The Astrophysical Journal Supplement Series, 162:346–374, 2006 February

ABUNDANCE GRADIENTS IN THE GALAXY

Alexander L. Rudolph,[1] Michel Fich,[2] Gwendolyn R. Bell,[3] Travis Norsen,[3] Janet P. Simpson,[4,5]
Michael R. Haas,[4] and Edwin F. Erickson[4]
Received 2001 May 23; accepted 2005 October 8

ABSTRACT

Six H ii regions at galactocentric distances of $R = 10$–15 kpc have been observed in the far-IR emission lines of [O iii] (52 μm, 88 μm), [N iii] (57 μm), and [S iii] (19 μm) using the Kuiper Airborne Observatory. These observations have been combined with Very Large Array radio continuum observations of these sources to determine the abundances of O^{++}, N^{++}, and S^{++} relative to hydrogen. In addition, eight of the most recent sets of measurements of ionic line strengths in H ii regions have been reanalyzed in order to attempt to reconcile differences in optical versus far-IR abundance determinations. We have in total 168 sets of observations of 117 H ii regions in our analysis. The new analysis included updating the atomic constants (transition probabilities and collision cross sections), recalculation of some of the physical conditions in the H ii regions (n_e and T_e), and the use of new photoionization models to determine stellar effective temperatures of the exciting stars. We also use the most recent data available for the distances for these objects, although for most we still rely on kinematic distance determinations. Our analysis finds little indication of differences between optical and infrared observations of the nitrogen abundances, but some differences are seen in the oxygen and sulfur abundances. A very significant offset continues to be seen between optical and infrared measurements of the N/O abundance ratio.

Subject headings: Galaxy: abundances — H ii regions — ISM: abundances

Online material: machine-readable tables

1. INTRODUCTION

When the first stars formed in galaxies, they were composed almost entirely of hydrogen and helium. However, as these first stars evolved and returned some of their processed interiors to the interstellar medium, the heavier elements (C, N, O, S, etc.) were then present to be incorporated into future generations of stars. The amount of these heavy elements observed today is clearly, then, a function of many processes fundamental to our understanding of galactic evolution: the star formation rate, the rate of element production and eventual return to the ISM as a function of stellar mass, and the initial mass function (IMF). Elemental abundances will be functions of time, and since physical conditions (e.g., Σ, the surface density of gas in the galactic disks) vary throughout many galaxies (including the Milky Way), the abundance will vary with position as well. Thus, the accurate and detailed measurement of galactic abundance gradients in galaxies is essential to develop an accurate picture of galactic evolution, and possibly dynamics (e.g., in barred galaxies, radial mixing of interstellar gas may occur).

The study of abundances in the Milky Way provides both special challenges and rewards. Due to our location in the plane of the Galaxy, extinction by dust can limit our view of the objects whose abundances we wish to study, and the determination of galactocentric distances can be difficult. However, it is possible, in our own Galaxy, to obtain a level of detail in our studies, both in the determination of abundances of individual objects, and in modeling overall galactic trends, that is difficult to obtain in external galaxies.

H ii regions are ideal objects with which to study abundance gradients. Since they are bright and hot they emit strongly in many lines observable over much of the Milky Way. Unlike stars, H ii regions probe the current state of abundances and unlike planetary nebulae and supernovae remnants, do not contaminate the surrounding ISM.

The seminal study of H ii region abundances in the Milky Way was by Shaver et al. (1983), who studied optical recombination and forbidden lines of H ii regions spanning a range of galactocentric radii from 5.0 to 13.6 kpc (all distances quoted have been scaled to $R_0 = 8.5$ kpc; see § 6) and found clear gradients of N/H and O/H. Subsequent optical studies by Fich & Silkey (1991) and Vílchez & Esteban (1996) have focused on the outer Galaxy ($R = 8.5$–18 kpc), showing some evidence for flattening of the gradient of N/H at large galactocentric radii. Most recently, Caplan et al. (2000) have observed a number of H ii regions optically over a range of $R = 6.6$–17.7 kpc, and Deharveng et al. (2000) have analyzed these data together with some other observations in the literature to determine the O/H gradient. They too find a significantly smaller gradient than that found by Shaver et al. and other observers.

Far-infrared (FIR) studies of H ii regions have extended all the way to the Galactic center (Lester et al. 1987; Simpson et al. 1995) and to the outer Galaxy as well (Rudolph et al. 1997; this work). Also the *Infrared Space Observatory* (*ISO*) was used to measure abundances in a large number of Galactic H ii regions (Peeters et al. 2002; Giveon et al. 2002; Martín-Hernández et al. 2002). One of the striking results of the FIR observations has been that a discrepancy has arisen in the determination of abundances determined optically versus those determined using FIR lines, particularly the ratio N/O (Rubin et al. 1988).

A number of factors complicate the comparison of these various studies. First, and most simply, the distances used by the various authors are not consistent, due to changes in the rotation curve used (Schmidt vs. flat rotation curve, and changes in R_0 and Θ_0). In addition, the atomic constants (Einstein A coefficients

[1] Physics Department, California State Polytechnic University, 3801 West Temple Avenue, Pomona, CA 91768.
[2] Guelph-Waterloo Program for Graduate Work in Physics, Physics Department, University of Waterloo, Waterloo, ON N2L 3G1, Canada.
[3] Department of Physics, Harvey Mudd College, Claremont, CA 91711.
[4] NASA-Ames Research Center, Mail Stop 245-6, Moffett Field, CA 94035.
[5] Also at the SETI Institute.

TABLE 1
SOURCE LIST

Source	Position (B1950)[a] R.A.	Decl.	Galactic Coordinates l	b	R (kpc)	d (kpc)	FWHM (arcsec)	Association
WB 73	21 20 14.3	51 57 58	93.86	1.55	11.7	7.4	16	...
S127 B	21 27 04.2	54 23 20	96.27	2.60	15.0	11.5	9	WB 85 B
S128	21 30 35.5	55 39 23	97.51	3.16	12.7	8.4	26	WB 91
S138	22 30 52.5	58 12 50	105.63	0.34	11.0	5.1	12	WB 191
S152	22 56 36.4	58 30 46	108.76	−0.95	11.4	5.4	30	WB 228, G108.76−0.95
WB 411	02 04 29.2	60 31 50	132.16	−0.73	12.9	5.6	10	KR138
W3 A	02 21 56.3	61 52 47	133.70	1.20	10.2	2.3	26	G133.7+1.2A
W3 B	02 21 50.4	61 52 21	133.70	1.20	10.2	2.3	11	G133.7+1.2B

[a] Positions are from VLA radio maps and are the positions used to point the KAO telescope. Units of right ascension are hours, minutes, and seconds, and units of declination are degrees, arcminutes, and arcseconds.

and collisional cross sections) have been updated in the past two decades. Finally, each study has used a slightly different scheme to determine corrections for unobserved ionization states (ionization correction factors or icfs), with the differences most striking between optical and FIR studies.

Henry & Worthey (1999) have recently reviewed observations of abundance gradients both in the Milky Way and in external galaxies. They concentrated on oxygen as the most abundant and least depleted element in the interstellar medium. They find reasonably good agreement, with a large amount of scatter, across studies that use H II regions, planetary nebulae, and supernova remnants, and they do not see any strong evidence for flattening of abundances in the outer Galaxy, at least for oxygen. However, they do not attempt to reanalyze the data in any self-consistent manner across studies, but rather simply take their results from the literature.

This paper has two purposes. The first is to present new FIR observations of H II regions in the range of galactocentric radius $R = 10-15$ kpc to fill in a gap in the FIR abundance observations. Table 1 lists the sources observed, including their positions, galactocentric distance, distance from the Sun, and angular size. The second is to present a complete redetermination of the abundances of all the optical and FIR H II region observations in the literature with a single, consistent program. This update includes the most up-to-date atomic constants and recent non-LTE stellar models to try to reconcile these discrepancies between the optical and FIR data sets. Equally important, we have collected from the literature the distances to all these sources and redetermined their galactocentric radii using a common rotation curve. This is especially important for the sources observed by Shaver et al. (1983), whose distances were previously determined using a Schmidt rather than a flat rotation curve.

2. OBSERVATIONS AND NEW DATA

The FIR observations of [S III] (19 μm), [O III] (52, 88 μm), and [N III] (57 μm) were made with the 91 cm telescope of the KAO using the facility Cryogenic Grating Spectrometer (CGS; Erickson et al. 1984, 1995) on flights of 1995 August 6, 10, and 12. The aperture sizes were $\sim 40''$ (the exact values are shown in Table 2), corresponding to a spectral resolution of ~ 90 km s^{-1}. Standard chopping techniques were employed throughout; the integration time was 10 or 20 s (depending on line strength); the chopper frequency was 11 or 13 Hz; the chopper amplitude was $\sim 5'$ on August 6 and 10 (except for Saturn on August 10, for which it was $\sim 7'$) and $\sim 6'$ on August 12; the chopper rotation angle was individually selected for each source to avoid background contamination.

Telescope pointing was done by offsetting from stars from the *HST* Guide Star Catalog (Lasker et al. 1990 and Jenkner et al. 1990). The infrared boresight established on the ground was verified in flight to an accuracy of $\pm 5''$.

The [S III] line and its adjacent continuum were measured with an array of 13 discrete Si : As impurity band conduction (IBC) detectors (Bharat 1994). The longer wavelength [O III] and [N III] lines and continua were measured with an array of 13 Ge : Sb photoconductors. Both detector arrays were flat-fielded and

TABLE 2
OBSERVED INFRARED LINE INTENSITIES AND RADIO CONTINUUM FLUXES

Source	[O III] 88 μm	[O III] 52 μm	[S III] 18 μm	[N III] 57 μm	Radio Flux (Jy)	Frequency (GHz)	Reference[a]
WB 73	1.25 ± 0.10	2.24 ± 0.46	2.37 ± 0.37	1.05 ± 0.24	0.23	8.44	5
S 127 B	0.68 ± 0.14	0.47 ± 0.17	1.18 ± 0.34	...	0.11	4.89	4
S 128	7.15 ± 0.27	10.26 ± 0.75	4.35 ± 0.70	3.58 ± 0.55	0.41	4.89	1
S 138	0.96 ± 0.08	2.57 ± 0.26	5.64 ± 0.73	1.23 ± 0.22	0.45	8.44	5
S 152	3.81 ± 0.23	9.09 ± 0.76	11.65 ± 0.83	2.44 ± 0.25	0.74	4.89	2
WB 411	2.07 ± 0.18	3.55 ± 0.30	4.06 ± 0.87	0.73 ± 0.19	0.55	4.89	1
W3 A	41.99 ± 0.55	273.62 ± 3.73	113.35 ± 1.88	26.60 ± 1.20	12.7	8.05	3
W3 B	6.90 ± 0.62	31.90 ± 1.38	12.86 ± 1.04	4.20 ± 0.63	4.2	8.05	3
Beam size (arcsec)	38	42	44	41	40		

NOTES.—FIR line intensities are in units of 10^{-11} ergs s^{-1} cm^{-2}. Radio fluxes are accurate to 5%. The radio fluxes are measured in a beam closely matched to the average beam size of the FIR observations.

[a] References for radio fluxes: (1) Fich 1986; (2) Fich 1993; (3) Afflerbach et al. 1996; (4) Rudolph et al. 1996; (5) A. L. Rudolph, unpublished results.

flux-calibrated using observations of Saturn at the same wavelengths. The brightness temperature for the disk of Saturn (Hanel et al. 1983; Bézard et al. 1986) was combined with the ring brightness temperature (Haas et al. 1982) using the technique of Matthews & Erickson (1977) to account for the geometry. Laboratory measurements were used to remove the differential instrumental response from the divided spectra. The zenith water vapor overburden was determined to be 8.35, 10.5, and 7.5 precipitable μm for the three flights from observations of Saturn in the telluric 85 μm H_2O line. The overburden for each source was calculated from the zenith value by correcting for the elevation angle of the telescope. The H II region spectra, divided by the Saturn spectra, were corrected for differential absorption using ratios of water vapor model transmission spectra (Lord 1992) and for differences ($\lesssim$10%) in diffraction assuming a circular aperture with an obscuring secondary (Born & Wolf 1964).

The continuum intensities were determined from the arithmetic mean of the detectors showing no line emission. The line intensities were obtained by summing the detectors with line emission, after subtracting the average continuum level from each detector, and then multiplying the difference by the detector width in μm. The final FIR fluxes are listed in Table 2, along with radio continuum fluxes determined from VLA observations. The quoted uncertainties include the uncertainties in the measured continuum level and in the individual line detectors but do not include the absolute calibration uncertainty, which is estimated to be $\pm$8% (1 σ), determined by flux reproducibility over many flight series. However, this calibration uncertainty is included in the ionic and final abundance uncertainties (see § 5). The beam sizes are also listed for each line.

3. DETERMINATION OF ELEMENTAL ABUNDANCES

The method of determining elemental abundances from nebular emission lines is well documented elsewhere (Osterbrock 2000; Pagel 1997; Dinerstein 1990; Simpson et al. 1995; Henry & Worthey 1999) and we will review only the major points here. For each step, we will briefly discuss the differences in application to optical and FIR data. The general method of determining abundances from emission lines proceeds as follows:

1. *Emission lines are observed*.—The majority of these lines are "collisionally excited" (to use the terminology of Osterbrock 2000) meaning that the ions are excited to upper energy levels by collisions, typically with hot electrons. Since the excitation levels of the most abundant elements, hydrogen and helium, are much higher than the thermal energy of electrons at typical H II region temperatures ($T = 4000$–$20{,}000$ K), their emission lines do not provide significant cooling to the regions. It is the common ions such as O II, O III, N II, N III, and others, whose excitation potentials are on the order of the electron thermal energy, that provide much of the H II region cooling, and are thus observable. These lines are also commonly referred to as "forbidden lines" as they are typically not observed in terrestrial laboratories, since their low downward transition probabilities lead to fast collisional de-excitation under those conditions. It is only in the relatively diffuse conditions of interstellar space that the excited ions survive long enough to radiate.

2. *Correct the observed line fluxes for extinction*.—The corrections for extinction are generally much larger in the optical than the FIR, and thus FIR observations allow one to look into much more obscured regions, such as the Galactic center, and to look at younger, more compact objects. However, the extinction in these highly obscured regions can be quite large and significant extinction corrections can be required in the FIR, especially at wavelengths shortward of 20 μm.

3. *Determine the physical conditions (n_e and T_e) in the* H II *region to determine the emissivity of the line*.—This is the one of the two most critical steps in the analysis. Because the lines are collisionally excited, primarily by hot electrons, the relevant parameters are n_e and T_e, the electron density and temperature. These can often be determined from various observed line ratios, including some of those observed to determine abundances. For example, the ratio of doublets of [O II] or [S II] in the optical or [O III] in the FIR can be used to determine electron density. Electron temperatures can sometimes be determined from [O III] lines observed in the optical, but it is often difficult to observe all the relevant lines, and the range of wavelengths covered is large, so extinction effects are important. Therefore, the preferred method of determining electron temperatures is to use hydrogen radio recombination lines (see, e.g., Shaver et al. 1983). (Note, however, that even this method has difficulties, for example, caused by temperature fluctuations in the gas; Peimbert 1967.)

Optical abundance determinations depend on both parameters but are *particularly* sensitive to the electron temperature. The size of the variation in abundance is itself a function of the temperature. Changes of $\pm$500 K lead to ionic abundance variations of $\pm$0.05–0.1 dex around $T_e = 10{,}000$ K, and up to $\pm$0.50 dex around $T_e = 4000$ K.

The FIR lines, by contrast, are extremely *insensitive* to electron temperature, since they come from transitions between fine-structure levels of the ground states of the ions. Changing the electron temperature by $\pm$1000 K changes the ionic abundances by $\pm$0.01 dex or less. On the other hand, some FIR lines are especially sensitive to density.

4. *Determine the ionic abundance relative to* H (*or another ion*).—Having determined the electron temperature and density, the ionic abundances are determined. The first step is to use a statistical equilibrium calculation involving a multilevel (typically five level) model of each ion to determine the relative populations of the levels for the ion. This information, together with the observed intensity ratios and relevant atomic constants then determine the ionic abundance.

Abundances determined from optical observations are generally produced from observations of the ratio of the line intensity to the intensity of a nearby hydrogen recombination line. Thus, optical lines are in general already in the form of an abundance relative to hydrogen. In contrast, the FIR lines are measured in absolute terms. A radio continuum observation is used to measure the hydrogen column density. A detailed discussion of the results and uncertainties created by this procedure is given in Rudolph et al. (1997).

5. *Determine the effective temperature ($T_{\rm eff}$) of the exciting star and the corresponding ionization correction factor* (*icf*).—This is the other most critical step in the analysis. In order to determine total abundances from ionic abundances, it is necessary to either measure all relevant ionization states of the atom (often difficult or impossible, if observing in a limited wavelength range), or to make some correction for the unmeasured ionization states. Some observers have used semiempirical methods to make this correction, while others have tried to model the ionization structure of the H II region to determine icfs. The latter method usually requires some means of determining the effective temperature of the star exciting the region, typically from line ratios.

6. *Correct the ionic abundance for unmeasured ionization states, using the icfs determined in Step 5 to produce the final atomic abundances*.—When more than one ionization state is

observed, these can be added together before correcting for the other, unobserved states. Thus, when both [O II] and [O III] are observed in the optical, they typically account for ≳80% of the oxygen, and thus this correction is small. When, more typically, only one ionization state is observed, this correction varies in size, depending on whether the measured ionization state is the dominant state of the atom.

4. PREVIOUS ABUNDANCE STUDIES: DISCREPANCIES IN OPTICAL VERSUS FAR-INFRARED ABUNDANCE DETERMINATIONS

The first study to systematically combine radio determinations of electron temperature and optical determinations of abundances was that of Shaver et al. (1983), which resulted in the first comprehensive study of abundance gradients in the Milky Way. Shaver et al. observed radio recombination lines for 67 H II regions resulting in determination of their electron temperatures. These temperatures were combined with optical spectroscopy of 33 of these sources, spanning a range of $R = 5.0-13.6$ kpc to determine their abundances and galactic abundance gradients of O/H, N/H, and S/H. They saw very clear gradients in O/H and N/H but none in S/H. Shaver et al. used an ionization correction scheme based on the assumptions that all the O is either singly or doubly ionized and that $N/O = N^+/O^+$, and they made a semiempirical correction to the sulfur abundance for the unobserved ionization state S^{++}. Shaver et al. also found a clear gradient of electron temperature with R in the sense of increasing T_e with R, which they attribute to the abundance gradients.

Fich & Silkey (1991) and Vílchez & Esteban (1996) both extended optical studies to the outer part of the Galaxy. Fich & Silkey obtained optical spectra of 18 outer Galaxy H II regions spanning a range of $R = 11.7-17.9$ kpc. They then determined abundances for these 18 regions, using a simplified version of the Shaver et al. ionization correction scheme.

Fich & Silkey only detected the [O III] doublet in 4 of their 18 sources, and therefore focused their analysis on nitrogen. When they compared their results with those of Shaver et al. (after rescaling the distances of Shaver et al. for a flat rotation curve and $R_0 = 8.5$ kpc, $\Theta_0 = 220$ km s^{-1}), they found evidence for a flattening of the N/H abundances in the outer Galaxy; namely, their abundances were higher than an extrapolation of the Shaver et al. nitrogen gradient, by a statistically significant amount.

Vílchez & Esteban observed 8 outer Galaxy H II regions, including 6 previously observed by Fich & Silkey, using a larger telescope and extending the spectral range of the observations into the near-infrared. They then analyzed their new observations together with ten more of Fich & Silkey's objects to determine abundances for these 18 objects spanning a range of $R = 8.4-17.9$ kpc. When Vílchez & Esteban fitted their outer Galaxy abundance data, they found slopes significantly flatter than those of Shaver et al. and concluded that the flattening seen by Fich & Silkey was real.

Deharveng et al. (2000) determined oxygen abundances for 34 H II regions observed in the optical and presented by Caplan et al. (2000). They found a significantly flatter slope to the oxygen abundances than found in previous studies but no evidence for an additional flattening at large galactocentric distances.

In order to make meaningful comparisons of our new results with these previously published results, we have refitted the Shaver et al. data with updated distances based on a modern rotation curve. Shaver et al. calculated the distances to their sources using a Schmidt rotation curve with $R_0 = 10$ kpc. As part of our complete reanalysis of previous work, we have determined distances to all the sources studied by Shaver et al. (as well as many others; see § 6). We have refitted the Shaver et al. data with these new distances to obtain the corrected values of the optically determined abundance gradients with which to compare FIR studies of H II regions and studies of other types of objects (e.g., B stars; Smartt & Rolleston 1997; Gummersbach et al. 1998; Rolleston et al. 2000).

Following Shaver et al. we recomputed the abundance gradients for their data set both including and excluding sources for which their ionization correction scheme could be applied. Table 3 shows these recomputed results. As we fitted the abundances as a function $a + b(R - 8.5)$ the abundance uncertainty is not well-defined at $R = 0$. The top row shows the fit including only those sources for which Shaver et al. had both [O II] and [O III] lines, which they considered "well-determined," but excluding the sources S38 and S48, which had abundances that deviated greatly from the fit generated by the others. The second row is a fit of all of the Shaver et al. sources. We find, as Shaver et al. did, that the fit is very different depending on which sources are included. The abundance gradients determined with rescaled distances are the same as the published values, within the uncertainties, not larger as one might expect if all galactocentric distances simply scaled due to the smaller scale of the Galaxy.

The first major studies of Milky Way abundances in the FIR were done by Lester et al. (1987), and Rubin et al. (1988). These studies focused on the abundance ratio N/O. Lester et al. observed 13 H II regions in the range $R = 0-10.2$ kpc, while Rubin et al. observed 6 H II regions, 3 in common with Lester et al., for a total of 16 regions observed in the two studies. Lester et al., in the absence of any direct way to estimate the degree of excitation in these regions, made the simple assumption that $N/O = N^{++}/O^{++}$, though they acknowledge that this assumption may be wrong. Rubin et al. analyzed all 16 regions and attempted to estimate the degree of excitation in the regions using the ratio He^+/H^+. The striking finding of these studies is that the FIR determinations of N/O are systematically 2–5 times higher than those determined from optical lines. Rubin et al. considered a number of possible reasons for this discrepancy and concluded that the most important is what they call the "geometry effect," the possibly incorrect assumption that $N/O = N^+/O^+$ or $N/O = N^{++}/O^{++}$ in the optical or FIR, respectively. A secondary effect they identify is the possible enhancement of the optical [O II] lines by recombination in the [O III] region of the nebula, leading to an underestimate of N/O (though only by ~20% in Orion, the region where they did detailed modeling). Lester et al. also concluded that there was evidence, from their data, for an enhancement of N/O in the inner Galaxy, which they attribute to secondary nitrogen production in regions where enhanced star formation has occurred in the last 10^7-10^8 yr. Rubin et al. after reanalyzing the Lester et al. data, and considering the uncertainties in correcting N^{++}/O^{++} to N/O, conclude that such a conclusion is possible but uncertain.

The next major study of Milky Way abundance gradients in the FIR was done by Simpson et al. (1995). Simpson et al. observed 13 H II regions in lines of [O III], [N III], [S III], and [Ne III], with the Kuiper Airborne Observatory. They analyzed these data along with previously published observations by the same group of another 5 regions for a total of 18 H II regions spanning a range of $R = 0-12.3$ kpc. Rudolph et al. (1997), in conjunction with the same observers, extended these observations to the outer Galaxy, observing lines of [O III], [N III], [S III], for an additional 5 sources with $R = 12.7-16.5$ kpc. Since these two groups used the same instrument on the same telescope, and reduced the data using a single method, they will be considered together from here on.

TABLE 3

Abundance Gradients from Previous Studies

Study	Slope	Abundance at 0 kpc	Abundance at 8.5 kpc	Range in R	Number of Points
		12 + log (N/H)			
S83[a]	-0.066 ± 0.020	8.12	7.56 ± 0.06	6.4–13.6	18
S83[b]	-0.113 ± 0.014	8.59	7.63 ± 0.03	5.0–13.6	33
S95/R97[c]	-0.111 ± 0.012	8.75 ± 0.11	7.81	0.0–16.5	20
A97[d]	-0.072 ± 0.006	8.42 ± 0.04	7.80	0.0–11.4	34
		12 + log (O/H)			
S83[a]	-0.064 ± 0.019	9.28	8.74 ± 0.05	6.3–13.6	18
S83[b]	-0.079 ± 0.016	9.42	8.75 ± 0.04	5.5–13.6	27
S95/R97[c]	-0.079 ± 0.009	9.21 ± 0.08	8.54	0.0–16.5	22
A97[d]	-0.064 ± 0.009	9.15 ± 0.06	8.61	0.0–11.4	34
D00[e]	-0.040 ± 0.005	8.82 ± 0.05	8.48	6.6–17.7	34
		12 + log (S/H)			
S83[a]	0.017 ± 0.043	6.91	7.06 ± 0.10	8.1–13.6	7
S83[b]	-0.015 ± 0.034	7.27	7.14 ± 0.08	6.5–13.6	8
S95/R97[c]	-0.079 ± 0.009	7.54 ± 0.08	6.87	0.0–16.5	22
A97[d]	-0.063 ± 0.006	7.55 ± 0.04	7.01	0.0–11.4	34

[a] Shaver et al. (1983) "well determined" values only.
[b] Shaver et al. (1983) all data.
[c] Simpson et al. (1995) and Rudolph et al. (1997).
[d] Afflerbach et al. (1997).
[e] Deharveng et al. (2000).

Simpson et al. (1995) and Rudolph et al. (1997) determined electron densities from observed [O III] line ratios. Simpson et al. took their electron temperatures from the literature, and Rudolph et al. assumed a value of 10^4 K for their sources in the outer Galaxy, since abundances determined from FIR lines are extremely insensitive to T_e. Both groups corrected ionic abundances to atomic abundances using H II region excitation models of Rubin (1985). To determine the effective temperature of the exciting star in each region, they used the observed ratio of [O III]/[S III] relative to an assumed constant ratio of O/S = 47. Both groups used radio continuum data to determine the hydrogen column density; Simpson et al. estimated the radio flux in the relevant area using data from the literature, while Rudolph et al. measured the radio flux in the appropriate beam directly from VLA images.

Most recently, Afflerbach et al. (1997) observed lines of [O III], [N III], [S III] for an additional 17 sources (one in common with Simpson et al.), also aboard the KAO, also using the same instrument as Simpson et al. and Rudolph et al. They then combined these data with those from the Simpson et al. sources, and with their own high-resolution VLA maps of these regions to do a self-consistent statistical equilibrium and ionization equilibrium model of each source. These models attempt to simultaneously fit the FIR lines and the radio continuum (including source geometry) to determine the atomic abundances, electron density and temperature, and ionization structure of the source. The 34 sources they modeled cover a range of $R =$ 0–11.4 kpc.

Together, Simpson et al. and Rudolph et al. found clear gradients in N/H and S/H (and by extension O/H) of -0.111 ± 0.012 dex kpc^{-1}, and -0.079 ± 0.009 dex kpc^{-1} (see Table 3 but note that as these were fitted as $a + bR$ the uncertainty at $R =$ 8.5 kpc is not well defined), while Afflerbach et al. found somewhat shallower gradients of -0.072 ± 0.006 dex kpc^{-1} for N/H, -0.064 ± 0.009 dex kpc^{-1} for O/H, and -0.063 ± 0.006 dex kpc^{-1} for S/H.[6] These results are also listed in Table 3. Rudolph et al. found that for the combined Simpson/Rudolph data set N/O was best fitted by a two-step model in which $\log(\mathrm{N/O}) = -0.50 \pm 0.02$ for $R < 6.2$ kpc and $\log(\mathrm{N/O}) = -0.83 \pm 0.04$ for $R > 6.2$ kpc. Afflerbach et al. merely noted that they saw no evidence for a gradient in N/O and quote a mean value of $\log(\mathrm{N/O}) = -0.78$.

In studying the N/H gradient determined from their data and that of Simpson et al., Rudolph et al. concluded that the N/H abundances did not flatten in the outer Galaxy. In fact, one result that Rudolph et al. noted was that the abundances they determined for the outer Galaxy H II regions S127 and S128 agreed quite well with those determined optically by Fich & Silkey and Vílchez & Esteban, suggesting that, rather then a flattening of N/H in the outer Galaxy, there is a systematic offset between the Shaver et al. and FIR determined N/H abundances in the inner Galaxy. Comparing the values of the nitrogen abundances at $R = 8.5$ kpc from the fits, there is some evidence for an offset between the optical and FIR determinations of $\sim$0.15–0.35 dex, corresponding to the optical nitrogen abundances being 30%–55% lower than the those determined from FIR lines, though such a difference is on the order of the uncertainties in the fits. Comparing the various fits in Table 3, it is interesting to note that the Afflerbach et al. fits agree quite well with the Shaver et al. fits for their "reliable" data points, while the Simpson et al.–Rudolph et al. fits agree better with the fits to all of the Shaver et al. data.

[6] Although Afflerbach et al. fit O/H and S/H separately, they find identical slopes for the two elements, indicating that O/S is constant with R. Afflerbach et al., like Simpson et al. and Rudolph et al., use the ratio of [O III]/[S III] relative to the value O/S = 47, appropriate for Orion, as a first guess at excitation in their models. Their final ratio of O/S, determined from their fitted intercepts, is O/S = 40.

The *Infrared Space Observatory* was used to obtain spectra of ions in H II regions. Two versions of the original data can be found in papers by Peeters et al. (2002) and Giveon et al. (2002). The Giveon et al. paper includes an analysis of the ionic and atomic abundances from their data, while the Peeters et al. data are analyzed in Martin-Hernandez et al. (2002). Neither of these analyses give abundance gradients for the atoms under study in this current paper.

Unlike the subtle differences noted for N/H, the optical and FIR determinations of N/O are strikingly different. In considering N/O as determined by all these studies (Shaver et al. 1983; Vílchez & Esteban 1996; Lester et al. 1987; Rubin et al. 1988; Simpson et al. 1995; Afflerbach et al. 1997; Rudolph et al. 1997), there is a clear, systematic offset between the optically determined and FIR-determined ratios, as noted by Rubin et al. (1988). Comparing N/O over the range $R = 6.4{-}13.6$, where Shaver et al. has reliable determinations of N/O, and over which the various FIR determinations of N/O are fairly consistent, the data of Shaver et al. give $\langle \log(\mathrm{N/O}) \rangle = -1.16$, Simpson et al. and Rudolph et al. give $\langle \log(\mathrm{N/O}) \rangle = -0.75$, and Afflerbach et al. give $\langle \log(\mathrm{N/O}) \rangle = -0.78$. Thus, there is a clear offset of 0.4 dex, or a factor of 2.5 between the optical and FIR determinations of N/O.

The variations seen both within and between the optical and FIR data sets, together with variations in methodology for determining abundances in the various studies, prompted us to undertake a complete reanalysis of the major abundance studies in the literature, beginning with the study of Shaver et al. We hoped that by using a single consistent method, we could reconcile these discrepancies (or at least rule out some of their causes), possibly settle some of the outstanding issues, such as whether there is a change in slope in abundance gradients with R, and determine a single best model for the variations of abundance in the Milky Way, based on the data currently available.

The following section begins by describing our method of determining abundances for the studies we analyzed, including the new data presented here, and then goes on to present the results of that analysis.

5. DETAILS OF NEW ABUNDANCE ANALYSIS

The studies we chose to reanalyze were those of Shaver et al. (1983), Fich & Silkey (1991), Simpson et al. (1995), Vílchez & Esteban (1996), Afflerbach et al. (1997), Rudolph et al. (1997), Deharveng et al. (2000; the data for this study were published by Caplan et al. 2000) and Martin-Hernandez et al. (2002; data in Peeters et al. 2002). The data from these eight studies were added to the new observations reported here to create a data set of observations of 117 distinct H II regions (listed in Table 4). Figure 1 shows the positions of these 103 objects projected onto the Galactic plane, using distances derived here and tabulated in Table 4 (see § 6). Twenty-four of these regions were observed by more than one observer, two of them (S127, S128) a total of six times.

The only recent major studies of H II regions we did not include in our analysis were those of Lester et al. (1987) and Rubin et al. (1988). Neither of these studies observed the [S III] lines necessary for the determination of effective temperature of the exciting star of the region (see §§ 3 and 4). Additionally, many of the objects first observed in these two FIR studies were included in Simpson et al.

We now report on the method used to analyze these data in detail. We generally followed the scheme outlined in § 3. For each step, we will describe the FIR and optical data sets separately, as we often used common analysis for studies in the same wavelength region.

5.1. *Flux Uncertainties*

All the FIR studies, including this one, quote statistical uncertainties for their fluxes. In addition, a systematic uncertainty of 7% was added to all FIR fluxes for the KAO data when used to determine abundances relative to hydrogen. This additional uncertainty is based on comparisons of fluxes of the same source between flight series on the KAO, and therefore is not included when calculating flux ratios, such as [O III]/[S III] or [N II]/[O III], taken from the same flight series.

Among the optical studies, only Vílchez & Esteban quoted uncertainties in their individual observed fluxes, so we assigned a 20% uncertainty to all the fluxes from Shaver et al. and Fich & Silkey and a 10% uncertainty to those of Caplan et al. as suggested by them.

5.2. *Extinction Correction*

All the KAO FIR studies presented here, including this one, followed a procedure for estimating extinction presented in Simpson & Rubin (1990), and Simpson et al. (1995). The FIR extinction is proportional to the optical depth of the silicate feature at 9.7 μm, $\tau_{9.7}$ (Simpson & Rubin 1990; Simpson et al. 1995), and falls with increasing wavelength. Simpson & Rubin (1990) assumed a spectral shape for the 18 μm silicate feature and that $\tau_\lambda \propto \lambda^{-2}$ for $\lambda \geq 22$ μm. They then estimated $\tau_\lambda/\tau_{9.7} =$ 0.395, 0.054, 0.044, and 0.019 for $\lambda = 19$, 52, 57, and 88 μm, respectively. By determining $\tau_{9.7}$ for each source, the relevant FIR extinction can be estimated.

For the *ISO* data of Peeters et al. (2002) we used the extinction method they outline. They did not use this in their analysis as they did not have accurate extinction information for many of their sources. However, we were able to find extinction values for a significant number, primarily for objects from their sample that are in common with others in our data sets. We have extinction corrected all the *ISO* sources for which we had such data.

For our new data, the optical depth of the silicate feature for the Sharpless sources, except S138, is estimated from the optical extinction. Although the optical extinction may not be caused by the same silicate grains as the 9.7 μm extinction, in general, the two interstellar dust components track each other well enough that an average relationship can be derived. We use $A_V/\tau_{9.7} \approx$ 12.5 and the extinction curve ($A_V/E_{B-V} = 3.09$) of Rieke & Lebofsky (1985) and Martin & Whittet (1990). The optical extinction is calculated from the relative extinction between Hα and Hβ. For S127 B and S128, we estimate $\tau_{9.7} = 0.26$ and 0.45 from the measured extinction at Hβ from Fich & Silkey (1991). For S152, we estimate $\tau_{9.7} = 0.26$ from the average relative extinction between Hα and Hβ from Hunter (1992). Antonopoulou & Pottasch (1987) directly determined $\tau_{9.7} = 0.16$ for S138 by performing a fit to the silicate feature.

The silicate feature optical depths for the embedded sources WB 73 and WB 411 are estimated from the *IRAS* LRS spectra following the method of Simpson & Rubin (1990) for model III. We find $\tau_{9.7} = 1.7$ and 2.1 for WB 73 and WB 411, respectively. This method is not used for W3 A and B because they are confused in the LRS beam. Hackwell et al. (1978) mapped $\tau_{9.7}$ over the W3 complex. Using their map, we estimate $\tau_{9.7} = 2.5$ and 4.0 for W3 A and B, respectively, by averaging over the beam area. We assign an uncertainty of 20% to all estimates of $\tau_{9.7}$, including those of previous studies. This uncertainty is propagated into the corrected fluxes by standard methods of error propagation.

The optical studies all used the hydrogen recombination lines they observed to estimate extinction. Shaver et al. fitted the

TABLE 4

H II Region Distances

Name	R (kpc)	d (kpc)	Type	Reference	Other Names	Observed By
G0.095+0.012	0.01	8.5	GC	S95		S95
G1.13−0.11	0.2	8.5	GC	S95		S95, P02
SgrC	0.3 ± 0.1	8.2 ± 0.1	K	LS95		P02
G9.61+0.20	3.0 ± 1.0	5.7 ± 1.1	SP	H94		A97
IR 17160	3.0 ± 0.1	5.7 ± 0.1	K	CH87		P02
G7.47+0.06	3.2 ± 1.0	5.4 ± 1.1	A	WAM82		A97
IR 17279	3.5 ± 0.1	5.1 ± 0.1	K	CH87		P02
G24.47+0.49	4.1 ± 0.2	9.8 ± 0.3	K	L89, CWC90		A97
G25.40−0.14	4.2 ± 0.2	9.8 ± 0.3	K	L89, CWC90		A97
IR 18116	4.3 ± 0.1	4.5 ± 0.1	K	G94		P02
IR 18317	4.5 ± 0.2	5.9 ± 0.2	K	WC89		P02
G23.95+0.15	4.5 ± 0.2	4.9 ± 0.3	K	L89, CWC90		S95
G29.96−0.02	4.5 ± 0.2	8.9 ± 0.5	K	CWC90		S95
G11.95−0.03	4.5 ± 0.4	4.2 ± 0.4	K	L89		A97
IR 18434	4.6 ± 0.1	5.7 ± 0.1	K	WC89		P02
W 43	4.7 ± 0.2	5.6 ± 0.4	K	L89, KB94	G30.8−0.0	S95
IR 18502	4.7 ± 0.1	7.1 ± 0.1	K	WC89		P02
IR 18469	4.8 ± 0.1	5.3 ± 0.1	K	B96		P02
RCW 166	5.0 ± 0.3	3.9 ± 0.3	K	S83		S83
G25.38−0.18	5.2 ± 0.2	11.4 ± 0.3	K	L89, CWC90		S95, A97
G8.14+0.23	5.2 ± 0.7	13.4 ± 0.7	K	L89, CWC90	G8.14−0.23	A97
S38	5.5 ± 0.5	3.1 ± 0.5	K	S83		S83
G12.21−0.10	5.6 ± 0.6	13.6 ± 0.6	K	CWC90		A97
IR 17591	5.5 ± 0.1	3.0 ± 0.1	K	B96		P02
S48	5.8 ± 0.8	2.9 ± 0.9	SP	BFS82		S83
G339.1−0.4	5.8 ± 0.3	3.0 ± 0.4	K	S83		S83
G333.6−0.2	5.8 ± 0.3	3.2 ± 0.4	K	CH87		S95
G37.87−0.40	5.9 ± 0.2	9.4 ± 0.5	K	L89, KB94		A97
G34.26+0.15	5.9 ± 0.4	3.6 ± 0.4	K	L89, CWC90		A97
RCW 117	6.0 ± 0.5	2.6 ± 0.5	K	S83		S83
RCW 121	6.0 ± 0.6	2.5 ± 0.7	K	S83		S83
G326.7+0.6	6.2 ± 0.2	3.0 ± 0.4	K	S83		S83
G45.13+0.14A	6.2 ± 0.2	7.5 ± 2.3	K	L89, KB94	G45.12+0.13	S95
RCW 94	6.3 ± 0.2	2.9 ± 0.4	K	S83		S83
G45.45+0.06	6.3 ± 0.2	7.6 ± 1.0	K	L89, KB94		S95
W 31	6.3 ± 2.7	14.5 ± 2.8	SP	C97	G10.2−0.4	S95
Omega Nebula	6.4 ± 0.2	2.2 ± 0.2	SP	CEN80	M17, G15.0−0.7	S83
G326.5+0.9	6.4 ± 0.3	2.7 ± 0.4	K	S83		S83
IR 19207	6.4 ± 0.1	5.6 ± 0.1	K	R70		P02
NGC 6604	6.5 ± 0.4	2.1 ± 0.4	SP	F94		S83
RCW 122	6.5 ± 0.8	2.0 ± 0.8	K	S83		S83
M16	6.6 ± 0.1	2.0 ± 0.1	SP	H93		S83, C00
S54	6.6 ± 0.7	2.1 ± 0.2	SP	C00		C00
G5.97−1.18	6.7 ± 0.2	1.8 ± 0.2	SP	V97	NGC 6530, M8	A97
W 51e	6.8 ± 0.4	7.5 ± 1.5	M	G81b	G49.5-0.4	S95
G316.8−0.1	6.9 ± 0.3	2.6 ± 0.5	K	CH87		S83
IR 18479	7.5 ± 0.1	1.2 ± 0.1	K	A97		P02
IR 18032	7.6 ± 0.2	1.0 ± 0.2	K	B96		P02
G32.80+0.19	7.6 ± 0.4	13.1 ± 0.5	K	L89, CWC90		A97
S88	7.7 ± 0.2	2.0 ± 0.6	SP	BFS82	G61.47+0.10	A97, C00
λ Cen	7.7 ± 0.2	3.6 ± 1.8	K	S83		S83
S93	7.7 ± 0.8	3.5 ± 0.4	SP	C00		C00
NGC 3576	7.92 ± 0.01	3.1 ± 0.4	SP	G97		S83, S95
S101	8.1 ± 0.8	2.5 ± 0.3	SP	C00		C00
Carina-2	8.11 ± 0.01	2.4 ± 0.2	SP	T88		S83
S98	8.4 ± 0.3	0.3 ± 2.8	K	FTD90		VE96
S104	8.4 ± 0.8	3.3 ± 0.3	SP	C00		C00
G81.7+0.5	8.5 ± 0.3	2.5 ± 1.6	K	L89	DR 21	A97, P02
S112	8.5 ± 0.8	2.0 ± 0.2	SP	C00		C00
S117	8.5 ± 0.8	1.2 ± 0.1	SP	C00		C00
RCW 40	8.66 ± 0.02	1.5 ± 0.1	SP	BB93	BBW224	S83
RCW 38	8.7 ± 0.1	1.7 ± 0.3	SP	MC79		S83
G75.84+0.40	8.7 ± 0.3	4.8 ± 2.5	K	L89		A97
S131	8.7 ± 0.9	1.0 ± 0.1	SP	C00		C00
NGC 3603	8.8 ± 0.2	7.0 ± 0.5	SP	D95		S95

TABLE 4—*Continued*

Name	R (kpc)	d (kpc)	Type	Reference	Other Names	Observed By
Orion Nebula	8.89 ± 0.06	0.48 ± 0.08	M	G81a		S83
RCW 39	9.0 ± 0.3	2.9 ± 0.8	K	S83		S83
RCW 34	9.2 ± 0.2	2.9 ± 0.6	SP	H88		S83
S99	9.4 ± 0.9	7.9 ± 0.8	SP	C00		C00
S100	9.4 ± 0.9	7.9 ± 0.8	SP	C00		C00
RCW 19	9.5 ± 0.1	2.4 ± 0.2	SP	BB93	BBW127	S83
K3-50A	9.6 ± 0.4	8.2 ± 0.7	K	L89	G70.29+1.60	S95, P02
S158	9.9 ± 0.5	2.8 ± 0.9	SP	B94	NGC7538A	S95
Rosette-1	10.0 ± 0.2	1.6 ± 0.2	SP	BFS82	S275	S83
G298.22−0.34...........	10.1 ± 0.4	10.8 ± 0.6	K	CH87		S95
S184	10.1 ± 1.0	2.8 ± 0.3	SP	C00		C00
W3.............................	10.2 ± 0.2	2.3 ± 0.4	SP	GG76		R05
S146	10.2 ± 0.7	3.6 ± 1.1	SP	BFS82	G108.19+0.58, WB 212	A97, C00, R05
S168	10.7 ± 1.1	3.7 ± 0.4	SP	C00		C00
S252	10.7 ± 0.3	2.2 ± 0.3	SP	H95		S83, C00
S153	10.8 ± 1.1	4.5 ± 0.5	SP	C00		C00
RCW 8	10.9 ± 0.5	3.5 ± 0.7	K	S83		S83
S255	11.0 ± 0.4	2.5 ± 0.4	SP	BFS82		S83
S257	11.0 ± 0.4	2.5 ± 0.4	SP	BFS82		S83, C00
RCW 16	11.0 ± 0.4	4.1 ± 0.6	SP	BFS82	S311	S83
S138	11.0 ± 0.5	5.1 ± 0.8	K	BFS82	G105.63−0.34, WB 191	A97, C00, P02, R05
S288	11.0 ± 1.0	3.0 ± 1.2	SP	BFS82	WB 952	R97
S206	11.1 ± 1.1	2.9 ± 0.3	SP	C00		C00
S142	10.2 ± 1.1	4.6 ± 0.5	SP	C00		C00
BFS31	11.3 ± 0.8	3.3 ± 0.9	K	BFS82		VE96
S148	11.4 ± 1.4	5.3 ± 0.5	SP	C00		C00
S152	11.4 ± 0.5	5.4 ± 0.7	K	BFS82	G108.76−0.95, WB 228	A97, C00, R05
WB 73	11.7 ± 0.5	7.4 ± 0.7	K	WB89		R05
BFS64	11.7 ± 0.8	5.8 ± 0.9	K	BFS82		FS91
S156	12.3 ± 1.5	6.4 ± 2.0	SP	BFS82		S95, C00, P02
S219	12.5 ± 0.6	4.2 ± 0.6	SP	BFS82		FS91, VE96, C00
RCW 6	12.6 ± 0.7	5.4 ± 0.8	K	S83		S83
IR 21190	12.7 ± 0.1	8.9 ± 0.1	K	W81		P02
S128	12.7 ± 0.6	8.4 ± 0.8	K	BFS82		FS91, VE96, R97, C00, P02, R05
WB 411	12.9 ± 0.8	5.6 ± 1.0	K	WB89	KR138	R05
S301	12.9 ± 0.8	5.8 ± 0.9	SP	BFS82		FS91
S271	13.2 ± 0.5	4.8 ± 0.5	SP	BFS82		FS91
S272	13.2 ± 0.5	4.8 ± 0.5	SP	BFS82		FS91
S284	13.2 ± 0.8	5.2 ± 0.8	SP	BFS82		S83
S241	13.2 ± 1.2	4.7 ± 1.2	SP	BFS82		FS91
S217	13.5 ± 0.6	5.2 ± 0.8	SP	BFS82		FS91, C00
G201.6+1.6	13.6 ± 1.8	5.3 ± 1.8	K	S83		S83
RCW 5	13.6 ± 2.2	6.3 ± 2.5	SP	BFS82	S298	S83, FS91
S211	14.1 ± 1.8	6.0 ± 1.8	K	BFS82		FS91, C00
S212	14.2 ± 0.6	6.0 ± 0.6	SP	BFS82		FS91, C00
S270	14.2 ± 2.7	5.9 ± 2.7	K	BFS82		FS91
WB 870.....................	14.6 ± 1.5	6.7 ± 1.6	K	WB89		R97
S285	14.7 ± 0.7	6.9 ± 0.7	SP	BFS82		FS91
S127	15.0 ± 0.9	11.5 ± 1.0	K	BFS82		FS91, VE96, R97, C00, P02, R05
S83	15.2 ± 1.5	18.3 ± 1.8	SP	C00		C00
BFS54	16.3 ± 2.7	8.7 ± 2.8	SP	BFS82	NGC 2284	FS91
WB 380.....................	16.5 ± 1.2	10.2 ± 1.4	K	WB89		R97
S207	16.8 ± 1.7	8.6 ± 0.9	SP	C00		C00
S208	16.8 ± 1.7	8.6 ± 0.9	SP	C00		C00
S209	17.0 ± 2.3	9.0 ± 2.4	K	BFS82		FS91, VE96, C00
S283	17.0 ± 2.8	9.1 ± 2.9	SP	BFS82		FS91, VE96
S266	17.9 ± 4.7	9.6 ± 4.8	K	BFS82		FS91, VE96

NOTE.—Table 4 is also available in machine-readable form in the electronic edition of the *Astrophysical Journal Supplement*.

REFERENCES.—(A97) Afflerbach et al. 1997; (B94) Balser et al. 1994; (BFS82) Blitz et al. 1982; (BB93) Brand & Blitz 1993; (B96) Bronfman et al. 1996; (C00) Caplan et al. 2000; (CH87) Caswell & Haynes 1987; (CF95) Chan & Fich 1995; (CEN80) Chini et al. 1980; (CWC90) Churchwell et al. 1990; (C97) Corbel et al. 1997; (D95) Drissen et al. 1995; (F94) Feinstein 1994; (FS91) Fich & Silkey 1991; (GG76) Georgelin & Georgelin 1976; (G94) Garay et al. 1994; (G97) Girardi et al. 1997; (GW94) Goldader & Wynn-Williams 1994; (H95) Haikala 1995; (H88) Heydari-Malayeri 1988; (H93) Hillenbrand et al. 1993; (H97) Hillenbrand 1997; (H94) Hofner et al. 1994; (KB94) Kuchar & Bania 1994; (L89) Lockman 1989; (LS95) Liszt & Spiker 1995; (M95) Mooney et al. 1995; (MC79) Muzzio & Celotti de Frecha 1979; (P02) Peeters et al. 2002; (R70) Reifenstein et al. 1970; (R97) Rudolph et al. 1997; (R05) this work; (S83) Shaver et al. 1983; (S95) Simpson et al. 1995; (T88) Tapia et al. 1988; (V97) van den Ancker et al. 1997; (VE96) Vilchez & Esteban 1996; (W81) Walmsley et al. 1981; (WAM82) Wink et al. 1982; (WB89) Wouterloot & Brand 1989; (WC89) Wood & Churchwell 1989.

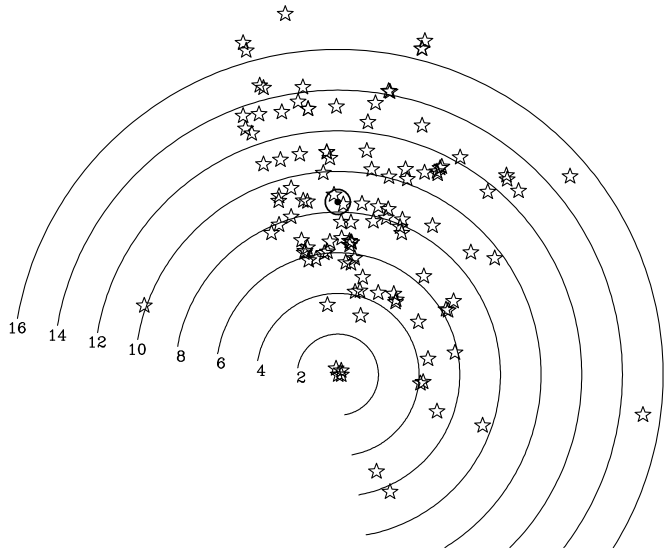

FIG. 1.—Plot of the Galactic positions of 117 sources analyzed in this study.

observed Balmer decrement to the theoretical one using the extinction law of Whitford (1958) to determine extinction corrections. From this fit they also derived $C(\mathrm{H}\beta)$, the extinction correction at the wavelength of the Hβ line. Fich & Silkey used the observed ratio of Hα to Hβ to derive $C(\mathrm{H}\beta)$ by assuming an intrinsic ratio of 2.859, and corrected their fluxes using the extinction law of Seaton (1979). Vílchez & Esteban compared the ratios of a number of Balmer lines to the theoretical values expected for case B recombination (Brocklehurst 1971) to determine $C(\mathrm{H}\beta)$ and to correct for extinction, also using the extinction law of Whitford (1958).

To determine if the use of older extinction laws might cause any systematic problems with the optical fluxes, we compared the extinction law of Whitford (1958) to the recent extinction law of Cardelli et al. (1989) and found that they agreed within 10% over the relevant wavelength range. Since Cardelli et al. also found their law in good agreement with that of Seaton (1979) we made no attempt to update the extinction corrections of the optical studies.

5.3. *Physical Conditions*

For our new data, we followed the procedure outlined in Rudolph et al. (1997), namely, we determined n_e, the electron density from the extinction-corrected ratio of the [O III] lines at 52 and 88 μm, and we estimated T_e, the electron temperature to be 10,000 K for all our sources, a value roughly correct for the outer Galaxy. Since the FIR abundance determinations are extremely insensitive to T_e (see § 3) this simple assumption is adequate.

For the other KAO FIR studies (Simpson et al.; Afflerbach et al.) we adopted their values of n_e and T_e. Both groups used the same [O III] line ratio as Rudolph et al. to estimate electron density. Simpson et al. compiled electron temperatures from the literature, and Afflerbach et al. derived their electron temperatures from their models. Again, given the insensitivity of the FIR analysis to T_e, we made no attempt to improve on these values.

Martin-Hernandez et al. (2002) estimate electron densities from their [O III] line ratios and we adopt their values. However, they use a constant electron temperature of 7500 K for all objects. Instead, we interpolate on the electron temperature relationship found by Deharveng et al. to estimate electron temperatures for all of the *ISO* object.

Among the optical studies, Shaver et al. and Vílchez & Esteban estimated their electron densities using the standard ratio of the [S II] doublet at $\lambda\lambda$6716, 6731, and we adopted these values. Deharveng et al. use the standard ratio of the [O II] doublet at $\lambda\lambda$3726, 3729, and we use the densities derived by them. Fich & Silkey did not resolve this doublet, and used electron densities estimated from radio continuum observations. For the sources observed by both Fich & Silkey and Vílchez & Esteban, we compared their estimates of n_e and found that the sulfur-determined densities were typically 10 times higher than those determined by radio continuum fluxes. Since the radio continuum flux comes from an average over the whole H II region while the sulfur lines come from the region emitting the forbidden lines used to determine abundances, we attempted to correct the electron densities of Fich & Silkey. For all the Fich & Silkey sources observed by Vílchez & Esteban, we used the latter's estimate of n_e. For the other Fich & Silkey sources we multiplied their estimate of n_e by 10. The one exception was S270, a compact H II region, where we used the n_e determined from the radio continuum, since in such a compact region, the radio continuum density is typically a better match to the fine-structure line emitting region (Rudolph et al. 1997).

As noted here and elsewhere, the determination of the electron temperature, T_e, is one of the most critical parameters for determining abundances from optical H II region data. Shaver et al. measured the electron temperature of each region from radio recombination lines, thereby avoiding the extinction problems that make such determinations difficult from the optical lines of O III. They then corrected for non-LTE effects and derive what they call the "line temperature" for [O II] (which they also use for [N II], [S II], and [S III]) and for [O III], using the models of Stasińska (1980).

Fich & Silkey, following Shaver et al. attempted to determine electron temperatures for their 18 sources using radio recombination lines, but they were only able to detect 8 of them and could only determine what they considered reliable values for 2 of them. For the other 16 sources, they instead used a combined linear fit of their and T_e data and that of Shaver et al. and estimated values of T_e from this fit.

Vílchez & Esteban determined electron temperatures for 3 of their 18 sources directly from the optical spectra, using the lines of [O II]. For the other sources, the electron temperature was determined indirectly by fitting various line ratios with photoionization models of Stasińska (1980, 1982).

Deharveng et al. determine electron temperature directly for six H II regions, calculate the Galactic electron temperature gradient, and then use the distances to the other H II regions to interpolate on this relationship to determine their electron temperatures.

Although the three optical studies we reanalyzed use very different methods of estimating electron temperature, we had no better way to determine this crucial parameter than the authors, so in all cases we used their values. However, we note that the sensitivity of ionic abundances derived from optical lines on electron temperature, combined with the inhomogeneity in methodology and resultant potentially large uncertainties in that parameter, suggest that this might be one of the potential causes of inconsistencies in determination of abundances from optical data (see § 8).

Simpson et al. and Rudolph et al. quote uncertainties in n_e propagated from the [O III] flux uncertainties used to determine the electron density, and we use these uncertainties in our analysis. For the other studies a 10% uncertainty was assumed for n_e. A similar 10% uncertainty was assumed for T_e for all eight studies (including this one).

TABLE 5
REFERENCES FOR ATOMIC PARAMETERS

Ion	Collision Strength, Ω	Transition Probability, A
O^+	Pradhan & Peng 1995	Pradhan & Peng 1995
O^{++}	Lennon & Burke 1994	Galavís et al. 1995
N^+	Lennon & Burke 1994	Galavís et al. 1995
N^{++}	Blum & Pradhan 1992	Galavís et al. 1995
S^+	Pradhan & Peng 1995	Pradhan & Peng 1995
S^{++}	Galavís et al. 1995	Pradhan & Peng 1995
S^{+++}	Saraph & Storey 1999	Mendoza 1983

5.4. *Determination of Ionic Abundances: Updated Atomic Constants*

The ionic abundances relative to hydrogen, and a number of relevant ion ratios were calculated from statistical equilibrium calculations using five-level models of the relevant ions. The atomic constants were compiled from the literature and represent the most current values of transition probabilities and collision cross sections available at the time of this work. Table 5 lists the references used for these atomic constants. The derived ionic abundances, along with the n_e and T_e of each source, are listed in Table 6.

5.5. *Determine the Effective Temperature ($T_{\rm eff}$) of the Exciting Star and the Corresponding Ionization Correction Factor for Each Ion*

The determination of the ionization structure of the H II region is one of the most difficult in the entire process. The early optical studies (including Shaver et al. and Fich & Silkey) used semiempirical ionization correction schemes, while FIR studies, beginning with Simpson et al., tried to determine the effective temperature of the exciting star from measured line ratios in order to apply photoionization models (Rubin 1985, in the case of Simpson et al. and Rudolph et al. and Mathis 1985 for Afflerbach et al.) to determine the ionization structure of the region. Both sets of models used by the FIR investigators used the LTE stellar atmospheres of Kurucz (1979). Recently, there have been published photoionization models of single-star H II regions (Stasińska & Schaerer 1997) which use non-LTE stellar atmosphere models which include the effects of line-blanketing and stellar winds ("CoStar" models; Schaerer & de Koter 1997), which are also available in electronic form. We have acquired the data from these models and incorporated them into our abundance code in order to allow us to calculate accurate icfs.

In order to use such models, it is necessary, in addition to knowing n_e and T_e of the H II region itself, to determine $T_{\rm eff}$, the effective temperature of the exciting star of the region (for simplicity, we have assumed a single exciting star throughout this analysis). For the FIR studies, we followed the method of Simpson et al., who used the observed ratio [O III]/[S III] relative to an assumed value of O/S to estimate stellar effective temperatures. Figure 2*a* shows a plot of this ratio as a function of $T_{\rm eff}$ for electron densities of 10 and 10^4 cm^{-3} taken from the models of Stasińska & Schaerer (1997). This ratio varies by more than an order of magnitude over the relevant range of $T_{\rm eff} = 33{,}000$–$50{,}000$ K, making it an extremely sensitive measure of $T_{\rm eff}$.

A similar ratio can be used to determine effective temperatures for optical H II region lines. Figure 2*b* shows a plot of [O III]/[S II] (a ratio commonly measured in optical studies) versus $T_{\rm eff}$ for the same electron densities also from the models of Stasińska & Schaerer. This ratio varies by almost 3 orders of magnitude over the same range of stellar effective temperature, making it even more sensitive than the FIR line ratio at determining $T_{\rm eff}$.

For both cases we assumed an underlying constant ratio of O/S = 47, the value determined for Orion (Rubin et al. 1991). The ratio O/S is expected to remain constant since both elements are produced by primary nucleosynthesis, and Simpson et al. conclude that the gradient in this ratio is no larger than -0.03 dex kpc^{-1}, corresponding to a variation of less than a factor of 3 in O/S. Such a variation leads to changes in $T_{\rm eff}$ of $\lesssim$1000 K.

For each source, the effective temperature of the source is determined from the relevant line ratio, if available, and n_e and T_e. The uncertainties in the line ratios, n_e, and T_e are propagated through the code to determine an uncertainty in $T_{\rm eff}$, and in the derived icfs. For sources in the optical that do not have the relevant lines (typically the [O II] line at 3727 Å) we adopt an effective temperature, following Shaver et al. of 36,000 K, and an uncertainty in $T_{\rm eff}$ of 2000 K.

To determine if our [O III]/[S II] ratio is correctly predicting effective temperatures, we compared the value of O II/(O II+O III) and O III/(O II+O III) calculated from the Stasińska & Schaerer models to the observed values for the sources for which both [O II] and [O III] lines were observed. Figure 3 shows a plot of this comparison. Although the relation is not a perfect 45 degree straight line, most of the points fall on such a line, giving us confidence that this method works well.

For the FIR studies, it is necessary to have a line of [S III] to determine $T_{\rm eff}$. Five of the regions observed in the FIR do not have such a measurement. In addition, Afflerbach et al. do not list fluxes for one of their observed sources, G34.26+0.15, which they state does not have a geometry consistent with a simple spherical model of the region.

5.6. *Final Abundances*

The final calculated abundances, along with the determined (or assumed) $T_{\rm eff}$ and derived icfs are listed in Table 6. For the sources where two ionization states were observed, the final abundance was determined by summing the two ionic abundances and dividing by the sum of the icfs. For other abundances relative to hydrogen, we simply divided the single measured ionic abundance by the relevant icf. An additional correction of 6% was added to all abundances relative to hydrogen to account for the additional electrons contributed by helium. This value represents the model value of He^+/H^+ for $T_{\rm eff} = 36{,}000$ K, a typical midrange value of effective temperature. This ratio varies from 0 to 0.10 and therefore this assumption will cause, at most, a 5% uncertainty in the final abundances.

For the abundance ratio, N/O, we followed a somewhat different procedure. Since Stasińska & Schaerer (1997) found that N/O $\approx N^+/O^+$ over a large range of $T_{\rm eff}$, we determined N/O directly from this ion ratio, even when [O III] lines were observed, since we believe this led to a more accurate determination of N/O. However, for the FIR observations, where only one ionization state of each atom was observed, we followed the standard procedure outlined above. Standard error propagation was followed throughout to arrive at the uncertainties in the final abundances quoted in Table 6. The asymmetric uncertainties listed in Table 6 are due to taking the logarithm of the abundances.

We compared the oxygen abundances we calculate using our method with those determined by Deharveng et al. (2000) for the 43 regions they analyzed and find essentially identical abundances:

TABLE 6

Final Abundances

Property	G0.095+0.012	G1.13−0.11	G1.13−0.11	SgrC	G9.61+0.20 B	IR 17160	IR 17279	G24.47+0.49
Reference	simpson95	peeters02	simpson95	peeters02	afflerbach97	peeters02	peeters02	afflerbach97
R	0.01	0.20	0.20	0.27	3.00	3.01	3.42	4.10
n_e	240 ± 20	545 ± 151	1000 ± 20	107 ± 55	650 ± 65	476 ± 122	127 ± 50	825 ± 82
T_e (10^3 K)	5.3 ± 0.5	4.3 ± 0.4	5.9 ± 0.6	4.4 ± 0.4	6.3 ± 0.6	5.4 ± 0.5	5.5 ± 0.6	6.1 ± 0.6
log (N^+/H^+)	...	$8.16^{+0.12}_{-0.17}$	...	$7.68^{+0.21}_{-0.41}$	...	$8.17^{+0.12}_{-0.17}$	$8.93^{+0.17}_{-0.28}$	...
log (N^{++}/H^+)	$7.57^{+0.09}_{-0.12}$	$7.92^{+0.13}_{-0.18}$	$8.02^{+0.09}_{-0.11}$	$6.58^{+0.23}_{-0.51}$	$7.33^{+0.09}_{-0.11}$	$7.64^{+0.12}_{-0.17}$	$8.28^{+0.18}_{-0.33}$	$7.64^{+0.07}_{-0.08}$
log (O^+/H^+)	...	...	...	...	...	...	...	...
log (O^{++}/H^+)	$7.64^{+0.09}_{-0.12}$	$8.27^{+0.12}_{-0.17}$	$8.30^{+0.08}_{-0.11}$	$6.85^{+0.21}_{-0.41}$	$7.51^{+0.07}_{-0.09}$	$7.95^{+0.12}_{-0.16}$	$8.47^{+0.17}_{-0.28}$	$7.82^{+0.06}_{-0.07}$
log (S^+/H^+)	...	...	...	...	...	...	...	...
log (S^{++}/H^+)	$7.17^{+0.09}_{-0.12}$	$6.89^{+0.14}_{-0.21}$	$7.19^{+0.09}_{-0.11}$	$5.23^{+0.23}_{-0.53}$	$7.15^{+0.14}_{-0.21}$	$5.97^{+0.14}_{-0.21}$	$6.99^{+0.19}_{-0.33}$	$7.16^{+0.12}_{-0.16}$
log (S^{+++}/H^+)	...	$5.92^{+0.14}_{-0.20}$	...	...	...	...	...	...
log (N^+/O^+)	...	...	...	...	...	...	...	...
log (N^{++}/O^{++})	$-0.07^{+0.13}_{-0.18}$	$-0.36^{+0.17}_{-0.28}$	$-0.28^{+0.12}_{-0.16}$	$-0.27^{+0.28}_{-1.10}$	$-0.18^{+0.11}_{-0.15}$	$-0.31^{+0.16}_{-0.26}$	$-0.18^{+0.23}_{-0.54}$	$-0.19^{+0.09}_{-0.11}$
$T_{\rm eff}$ (10^3 K)	34.2 ± 0.3	36.2 ± 0.5	35.5 ± 0.3	39.0 ± 4.5	33.9 ± 0.4	41.6 ± 2.1	37.3 ± 3.4	34.5 ± 0.3
icf (N^+)	...	0.53 ± 0.06	...	0.31 ± 0.29	...	0.12 ± 0.03	0.45 ± 0.34	...
icf (N^{++})	0.10 ± 0.02	0.36 ± 0.05	0.25 ± 0.05	0.47 ± 0.21	0.09 ± 0.02	0.61 ± 0.03	0.40 ± 0.13	0.14 ± 0.03
log (N/H)	$8.57^{+0.13}_{-0.18}$	$8.35^{+0.17}_{-0.28}$	$8.62^{+0.11}_{-0.15}$	$7.71^{+0.28}_{-1.11}$	$8.37^{+0.14}_{-0.20}$	$8.28^{+0.16}_{-0.27}$	$9.02^{+0.23}_{-0.54}$	$8.50^{+0.11}_{-0.15}$
icf (O^+)	...	...	...	...	...	...	...	...
icf (O^{++})	0.05 ± 0.02	0.36 ± 0.09	0.20 ± 0.07	0.51 ± 0.30	0.04 ± 0.02	0.78 ± 0.08	0.42 ± 0.19	0.08 ± 0.03
log (O/H)	$8.97^{+0.17}_{-0.30}$	$8.72^{+0.15}_{-0.23}$	$9.00^{+0.16}_{-0.24}$	$7.14^{+0.26}_{-0.70}$	$8.92^{+0.21}_{-0.42}$	$8.06^{+0.12}_{-0.17}$	$8.85^{+0.24}_{-0.60}$	$8.95^{+0.18}_{-0.32}$
icf (S^+)	...	...	...	...	...	...	...	...
icf (S^{++})	0.75 ± 0.01	...	0.73 ± 0.01	0.58 ± 0.20	0.79 ± 0.02	0.39 ± 0.06	0.66 ± 0.18	0.77 ± 0.01
log (S/H)	$7.30^{+0.09}_{-0.12}$	$6.94^{+0.18}_{-0.33}$	$7.33^{+0.09}_{-0.11}$	$5.47^{+0.26}_{-0.74}$	$7.25^{+0.14}_{-0.21}$	$6.39^{+0.15}_{-0.23}$	$7.18^{+0.21}_{-0.42}$	$7.28^{+0.12}_{-0.16}$
log (N/O)	$-0.39^{+0.13}_{-0.18}$	$-0.35^{+0.17}_{-0.28}$	$-0.38^{+0.12}_{-0.16}$	$-0.23^{+0.28}_{-1.10}$	$-0.55^{+0.11}_{-0.15}$	$-0.21^{+0.16}_{-0.26}$	$-0.16^{+0.23}_{-0.54}$	$-0.45^{+0.09}_{-0.11}$

Property	G25.40−0.14	IR 18116	IR 18317	G23.95+0.15	G29.96−0.02	IR 18434	W43N	W43C	W43S
Reference	afflerbach97	peeters02	peeters02	simpson95	simpson95	peeters02	simpson95	simpson95	simpson95
R	4.20	4.29	4.48	4.50	4.50	4.55	4.70	4.70	4.70
n_e	1200 ± 120	753 ± 188	1543 ± 567	3500 ± 900	1500 ± 200	817 ± 215	800 ± 40	700 ± 50	700 ± 40
T_e (10^3 K)	6.7 ± 0.7	5.9 ± 0.6	5.9 ± 0.6	6.0 ± 0.6	6.1 ± 0.6	6.0 ± 0.6	6.5 ± 0.7	6.5 ± 0.7	6.5 ± 0.7
log (N^+/H^+)	...	$7.66^{+0.12}_{-0.16}$	$8.60^{+0.15}_{-0.23}$	...	...	$8.09^{+0.12}_{-0.16}$	...	...	...
log (N^{++}/H^+)	$7.38^{+0.07}_{-0.09}$	$7.01^{+0.12}_{-0.17}$	$7.60^{+0.15}_{-0.23}$	$7.77^{+0.13}_{-0.18}$	$7.70^{+0.10}_{-0.13}$	$7.70^{+0.12}_{-0.17}$	$7.78^{+0.09}_{-0.11}$	$8.07^{+0.09}_{-0.11}$	$8.03^{+0.09}_{-0.11}$
log (O^+/H^+)	...	...	...	...	...	...	...	...	...
log (O^{++}/H^+)	$7.51^{+0.07}_{-0.08}$	$7.31^{+0.11}_{-0.15}$	$7.70^{+0.15}_{-0.22}$	$7.79^{+0.13}_{-0.18}$	$7.97^{+0.10}_{-0.13}$	$8.02^{+0.12}_{-0.16}$	$8.06^{+0.09}_{-0.11}$	$8.40^{+0.09}_{-0.11}$	$8.32^{+0.09}_{-0.11}$
log (S^+/H^+)	...	...	...	...	...	...	...	...	...
log (S^{++}/H^+)	$6.98^{+0.17}_{-0.27}$	$6.22^{+0.13}_{-0.19}$	$7.04^{+0.16}_{-0.26}$	$7.14^{+0.13}_{-0.18}$	$6.66^{+0.11}_{-0.15}$	$6.89^{+0.13}_{-0.20}$	$7.09^{+0.09}_{-0.11}$	$7.25^{+0.09}_{-0.11}$	$7.20^{+0.09}_{-0.11}$
log (S^{+++}/H^+)	...	...	$5.01^{+0.17}_{-0.27}$	...	...	$5.53^{+0.12}_{-0.18}$	...	...	...
log (N^+/O^+)	...	...	...	...	...	...	...	...	...
log (N^{++}/O^{++})	$-0.13^{+0.09}_{-0.12}$	$-0.31^{+0.16}_{-0.25}$	$-0.09^{+0.20}_{-0.37}$	$-0.02^{+0.17}_{-0.29}$	$-0.27^{+0.14}_{-0.20}$	$-0.32^{+0.16}_{-0.26}$	$-0.28^{+0.12}_{-0.17}$	$-0.34^{+0.12}_{-0.17}$	$-0.29^{+0.12}_{-0.17}$
$T_{\rm eff}$ (10^3 K)	34.2 ± 0.4	35.5 ± 0.5	34.5 ± 0.5	34.4 ± 0.5	35.9 ± 0.4	35.6 ± 0.4	35.2 ± 0.3	35.7 ± 0.3	35.6 ± 0.3
icf (N^+)	...	0.59 ± 0.05	0.71 ± 0.08	...	...	0.58 ± 0.05	...	...	...
icf (N^{++})	0.12 ± 0.03	0.25 ± 0.08	0.14 ± 0.05	0.15 ± 0.04	0.33 ± 0.08	0.26 ± 0.07	0.21 ± 0.04	0.27 ± 0.05	0.25 ± 0.05
log (N/H)	$8.30^{+0.14}_{-0.20}$	$7.75^{+0.16}_{-0.26}$	$8.64^{+0.20}_{-0.38}$	$8.60^{+0.17}_{-0.29}$	$8.18^{+0.14}_{-0.21}$	$8.24^{+0.16}_{-0.26}$	$8.47^{+0.12}_{-0.17}$	$8.64^{+0.12}_{-0.16}$	$8.63^{+0.12}_{-0.16}$
icf (O^+)	...	...	...	...	...	...	...	...	...
icf (O^{++})	0.06 ± 0.03	0.19 ± 0.11	0.08 ± 0.05	0.08 ± 0.04	0.31 ± 0.14	0.21 ± 0.11	0.15 ± 0.05	0.22 ± 0.08	0.20 ± 0.07
log (O/H)	$8.76^{+0.24}_{-0.60}$	$8.03^{+0.27}_{-0.86}$	$8.81^{+0.29}_{-1.34}$	$8.91^{+0.28}_{-0.96}$	$8.48^{+0.21}_{-0.44}$	$8.70^{+0.25}_{-0.65}$	$8.90^{+0.17}_{-0.29}$	$9.06^{+0.17}_{-0.27}$	$9.01^{+0.16}_{-0.26}$

TABLE 6—*Continued*

Property	G25.40−0.14	IR 18116	IR 18317	G23.95+0.15	G29.96−0.02	IR 18434	W43N	W43C	W43S
icf (S^+)	...	...	...	...	...	...	...	...	...
icf (S^{++})	0.79 ± 0.02	0.73 ± 0.02	...	0.81 ± 0.03	0.71 ± 0.02	...	0.74 ± 0.01	0.72 ± 0.01	0.73 ± 0.01
log (S/H)	$7.08^{+0.17}_{-0.28}$	$6.35^{+0.13}_{-0.19}$	$7.04^{+0.22}_{-0.45}$	$7.24^{+0.13}_{-0.18}$	$6.80^{+0.11}_{-0.15}$	$6.91^{+0.17}_{-0.29}$	$7.23^{+0.09}_{-0.11}$	$7.39^{+0.09}_{-0.11}$	$7.34^{+0.09}_{-0.11}$
log (N/O)	$-0.45^{+0.09}_{-0.12}$	$-0.41^{+0.16}_{-0.25}$	$-0.36^{+0.20}_{-0.37}$	$-0.31^{+0.17}_{-0.29}$	$-0.30^{+0.14}_{-0.20}$	$-0.41^{+0.16}_{-0.26}$	$-0.43^{+0.12}_{-0.17}$	$-0.42^{+0.12}_{-0.17}$	$-0.39^{+0.12}_{-0.17}$

Property	IR 18502	IR 18469	RCW 166-1	G8.14+0.23	G25.38−0.18	G25.38−0.18	S38	IR 17591
Reference	peeters02	peeters02	shaver83	afflerbach97	afflerbach97	simpson95	shaver83	peeters02
R	4.74	4.83	5.00	5.20	5.20	5.20	5.50	5.53
n_e	1181 ± 334	146 ± 55	1000 ± 100	800 ± 80	1200 ± 120	1600 ± 200	100 ± 10	462 ± 121
T_e (10^3 K)	6.0 ± 0.6	6.1 ± 0.6	4.8 ± 0.5	7.2 ± 0.7	6.7 ± 0.7	6.0 ± 0.6	5.5 ± 0.6	6.3 ± 0.6
log (N^+/H^+)	...	$8.79^{+0.17}_{-0.27}$	$8.43^{+0.12}_{-0.16}$	...	...	...	$8.14^{+0.11}_{-0.15}$	$7.49^{+0.12}_{-0.16}$
log (N^{++}/H^+)	$7.26^{+0.13}_{-0.19}$	$8.37^{+0.18}_{-0.30}$	...	$7.37^{+0.08}_{-0.09}$	$7.79^{+0.07}_{-0.08}$	$8.13^{+0.10}_{-0.13}$	...	$7.04^{+0.13}_{-0.18}$
log (O^+/H^+)	...	...	...	...	...	...	$9.58^{+0.17}_{-0.28}$	...
log (O^{++}/H^+)	$7.67^{+0.12}_{-0.17}$	$8.74^{+0.16}_{-0.26}$	...	$7.66^{+0.07}_{-0.08}$	$8.11^{+0.06}_{-0.07}$	$8.47^{+0.10}_{-0.13}$	$8.17^{+0.23}_{-0.50}$	$7.98^{+0.12}_{-0.16}$
log (S^+/H^+)	...	...	$6.74^{+0.11}_{-0.16}$	...	...	...	$6.72^{+0.14}_{-0.21}$	...
log (S^{++}/H^+)	$6.51^{+0.14}_{-0.20}$	$7.12^{+0.18}_{-0.31}$	...	$6.91^{+0.10}_{-0.13}$	$6.97^{+0.08}_{-0.09}$	$7.22^{+0.10}_{-0.13}$	...	$5.50^{+0.14}_{-0.21}$
log (S^{+++}/H^+)	$5.37^{+0.13}_{-0.20}$	...	...	...	...	...	...	...
log (N^+/O^+)	...	...	...	...	...	...	$-1.44^{+0.19}_{-0.36}$	...
log (N^{++}/O^{++})	$-0.41^{+0.17}_{-0.29}$	$-0.37^{+0.22}_{-0.49}$	...	$-0.29^{+0.10}_{-0.12}$	$-0.33^{+0.09}_{-0.11}$	$-0.34^{+0.13}_{-0.19}$	...	$-0.94^{+0.16}_{-0.27}$
$T_{\rm eff}$ (10^3 K)	35.6 ± 0.5	38.8 ± 3.2	36.0 ± 2.0	34.8 ± 0.3	35.6 ± 0.2	35.8 ± 0.3	34.9 ± 0.6	50.3 ± 2.0
icf (N^+)	...	0.31 ± 0.22	0.53 ± 0.22	...	...	...	0.71 ± 0.07	0.06 ± 0.00
icf (N^{++})	0.27 ± 0.09	0.46 ± 0.14	...	0.16 ± 0.03	0.27 ± 0.04	0.31 ± 0.06	...	0.57 ± 0.01
log (N/H)	$7.83^{+0.18}_{-0.32}$	$8.93^{+0.23}_{-0.50}$	$8.71^{+0.21}_{-0.41}$	$8.18^{+0.10}_{-0.14}$	$8.36^{+0.09}_{-0.11}$	$8.64^{+0.13}_{-0.18}$	$8.29^{+0.12}_{-0.16}$	$7.63^{+0.17}_{-0.27}$
icf (O^+)	...	...	...	...	...	...	0.73 ± 0.07	...
icf (O^{++})	0.22 ± 0.13	0.51 ± 0.21	...	0.09 ± 0.03	0.22 ± 0.06	0.27 ± 0.10	0.09 ± 0.07	0.89 ± 0.01
log (O/H)	$8.32^{+0.27}_{-0.83}$	$9.03^{+0.23}_{-0.51}$	...	$8.70^{+0.15}_{-0.23}$	$8.78^{+0.12}_{-0.17}$	$9.03^{+0.18}_{-0.32}$	$9.60^{+0.26}_{-0.77}$	$8.03^{+0.12}_{-0.16}$
icf (S^+)	...	...	0.07 ± 0.02	...	...	...	0.15 ± 0.02	...
icf (S^{++})	...	0.57 ± 0.16	...	0.76 ± 0.01	0.73 ± 0.01	0.72 ± 0.02	...	0.22 ± 0.01
log (S/H)	$6.54^{+0.18}_{-0.32}$	$7.36^{+0.20}_{-0.39}$	$7.92^{+0.18}_{-0.31}$	$7.03^{+0.10}_{-0.13}$	$7.10^{+0.08}_{-0.09}$	$7.36^{+0.10}_{-0.13}$	$7.55^{+0.15}_{-0.22}$	$6.15^{+0.14}_{-0.22}$
log (N/O)	$-0.50^{+0.17}_{-0.29}$	$-0.33^{+0.22}_{-0.49}$	...	$-0.52^{+0.10}_{-0.12}$	$-0.41^{+0.09}_{-0.11}$	$-0.39^{+0.13}_{-0.19}$	$-1.43^{+0.19}_{-0.36}$	$-0.75^{+0.16}_{-0.27}$

Property	G333.61−0.21	G339.1−0.4	S48	G37.87−0.40	RCW 117	RCW 121	IR 19207	G45.13+0.14 A
Reference	simpson95	shaver83	shaver83	afflerbach97	shaver83	shaver83	peeters02	simpson95
R	5.80	5.80	5.80	5.90	6.00	6.00	6.06	6.20
n_e	4600 ± 400	630 ± 63	100 ± 10	1100 ± 110	1580 ± 158	790 ± 79	485 ± 128	2000 ± 500
T_e (10^3 K)	6.2 ± 0.6	4.8 ± 0.5	4.8 ± 0.5	8.7 ± 0.9	6.4 ± 0.6	4.9 ± 0.5	6.5 ± 0.7	7.9 ± 0.8
log (N^+/H^+)	...	$8.35^{+0.11}_{-0.15}$	$8.23^{+0.12}_{-0.16}$	...	$7.99^{+0.11}_{-0.14}$	$8.21^{+0.14}_{-0.22}$	$7.07^{+0.12}_{-0.17}$	...
log (N^{++}/H^+)	$7.43^{+0.09}_{-0.12}$	...	...	$7.07^{+0.07}_{-0.09}$	...	...	$7.16^{+0.13}_{-0.18}$	$6.89^{+0.14}_{-0.21}$
log (O^+/H^+)	...	...	$9.35^{+0.18}_{-0.31}$	...	...	...	...	...
log (O^{++}/H^+)	$7.72^{+0.09}_{-0.12}$	$8.58^{+0.19}_{-0.34}$	$9.24^{+0.20}_{-0.37}$	$7.59^{+0.06}_{-0.07}$	$8.71^{+0.14}_{-0.20}$	$9.02^{+0.22}_{-0.48}$	$7.79^{+0.11}_{-0.15}$	$7.46^{+0.13}_{-0.18}$
log (S^+/H^+)	...	$6.99^{+0.11}_{-0.15}$	$6.83^{+0.12}_{-0.16}$	...	$6.22^{+0.10}_{-0.14}$	$6.33^{+0.11}_{-0.14}$	...	...
log (S^{++}/H^+)	$6.68^{+0.09}_{-0.11}$	...	...	$6.23^{+0.13}_{-0.18}$	...	...	$5.44^{+0.14}_{-0.21}$	$6.02^{+0.13}_{-0.19}$
log (S^{+++}/H^+)	...	...	...	...	...	...	$5.90^{+0.12}_{-0.17}$	...
log (N^+/O^+)	...	...	$-1.12^{+0.20}_{-0.40}$	...	...	...	...	...
log (N^{++}/O^{++})	$-0.29^{+0.12}_{-0.17}$	...	...	$-0.52^{+0.09}_{-0.12}$	...	...	$-0.63^{+0.16}_{-0.26}$	$-0.57^{+0.18}_{-0.31}$

TABLE 6—*Continued*

Property	G333.61−0.21	G339.1−0.4	S48	G37.87−0.40	RCW 117	RCW 121	IR 19207	G45.13+0.14 A
$T_{\rm eff}$ (10^3 K)	35.2 ± 0.3	34.6 ± 0.5	38.9 ± 3.1	36.0 ± 0.4	36.1 ± 0.4	38.7 ± 3.6	50.3 ± 2.0	36.2 ± 0.5
icf (N^+)	...	0.71 ± 0.07	0.32 ± 0.21	...	0.50 ± 0.05	0.25 ± 0.25	0.06 ± 0.00	...
icf (N^{++})	0.24 ± 0.05	...	...	0.35 ± 0.06	...	...	0.57 ± 0.01	0.39 ± 0.05
log (N/H)	$8.05^{+0.12}_{-0.17}$	$8.50^{+0.12}_{-0.16}$	$8.72^{+0.25}_{-0.65}$	$7.53^{+0.10}_{-0.14}$	$8.29^{+0.11}_{-0.15}$	$8.81^{+0.27}_{-0.81}$	$7.42^{+0.16}_{-0.27}$	$7.29^{+0.15}_{-0.23}$
icf (O^+)	...	...	0.34 ± 0.22	...	...	...	...	...
icf (O^{++})	0.18 ± 0.07	0.08 ± 0.05	0.50 ± 0.20	0.34 ± 0.11	0.37 ± 0.11	0.57 ± 0.25	0.89 ± 0.01	0.41 ± 0.09
log (O/H)	$8.48^{+0.18}_{-0.31}$	$9.67^{+0.29}_{-1.44}$	$9.60^{+0.25}_{-0.63}$	$8.06^{+0.15}_{-0.22}$	$9.13^{+0.17}_{-0.29}$	$9.27^{+0.26}_{-0.73}$	$7.84^{+0.11}_{-0.15}$	$7.84^{+0.15}_{-0.23}$
icf (S^+)	...	0.10 ± 0.01	0.09 ± 0.02	...	0.06 ± 0.00	0.05 ± 0.02	...	...
icf (S^{++})	0.76 ± 0.02	...	...	0.71 ± 0.02	...	...	...	0.70 ± 0.04
log (S/H)	$6.80^{+0.09}_{-0.12}$	$8.00^{+0.11}_{-0.16}$	$7.87^{+0.15}_{-0.23}$	$6.38^{+0.13}_{-0.18}$	$7.46^{+0.11}_{-0.14}$	$7.59^{+0.16}_{-0.25}$	$6.03^{+0.18}_{-0.31}$	$6.17^{+0.13}_{-0.19}$
log (N/O)	$-0.43^{+0.12}_{-0.17}$	...	$-1.10^{+0.20}_{-0.40}$	$-0.53^{+0.09}_{-0.12}$	...	...	$-0.44^{+0.16}_{-0.26}$	$-0.55^{+0.18}_{-0.31}$

Property	G326.7+0.6	W31 B2	W31 B4	G45.45+0.06	RCW 94-1	RCW 94-2	G326.5+0.9	Omega (M17)
Reference	shaver83	simpson95	simpson95	simpson95	shaver83	shaver83	shaver83	shaver83
R	6.20	6.30	6.30	6.30	6.30	6.30	6.40	6.40
n_e	630 ± 63	500 ± 60	1000 ± 100	1000 ± 100	100 ± 10	100 ± 10	1000 ± 100	1000 ± 100
T_e (10^3 K)	6.9 ± 0.7	6.8 ± 0.7	6.8 ± 0.7	7.2 ± 0.7	3.9 ± 0.4	5.1 ± 0.5	6.8 ± 0.7	7.0 ± 0.7
log (N^+/H^+)	$7.77^{+0.10}_{-0.14}$	...	...	...	$8.38^{+0.15}_{-0.24}$	$8.19^{+0.11}_{-0.16}$	$8.04^{+0.11}_{-0.14}$	$7.06^{+0.12}_{-0.16}$
log (N^{++}/H^+)	...	$7.86^{+0.10}_{-0.13}$	$7.93^{+0.09}_{-0.12}$	$7.67^{+0.10}_{-0.12}$	...	...	...	...
log (O^+/H^+)	...	...	...	...	...	$8.99^{+0.17}_{-0.29}$	...	$8.32^{+0.13}_{-0.20}$
log (O^{++}/H^+)	$8.38^{+0.17}_{-0.28}$	$8.05^{+0.10}_{-0.13}$	$8.11^{+0.09}_{-0.12}$	$8.24^{+0.09}_{-0.12}$	$9.15^{+0.26}_{-0.70}$	$8.81^{+0.24}_{-0.59}$	...	$8.70^{+0.12}_{-0.17}$
log (S^+/H^+)	$6.20^{+0.10}_{-0.13}$	...	...	...	$6.73^{+0.12}_{-0.16}$	$6.61^{+0.11}_{-0.15}$	$6.31^{+0.11}_{-0.14}$	$5.98^{+0.10}_{-0.13}$
log (S^{++}/H^+)	...	$7.18^{+0.10}_{-0.13}$	$7.13^{+0.09}_{-0.12}$	$6.98^{+0.10}_{-0.12}$	...	...	...	...
log (S^{+++}/H^+)	...	...	...	...	...	...	...	...
log (N^+/O^+)	...	...	...	...	...	$-0.80^{+0.20}_{-0.37}$	...	$-1.26^{+0.17}_{-0.28}$
log (N^{++}/O^{++})	...	$-0.19^{+0.14}_{-0.20}$	$-0.17^{+0.13}_{-0.18}$	$-0.57^{+0.13}_{-0.18}$	...	...	...	...
$T_{\rm eff}$ (10^3 K)	35.8 ± 0.4	35.1 ± 0.3	35.2 ± 0.3	35.8 ± 0.3	39.1 ± 4.1	36.6 ± 3.8	36.0 ± 2.0	38.7 ± 2.1
icf (N^+)	0.56 ± 0.05	...	...	...	0.31 ± 0.27	0.53 ± 0.42	0.53 ± 0.22	0.24 ± 0.14
icf (N^{++})	...	0.18 ± 0.04	0.21 ± 0.04	0.31 ± 0.06	...	...	...	...
log (N/H)	$8.02^{+0.11}_{-0.14}$	$8.61^{+0.13}_{-0.19}$	$8.60^{+0.12}_{-0.17}$	$8.19^{+0.12}_{-0.17}$	$8.89^{+0.26}_{-0.75}$	$8.47^{+0.21}_{-0.43}$	$8.32^{+0.20}_{-0.39}$	$7.68^{+0.26}_{-0.78}$
icf (O^+)	...	...	...	...	...	0.55 ± 0.44	...	0.25 ± 0.15
icf (O^{++})	0.25 ± 0.13	0.12 ± 0.05	0.15 ± 0.05	0.27 ± 0.10	0.51 ± 0.28	0.38 ± 0.19	...	0.58 ± 0.14
log (O/H)	$8.98^{+0.27}_{-0.87}$	$8.98^{+0.19}_{-0.34}$	$8.93^{+0.17}_{-0.29}$	$8.80^{+0.17}_{-0.29}$	$9.44^{+0.28}_{-0.99}$	$9.21^{+0.28}_{-0.96}$	...	$8.85^{+0.17}_{-0.29}$
icf (S^+)	0.08 ± 0.01	...	...	...	0.09 ± 0.03	0.11 ± 0.03	0.07 ± 0.02	0.05 ± 0.01
icf (S^{++})	...	0.74 ± 0.01	0.74 ± 0.01	0.72 ± 0.01	...	...	...	...
log (S/H)	$7.30^{+0.11}_{-0.14}$	$7.31^{+0.10}_{-0.13}$	$7.26^{+0.09}_{-0.12}$	$7.13^{+0.10}_{-0.12}$	$7.77^{+0.17}_{-0.28}$	$7.57^{+0.16}_{-0.26}$	$7.49^{+0.17}_{-0.30}$	$7.27^{+0.12}_{-0.16}$
log (N/O)	...	$-0.37^{+0.14}_{-0.20}$	$-0.32^{+0.13}_{-0.18}$	$-0.61^{+0.13}_{-0.18}$	...	$-0.78^{+0.20}_{-0.37}$	...	$-1.24^{+0.17}_{-0.28}$

Property	RCW 122	NCG 6604-1	NGC 6604-3	S54	M16	M16	G5.97−1.18	W51e
Reference	shaver83	shaver83	shaver83	caplan00	caplan00	shaver83	afflerbach97	simpson95
R	6.50	6.50	6.50	6.55	6.60	6.60	6.70	6.80
n_e	790 ± 79	15 ± 1	199 ± 19	245 ± 24	71 ± 7	630 ± 63	1400 ± 140	1600 ± 200
T_e (10^3 K)	6.1 ± 0.6	5.7 ± 0.6	7.0 ± 0.7	6.6 ± 0.7	6.8 ± 0.7	6.6 ± 0.7	6.7 ± 0.7	7.1 ± 0.7
log (N^+/H^+)	$8.13^{+0.11}_{-0.14}$	$7.89^{+0.11}_{-0.15}$	$7.63^{+0.10}_{-0.13}$	...	...	$7.46^{+0.10}_{-0.13}$	...	...
log (N^{++}/H^+)	...	...	...	...	...	...	$7.52^{+0.07}_{-0.09}$	$7.69^{+0.10}_{-0.13}$

TABLE 6—*Continued*

Property	RCW 122	NCG 6604-1	NGC 6604-3	S54	M16	M16	G5.97−1.18	W51e
log (O^+/H^+)	$9.13^{+0.15}_{-0.22}$	$8.92^{+0.17}_{-0.28}$	$8.59^{+0.15}_{-0.24}$	$8.47^{+0.14}_{-0.20}$	$8.13^{+0.13}_{-0.20}$	$8.55^{+0.14}_{-0.21}$	...	...
log (O^{++}/H^+)	$8.19^{+0.19}_{-0.33}$	$8.61^{+0.15}_{-0.24}$	$8.28^{+0.13}_{-0.18}$	$7.99^{+0.17}_{-0.27}$	$8.28^{+0.16}_{-0.26}$	$8.45^{+0.13}_{-0.18}$	$8.16^{+0.06}_{-0.07}$	$8.20^{+0.10}_{-0.13}$
log (S^+/H^+)	$6.46^{+0.11}_{-0.14}$	$6.40^{+0.11}_{-0.14}$	$6.07^{+0.10}_{-0.13}$	...	...	$6.01^{+0.10}_{-0.13}$	...	...
log (S^{++}/H^+)	...	$7.29^{+0.20}_{-0.39}$	...	...	...	...	$6.98^{+0.08}_{-0.09}$	$6.78^{+0.10}_{-0.13}$
log (S^{+++}/H^+)	...	...	...	...	...	...	...	...
log (N^+/O^+)	$-1.01^{+0.17}_{-0.29}$	$-1.03^{+0.19}_{-0.35}$	$-0.97^{+0.17}_{-0.29}$	...	...	$-1.09^{+0.17}_{-0.27}$	...	...
log (N^{++}/O^{++})	...	...	...	...	...	...	$-0.64^{+0.09}_{-0.12}$	$-0.51^{+0.13}_{-0.19}$
T_{eff} (10^3 K)	34.8 ± 0.5	36.7 ± 4.2	36.2 ± 0.3	36.0 ± 2.0	36.0 ± 2.0	36.3 ± 0.3	35.6 ± 0.2	36.2 ± 0.3
icf (N^+)	0.67 ± 0.06	0.60 ± 0.38	0.56 ± 0.04	...	...	0.51 ± 0.05	...	...
icf (N^{++})	...	...	...	...	...	...	0.28 ± 0.05	0.38 ± 0.04
log (N/H)	$8.30^{+0.11}_{-0.15}$	$8.11^{+0.20}_{-0.37}$	$7.88^{+0.10}_{-0.13}$	...	...	$7.76^{+0.10}_{-0.14}$	$8.07^{+0.10}_{-0.13}$	$8.11^{+0.10}_{-0.14}$
icf (O^+)	0.71 ± 0.07	0.62 ± 0.39	0.58 ± 0.04	0.59 ± 0.22	0.63 ± 0.20	0.53 ± 0.05	...	...
icf (O^{++})	0.10 ± 0.06	0.32 ± 0.19	0.33 ± 0.06	0.28 ± 0.60	0.25 ± 0.55	0.42 ± 0.02	0.23 ± 0.07	0.39 ± 0.07
log (O/H)	$9.18^{+0.22}_{-0.48}$	$9.09^{+0.21}_{-0.44}$	$8.77^{+0.19}_{-0.34}$	$8.59^{+0.20}_{-0.39}$	$8.51^{+0.20}_{-0.38}$	$8.81^{+0.18}_{-0.32}$	$8.79^{+0.13}_{-0.19}$	$8.61^{+0.12}_{-0.16}$
icf (S^+)	0.09 ± 0.01	...	0.10 ± 0.00	...	...	0.07 ± 0.00	...	...
icf (S^{++})	...	...	...	...	...	...	0.73 ± 0.01	0.70 ± 0.02
log (S/H)	$7.51^{+0.11}_{-0.15}$	$7.34^{+0.22}_{-0.47}$	$7.08^{+0.10}_{-0.13}$	...	...	$7.16^{+0.10}_{-0.13}$	$7.12^{+0.08}_{-0.09}$	$6.94^{+0.10}_{-0.13}$
log (N/O)	$-0.98^{+0.17}_{-0.29}$	$-1.01^{+0.19}_{-0.35}$	$-0.95^{+0.17}_{-0.29}$	...	...	$-1.07^{+0.17}_{-0.27}$	$-0.72^{+0.09}_{-0.12}$	$-0.50^{+0.13}_{-0.19}$

Property	IR 18479	IR 18032	G32.80+0.19	S93	S88B	S88	Lambda Cen-1	Lambda Cen-2
Reference	peeters02	peeters02	afflerbach97	caplan00	afflerbach97	caplan00	shaver83	shaver83
R	7.53	7.55	7.60	7.65	7.70	7.70	7.70	7.70
n_e	836 ± 339	512 ± 214	2500 ± 250	269 ± 26	5750 ± 575	99 ± 9	400 ± 40	100 ± 10
T_e (10^3 K)	7.1 ± 0.7	7.1 ± 0.7	10.8 ± 1.1	7.1 ± 0.7	9.8 ± 1.0	7.1 ± 0.7	6.8 ± 0.7	6.8 ± 0.7
log (N^+/H^+)	...	$8.15^{+0.17}_{-0.29}$	...	...	...	...	$7.72^{+0.10}_{-0.13}$	$7.30^{+0.10}_{-0.14}$
log (N^{++}/H^+)	$6.79^{+0.18}_{-0.32}$	$7.42^{+0.18}_{-0.30}$	$7.24^{+0.10}_{-0.13}$	...	$7.19^{+0.12}_{-0.16}$	...	...	...
log (O^+/H^+)	...	...	...	$8.49^{+0.13}_{-0.19}$	...	$8.44^{+0.15}_{-0.22}$	$8.82^{+0.15}_{-0.23}$	$8.53^{+0.16}_{-0.25}$
log (O^{++}/H^+)	$7.61^{+0.16}_{-0.25}$	$7.63^{+0.17}_{-0.27}$	$7.53^{+0.07}_{-0.08}$	$7.60^{+0.16}_{-0.25}$	$7.69^{+0.07}_{-0.08}$	$7.52^{+0.16}_{-0.25}$	$8.24^{+0.13}_{-0.19}$	$8.47^{+0.13}_{-0.19}$
log (S^+/H^+)	...	...	...	...	...	...	$6.34^{+0.10}_{-0.13}$	$5.77^{+0.10}_{-0.13}$
log (S^{++}/H^+)	$5.56^{+0.19}_{-0.35}$	$6.67^{+0.18}_{-0.33}$	$6.58^{+0.20}_{-0.38}$	...	$6.41^{+0.15}_{-0.24}$	...	...	...
log (S^{+++}/H^+)	...	...	...	...	...	...	...	...
log (N^+/O^+)	...	...	...	...	...	...	$-1.10^{+0.17}_{-0.29}$	$-1.22^{+0.18}_{-0.31}$
log (N^{++}/O^{++})	$-0.83^{+0.23}_{-0.49}$	$-0.21^{+0.23}_{-0.49}$	$-0.28^{+0.12}_{-0.16}$	...	$0.50^{+0.13}_{-0.19}$	...	...	...
T_{eff} (10^3 K)	42.3 ± 9.3	35.2 ± 0.6	35.1 ± 0.6	36.0 ± 2.0	35.7 ± 0.4	36.0 ± 2.0	35.4 ± 0.4	42.8 ± 5.7
icf (N^+)	...	0.63 ± 0.08	...	...	...	...	0.62 ± 0.04	0.16 ± 0.06
icf (N^{++})	0.62 ± 0.04	0.20 ± 0.09	0.21 ± 0.08	...	0.32 ± 0.08	...	...	...
log (N/H)	$6.99^{+0.18}_{-0.32}$	$8.22^{+0.23}_{-0.52}$	$7.92^{+0.19}_{-0.33}$	...	$7.68^{+0.15}_{-0.23}$	...	$7.92^{+0.10}_{-0.14}$	$8.10^{+0.18}_{-0.31}$
icf (O^+)	...	...	...	0.59 ± 0.22	...	0.62 ± 0.20	0.65 ± 0.04	0.17 ± 0.07
icf (O^{++})	0.82 ± 0.11	0.14 ± 0.11	0.14 ± 0.10	0.29 ± 0.60	0.29 ± 0.14	0.26 ± 0.56	0.16 ± 0.07	0.74 ± 0.09
log (O/H)	$7.70^{+0.16}_{-0.27}$	$8.48^{+0.28}_{-1.12}$	$8.37^{+0.27}_{-0.93}$	$8.54^{+0.20}_{-0.36}$	$8.23^{+0.21}_{-0.44}$	$8.49^{+0.20}_{-0.40}$	$8.92^{+0.19}_{-0.34}$	$8.80^{+0.19}_{-0.36}$
icf (S^+)	...	...	...	...	...	...	0.09 ± 0.01	0.07 ± 0.02
icf (S^{++})	0.34 ± 0.20	0.74 ± 0.02	0.76 ± 0.04	...	0.72 ± 0.03	...	...	...
log (S/H)	$6.03^{+0.27}_{-0.81}$	$6.81^{+0.18}_{-0.33}$	$6.70^{+0.20}_{-0.38}$	...	$6.55^{+0.15}_{-0.24}$	...	$7.36^{+0.10}_{-0.14}$	$6.93^{+0.16}_{-0.26}$
log (N/O)	$-0.71^{+0.23}_{-0.49}$	$-0.36^{+0.23}_{-0.49}$	$-0.45^{+0.12}_{-0.16}$	...	$-0.55^{+0.13}_{-0.19}$	...	$-1.08^{+0.17}_{-0.29}$	$-1.21^{+0.18}_{-0.31}$

TABLE 6—*Continued*

Property	NGC 3576	NGC 3576	S101	Carina-2	S104	S98	G81.7+0.5 (DR21)	DR21	S112
Reference	simpson95	shaver83	caplan00	shaver83	caplan00	vilchez96ind	afflerbach97	peeters02	caplan00
R	7.92	7.92	8.10	8.11	8.40	8.40	8.50	8.50	8.50
n_e	8400 ± 2300	1260 ± 126	7 ± 0	630 ± 63	56 ± 5	100 ± 10	2100 ± 210	320 ± 114	66 ± 6
T_e (10^3 K)	7.5 ± 0.8	8.0 ± 0.8	7.3 ± 0.7	7.8 ± 0.8	7.4 ± 0.7	10.0 ± 1.0	9.3 ± 0.9	7.4 ± 0.7	7.4 ± 0.7
log (N^+/H^+)	...	$7.13^{+0.11}_{-0.15}$	...	$7.41^{+0.12}_{-0.16}$	...	$6.89^{+0.08}_{-0.10}$	...	...	...
log (N^{++}/H^+)	$7.67^{+0.13}_{-0.19}$	...	...	...	...	...	$6.77^{+0.08}_{-0.10}$	...	...
log (O^+/H^+)	...	...	$8.00^{+0.13}_{-0.19}$	$8.32^{+0.14}_{-0.20}$	$8.24^{+0.13}_{-0.19}$	$8.18^{+0.13}_{-0.19}$	...	...	$8.13^{+0.13}_{-0.19}$
log (O^{++}/H^+)	$8.45^{+0.13}_{-0.19}$	$8.52^{+0.12}_{-0.16}$	$8.02^{+0.16}_{-0.25}$	$8.42^{+0.14}_{-0.22}$	$8.10^{+0.16}_{-0.25}$	$7.19^{+0.16}_{-0.26}$	$6.94^{+0.07}_{-0.08}$	$6.55^{+0.15}_{-0.23}$	$8.12^{+0.16}_{-0.24}$
log (S^+/H^+)	...	$5.69^{+0.10}_{-0.12}$	...	$6.05^{+0.10}_{-0.13}$	...	$6.03^{+0.08}_{-0.10}$	...	...	...
log (S^{++}/H^+)	$6.87^{+0.13}_{-0.19}$	$6.94^{+0.17}_{-0.28}$	...	$6.97^{+0.17}_{-0.29}$	...	$6.14^{+0.10}_{-0.12}$	$6.49^{+0.23}_{-0.55}$	$4.73^{+0.17}_{-0.29}$	...
log (S^{+++}/H^+)	...	...	...	...	...	...	...	...	...
log (N^+/O^+)	...	...	...	$-0.91^{+0.17}_{-0.29}$	...	$-1.29^{+0.15}_{-0.24}$	...	...	...
log (N^{++}/O^{++})	$-0.79^{+0.17}_{-0.30}$	...	...	...	...	...	$-0.16^{+0.10}_{-0.13}$	...	...
$T_{\rm eff}$ (10^3 K)	36.5 ± 1.8	37.2 ± 2.2	36.0 ± 2.0	36.3 ± 2.0	36.0 ± 2.0	35.6 ± 0.5	34.0 ± 0.7	40.3 ± 2.8	36.0 ± 2.0
icf (N^+)	...	0.36 ± 0.24	...	0.51 ± 0.27	...	0.64 ± 0.05	...	...	...
icf (N^{++})	0.46 ± 0.05	...	...	...	...	...	0.11 ± 0.05	...	...
log (N/H)	$8.00^{+0.14}_{-0.20}$	$7.57^{+0.24}_{-0.59}$	...	$7.71^{+0.22}_{-0.46}$	...	$7.09^{+0.09}_{-0.11}$	$7.73^{+0.22}_{-0.45}$	...	...
icf (O^+)	...	...	0.70 ± 0.15	0.53 ± 0.29	0.64 ± 0.19	0.66 ± 0.05	...	...	0.63 ± 0.20
icf (O^{++})	0.54 ± 0.10	0.50 ± 0.13	0.19 ± 0.44	0.42 ± 0.11	0.25 ± 0.54	0.17 ± 0.10	0.05 ± 0.04	0.65 ± 0.23	0.25 ± 0.55
log (O/H)	$8.72^{+0.15}_{-0.22}$	$8.83^{+0.15}_{-0.23}$	$8.31^{+0.19}_{-0.36}$	$8.67^{+0.19}_{-0.34}$	$8.48^{+0.19}_{-0.35}$	$8.22^{+0.20}_{-0.38}$	$8.25^{+0.29}_{-1.39}$	$6.74^{+0.20}_{-0.38}$	$8.43^{+0.19}_{-0.35}$
icf (S^+)	...	...	...	...	...	...	...	...	...
icf (S^{++})	0.66 ± 0.20	...	...	...	...	...	0.82 ± 0.04	0.47 ± 0.13	...
log (S/H)	$7.05^{+0.17}_{-0.30}$	$6.96^{+0.18}_{-0.33}$	...	$7.02^{+0.19}_{-0.35}$	...	$6.39^{+0.12}_{-0.17}$	$6.58^{+0.23}_{-0.55}$	$5.07^{+0.20}_{-0.38}$	...
log (N/O)	$-0.72^{+0.17}_{-0.30}$	...	...	$-0.89^{+0.17}_{-0.29}$	...	$-1.27^{+0.15}_{-0.24}$	$-0.52^{+0.10}_{-0.13}$	...	...

Property	S117	RCW 40	G75.84+0.40	S131	RCW 38-1	RCW 38-2	NGC 3603 P1	NGC 3603 P2
Reference	caplan00	shaver83	afflerbach97	caplan00	shaver83	shaver83	simpson95	simpson95
R	8.50	8.66	8.70	8.70	8.70	8.70	8.80	8.80
n_e	16 ± 1	125 ± 12	2100 ± 210	18 ± 1	2511 ± 251	10000 ± 1000	1100 ± 50	1100 ± 40
T_e (10^3 K)	6.8 ± 0.7	6.9 ± 0.7	8.8 ± 0.9	7.5 ± 0.7	7.4 ± 0.7	7.4 ± 0.7	6.9 ± 0.7	6.9 ± 0.7
log (N^+/H^+)	...	$7.62^{+0.10}_{-0.13}$	...	...	$7.41^{+0.12}_{-0.16}$	$7.04^{+0.13}_{-0.18}$	...	...
log (N^{++}/H^+)	...	...	$7.34^{+0.07}_{-0.08}$	...	...	...	$7.82^{+0.09}_{-0.11}$	$7.82^{+0.09}_{-0.11}$
log (O^+/H^+)	$8.27^{+0.14}_{-0.20}$	$8.76^{+0.15}_{-0.24}$	...	$8.11^{+0.13}_{-0.19}$	...	...	...	...
log (O^{++}/H^+)	$8.31^{+0.16}_{-0.27}$	$8.10^{+0.13}_{-0.19}$	$7.94^{+0.06}_{-0.07}$	$8.06^{+0.15}_{-0.24}$	$8.58^{+0.12}_{-0.17}$	$8.65^{+0.12}_{-0.17}$	$8.58^{+0.09}_{-0.11}$	$8.61^{+0.09}_{-0.11}$
log (S^+/H^+)	...	$6.26^{+0.10}_{-0.13}$	...	...	$5.96^{+0.10}_{-0.13}$	$6.04^{+0.10}_{-0.12}$	...	...
log (S^{++}/H^+)	...	$7.02^{+0.19}_{-0.33}$	$6.49^{+0.08}_{-0.09}$	...	$7.01^{+0.17}_{-0.29}$	$7.49^{+0.17}_{-0.29}$	$7.00^{+0.09}_{-0.11}$	$6.98^{+0.09}_{-0.11}$
log (S^{+++}/H^+)	...	...	...	...	...	...	...	...
log (N^+/O^+)	...	$-1.14^{+0.18}_{-0.30}$	...	...	...	...	...	...
log (N^{++}/O^{++})	...	...	$-0.61^{+0.09}_{-0.11}$	...	...	...	$-0.76^{+0.12}_{-0.16}$	$-0.79^{+0.12}_{-0.16}$
$T_{\rm eff}$ (10^3 K)	36.0 ± 2.0	35.6 ± 0.6	36.2 ± 0.2	36.0 ± 2.0	36.8 ± 2.3	35.4 ± 0.5	37.3 ± 1.2	37.8 ± 1.3
icf (N^+)	...	0.63 ± 0.06	...	...	0.40 ± 0.29	0.54 ± 0.07	...	...
icf (N^{++})	...	...	0.40 ± 0.02	...	...	...	0.44 ± 0.04	0.46 ± 0.05
log (N/H)	...	$7.82^{+0.11}_{-0.14}$	$7.74^{+0.07}_{-0.08}$	...	$7.81^{+0.24}_{-0.56}$	$7.31^{+0.14}_{-0.20}$	$8.17^{+0.09}_{-0.12}$	$8.16^{+0.10}_{-0.12}$
icf (O^+)	0.68 ± 0.17	0.65 ± 0.06	...	0.67 ± 0.17	...	...	...	...
icf (O^{++})	0.22 ± 0.49	0.18 ± 0.13	0.42 ± 0.04	0.22 ± 0.50	0.50 ± 0.13	0.23 ± 0.13	0.50 ± 0.07	0.52 ± 0.08
log (O/H)	$8.59^{+0.20}_{-0.39}$	$8.85^{+0.19}_{-0.35}$	$8.32^{+0.07}_{-0.09}$	$8.38^{+0.19}_{-0.35}$	$8.88^{+0.15}_{-0.24}$	$9.29^{+0.27}_{-0.81}$	$8.88^{+0.10}_{-0.13}$	$8.89^{+0.10}_{-0.13}$
icf (S^+)	...	...	...	...	...	...	...	...

TABLE 6—*Continued*

Property	S117	RCW 40	G75.84+0.40	S131	RCW 38-1	RCW 38-2	NGC 3603 P1	NGC 3603 P2
icf (S^{++})	. . .	. . .	0.70 ± 0.02	. . .	. . .	. . .	0.61 ± 0.10	0.57 ± 0.09
log (S/H)	. . .	$7.09^{+0.20}_{-0.39}$	$6.65^{+0.08}_{-0.09}$	. . .	$7.05^{+0.19}_{-0.35}$	$7.51^{+0.19}_{-0.35}$	$7.21^{+0.11}_{-0.14}$	$7.22^{+0.11}_{-0.15}$
log (N/O)	. . .	$-1.13^{+0.18}_{-0.30}$	$-0.58^{+0.09}_{-0.11}$	. . .	. . .	. . .	$-0.71^{+0.12}_{-0.16}$	$-0.73^{+0.12}_{-0.16}$

Property	M42	Orion	RCW 39	RCW 34	S100	RCW 19	K3-50A IR 1959	K3-50 A	G298.22-0.34
Reference	caplan00	shaver83	shaver83	shaver83	caplan00	shaver83	peeters02	simpson95	simpson95
R	8.80	8.89	9.00	9.20	9.40	9.50	9.60	9.60	10.10
n_e	3665 ± 366	3980 ± 398	400 ± 40	100 ± 10	100 ± 10	250 ± 25	484 ± 129	1200 ± 500	2200 ± 300
T_e (10^3 K)	8.4 ± 0.8	8.7 ± 0.9	7.5 ± 0.8	6.5 ± 0.7	7.8 ± 0.8	7.6 ± 0.8	7.8 ± 0.8	9.1 ± 0.9	8.6 ± 0.9
log (N^+/H^+)	. . .	$7.11^{+0.11}_{-0.15}$	$7.03^{+0.13}_{-0.18}$	$7.53^{+0.10}_{-0.13}$	. . .	$7.53^{+0.10}_{-0.13}$	. . .	. . .	. . .
log (N^{++}/H^+)	. . .	. . .	. . .	. . .	. . .	. . .	$6.66^{+0.15}_{-0.22}$	$6.65^{+0.18}_{-0.31}$	$7.13^{+0.10}_{-0.13}$
log (O^+/H^+)	$8.46^{+0.13}_{-0.18}$	$8.08^{+0.11}_{-0.14}$	. . .	$8.74^{+0.16}_{-0.25}$	. . .	$8.70^{+0.14}_{-0.22}$	. . .	. . .	. . .
log (O^{++}/H^+)	$8.30^{+0.14}_{-0.22}$	$8.37^{+0.13}_{-0.19}$	$8.30^{+0.15}_{-0.24}$	$8.42^{+0.13}_{-0.20}$	$8.41^{+0.15}_{-0.24}$	$7.46^{+0.12}_{-0.16}$	$7.63^{+0.12}_{-0.17}$	$7.41^{+0.17}_{-0.28}$	$7.95^{+0.10}_{-0.13}$
log (S^+/H^+)	. . .	$5.50^{+0.09}_{-0.11}$	$6.11^{+0.10}_{-0.13}$	$6.05^{+0.10}_{-0.14}$	. . .	$6.30^{+0.10}_{-0.13}$	. . .	. . .	. . .
log (S^{++}/H^+)	. . .	$6.87^{+0.16}_{-0.26}$	. . .	. . .	. . .	. . .	$5.71^{+0.14}_{-0.21}$	$5.80^{+0.18}_{-0.31}$	$6.35^{+0.10}_{-0.13}$
log (S^{+++}/H^+)	. . .	. . .	. . .	. . .	. . .	. . .	$5.46^{+0.12}_{-0.17}$	. . .	. . .
log (N^+/O^+)	. . .	$-0.97^{+0.15}_{-0.22}$	. . .	$-1.21^{+0.18}_{-0.31}$	. . .	$-1.18^{+0.17}_{-0.28}$	. . .	. . .	. . .
log (N^{++}/O^{++})	. . .	. . .	. . .	. . .	. . .	. . .	$-0.98^{+0.18}_{-0.31}$	$-0.76^{+0.23}_{-0.51}$	$-0.82^{+0.14}_{-0.20}$
T_{eff} (10^3 K)	36.0 ± 2.0	36.2 ± 0.5	35.9 ± 0.4	38.4 ± 2.2	36.0 ± 2.0	34.1 ± 0.3	41.1 ± 2.2	37.5 ± 2.8	37.2 ± 1.4
icf (N^+)	. . .	0.46 ± 0.07	0.56 ± 0.04	0.36 ± 0.16	. . .	0.80 ± 0.05	. . .	. . .	. . .
icf (N^{++})	. . .	. . .	. . .	. . .	. . .	. . .	0.59 ± 0.11	0.45 ± 0.10	0.45 ± 0.05
log (N/H)	. . .	$7.45^{+0.13}_{-0.18}$	$7.29^{+0.13}_{-0.19}$	$7.98^{+0.22}_{-0.45}$	. . .	$7.62^{+0.10}_{-0.13}$	$6.89^{+0.16}_{-0.26}$	$6.99^{+0.19}_{-0.35}$	$7.48^{+0.11}_{-0.14}$
icf (O^+)	0.52 ± 0.25	0.49 ± 0.08	. . .	0.37 ± 0.17	. . .	0.83 ± 0.05	. . .	. . .	. . .
icf (O^{++})	0.36 ± 0.72	0.46 ± 0.07	0.28 ± 0.14	0.47 ± 0.14	0.26 ± 0.56	0.04 ± 0.02	0.73 ± 0.19	0.51 ± 0.17	0.52 ± 0.08
log (O/H)	$8.69^{+0.18}_{-0.32}$	$8.55^{+0.16}_{-0.26}$	$8.85^{+0.25}_{-0.66}$	$8.91^{+0.20}_{-0.37}$	$8.99^{+0.27}_{-0.82}$	$8.73^{+0.18}_{-0.30}$	$7.77^{+0.16}_{-0.24}$	$7.70^{+0.21}_{-0.40}$	$8.24^{+0.12}_{-0.16}$
icf (S^+)	. . .	. . .	0.09 ± 0.01	0.10 ± 0.02	. . .	0.14 ± 0.01	. . .	. . .	. . .
icf (S^{++})	. . .	. . .	. . .	. . .	. . .	. . .	. . .	0.59 ± 0.22	0.61 ± 0.12
log (S/H)	. . .	$6.89^{+0.18}_{-0.31}$	$7.18^{+0.10}_{-0.13}$	$7.07^{+0.12}_{-0.17}$	. . .	$7.17^{+0.10}_{-0.13}$	$5.91^{+0.18}_{-0.30}$	$6.03^{+0.22}_{-0.48}$	$6.57^{+0.13}_{-0.18}$
log (N/O)	. . .	$-0.94^{+0.15}_{-0.22}$	. . .	$-1.19^{+0.18}_{-0.31}$	. . .	$-1.16^{+0.17}_{-0.28}$	$-0.88^{+0.18}_{-0.31}$	$-0.70^{+0.23}_{-0.51}$	$-0.76^{+0.14}_{-0.20}$

Property	S184	W3A IR 02219a	W3A IR 02219b	W3 A	W3 B	S142	Rosette-1	S146
Reference	caplan00	peeters02	peeters02	This work	This work	caplan00	shaver83	afflerbach97
R	10.10	10.20	10.20	10.20	10.20	10.20	10.20	10.21
n_e	116 ± 11	2834 ± 952	2834 ± 952	7500 ± 650	3500 ± 800	67 ± 6	100 ± 10	650 ± 65
T_e (10^3 K)	8.0 ± 0.8	8.4 ± 0.8	8.4 ± 0.8	10.0 ± 1.0	10.0 ± 1.0	8.1 ± 0.8	8.7 ± 0.9	8.5 ± 0.8
log (N^+/H^+)	. . .	. . .	. . .	. . .	. . .	. . .	$7.41^{+0.09}_{-0.12}$	. . .
log (N^{++}/H^+)	. . .	$7.25^{+0.15}_{-0.24}$	. . .	$7.78^{+0.06}_{-0.07}$	$7.19^{+0.11}_{-0.15}$	. . .	. . .	$7.12^{+0.08}_{-0.09}$
log (O^+/H^+)	$8.07^{+0.13}_{-0.18}$	. . .	. . .	. . .	. . .	$7.77^{+0.13}_{-0.18}$	$8.42^{+0.14}_{-0.21}$	. . .
log (O^{++}/H^+)	$8.06^{+0.15}_{-0.23}$	$8.05^{+0.14}_{-0.20}$	. . .	$8.58^{+0.06}_{-0.06}$	$7.91^{+0.10}_{-0.13}$	$8.07^{+0.15}_{-0.23}$	$6.75^{+0.14}_{-0.20}$	$7.87^{+0.06}_{-0.07}$
log (S^+/H^+)	. . .	. . .	. . .	. . .	. . .	. . .	$6.29^{+0.09}_{-0.12}$	. . .
log (S^{++}/H^+)	. . .	$6.11^{+0.15}_{-0.24}$	$5.97^{+0.15}_{-0.24}$	$7.05^{+0.10}_{-0.12}$	$6.72^{+0.16}_{-0.26}$	. . .	$6.90^{+0.16}_{-0.27}$	$6.54^{+0.09}_{-0.12}$
log (S^{+++}/H^+)	. . .	$6.23^{+0.13}_{-0.19}$	$6.26^{+0.13}_{-0.19}$	. . .	. . .	. . .	. . .	. . .
log (N^+/O^+)	. . .	. . .	. . .	. . .	. . .	. . .	$-1.01^{+0.16}_{-0.26}$	. . .
log (N^{++}/O^{++})	. . .	$-0.80^{+0.19}_{-0.36}$	. . .	$-0.80^{+0.08}_{-0.10}$	$-0.72^{+0.14}_{-0.22}$	. . .	. . .	$-0.75^{+0.10}_{-0.12}$
T_{eff} (10^3 K)	36.0 ± 2.0	40.1 ± 2.1	36.0 ± 2.0	36.3 ± 0.3	35.6 ± 0.5	36.0 ± 2.0	33.4 ± 2.0	36.0 ± 0.3

TABLE 6—*Continued*

Property	S184	W3A IR 02219a	W3A IR 02219b	W3 A	W3 B	S142	Rosette-1	S146
icf (N^+)	...	...	...	...	...	...	0.92 ± 0.29	...
icf (N^{++})	...	0.56 ± 0.08	...	0.44 ± 0.02	0.29 ± 0.08	...	...	0.33 ± 0.05
log (N/H)	...	$7.51^{+0.16}_{-0.26}$	...	$8.13^{+0.06}_{-0.07}$	$7.73^{+0.16}_{-0.25}$	...	$7.45^{+0.11}_{-0.16}$	$7.59^{+0.10}_{-0.13}$
icf (O^+)	0.62 ± 0.20	...	...	...	...	0.63 ± 0.20	0.95 ± 0.29	...
icf (O^{++})	0.27 ± 0.57	0.73 ± 0.17	...	0.50 ± 0.03	0.24 ± 0.13	0.25 ± 0.55	0.02 ± 0.04	0.32 ± 0.09
log (O/H)	$8.37^{+0.19}_{-0.33}$	$8.19^{+0.16}_{-0.26}$	...	$8.88^{+0.06}_{-0.07}$	$8.53^{+0.26}_{-0.73}$	$8.25^{+0.18}_{-0.33}$	$8.43^{+0.19}_{-0.33}$	$8.36^{+0.12}_{-0.17}$
icf (S^+)	...	...	...	...	...	...	...	...
icf (S^{++})	...	...	...	0.69 ± 0.03	0.73 ± 0.03	...	...	0.71 ± 0.01
log (S/H)	...	$6.47^{+0.19}_{-0.34}$	$6.44^{+0.19}_{-0.35}$	$7.21^{+0.10}_{-0.12}$	$6.86^{+0.16}_{-0.26}$	...	$7.00^{+0.18}_{-0.32}$	$6.69^{+0.09}_{-0.12}$
log (N/O)	...	$-0.69^{+0.19}_{-0.36}$	...	$-0.75^{+0.08}_{-0.10}$	$-0.80^{+0.14}_{-0.22}$	...	$-1.00^{+0.16}_{-0.26}$	$-0.77^{+0.10}_{-0.12}$

Property	S146	S168	S252	S252-1	S252-2	S153	RCW 8	S138	S138 IR 22308a
Reference	caplan00	caplan00	caplan00	shaver83	shaver83	caplan00	shaver83	afflerbach97	peeters02
R	10.21	10.65	10.70	10.70	10.70	10.80	10.90	11.00	11.00
n_e	470 ± 47	137 ± 13	144 ± 14	251 ± 25	100 ± 10	106 ± 10	316 ± 31	175 ± 17	768 ± 286
T_e (10^3 K)	8.5 ± 0.8	8.2 ± 0.8	8.2 ± 0.8	8.7 ± 0.9	8.5 ± 0.8	9.3 ± 0.9	7.5 ± 0.8	11.2 ± 1.1	8.4 ± 0.8
log (N^+/H^+)	...	...	...	$6.96^{+0.10}_{-0.13}$	$7.49^{+0.13}_{-0.19}$	...	$7.60^{+0.10}_{-0.13}$	...	...
log (N^{++}/H^+)	...	...	...	...	...	...	...	$6.63^{+0.12}_{-0.17}$	...
log (O^+/H^+)	$8.45^{+0.12}_{-0.17}$	$8.41^{+0.13}_{-0.19}$	$7.92^{+0.12}_{-0.18}$	$8.06^{+0.14}_{-0.21}$	...	$8.04^{+0.12}_{-0.17}$	$8.72^{+0.14}_{-0.22}$	...	...
log (O^{++}/H^+)	$7.91^{+0.14}_{-0.22}$	$7.17^{+0.15}_{-0.22}$	$8.15^{+0.15}_{-0.22}$	$8.10^{+0.11}_{-0.15}$	$7.57^{+0.11}_{-0.15}$	...	$6.98^{+0.15}_{-0.24}$	$7.07^{+0.07}_{-0.08}$	$7.27^{+0.15}_{-0.23}$
log (S^+/H^+)	...	...	...	$5.69^{+0.10}_{-0.12}$	$5.06^{+0.12}_{-0.16}$	...	$6.30^{+0.10}_{-0.13}$	...	...
log (S^{++}/H^+)	...	...	...	$7.21^{+0.16}_{-0.27}$	$6.66^{+0.16}_{-0.27}$	...	...	$6.36^{+0.14}_{-0.21}$	$6.44^{+0.17}_{-0.28}$
log (S^{+++}/H^+)	...	...	...	...	...	...	...	...	...
log (N^+/O^+)	...	...	...	$-1.11^{+0.16}_{-0.26}$	...	...	$-1.11^{+0.17}_{-0.28}$	...	...
log (N^{++}/O^{++})	...	...	...	...	...	...	...	$-0.43^{+0.14}_{-0.20}$	...
$T_{\rm eff}$ (10^3 K)	36.0 ± 2.0	36.0 ± 2.0	36.0 ± 2.0	35.2 ± 0.5	35.3 ± 0.5	36.0 ± 2.0	33.4 ± 2.0	34.8 ± 0.4	34.9 ± 0.6
icf (N^+)	...	...	...	0.66 ± 0.06	0.67 ± 0.06	...	0.91 ± 0.33	...	...
icf (N^{++})	...	...	...	...	...	...	...	0.14 ± 0.04	...
log (N/H)	...	...	...	$7.14^{+0.10}_{-0.14}$	$7.66^{+0.14}_{-0.20}$	...	$7.64^{+0.12}_{-0.17}$	$7.49^{+0.16}_{-0.26}$	...
icf (O^+)	0.58 ± 0.22	0.61 ± 0.21	0.61 ± 0.21	0.69 ± 0.06	...	0.62 ± 0.20	0.95 ± 0.34	...	...
icf (O^{++})	0.30 ± 0.63	0.27 ± 0.57	0.27 ± 0.58	0.12 ± 0.08	0.12 ± 0.08	...	0.02 ± 0.05	0.08 ± 0.04	0.11 ± 0.08
log (O/H)	$8.56^{+0.18}_{-0.31}$	$8.44^{+0.19}_{-0.34}$	$8.35^{+0.18}_{-0.32}$	$8.38^{+0.17}_{-0.28}$	$8.47^{+0.28}_{-1.06}$	$8.25^{+0.18}_{-0.30}$	$8.72^{+0.20}_{-0.38}$	$8.16^{+0.21}_{-0.42}$	$8.24^{+0.29}_{-1.20}$
icf (S^+)	...	...	...	...	...	...	0.15 ± 0.05	...	...
icf (S^{++})	...	...	...	...	...	...	...	0.74 ± 0.01	0.75 ± 0.03
log (S/H)	...	...	...	$7.22^{+0.18}_{-0.32}$	$6.67^{+0.19}_{-0.35}$	...	$7.13^{+0.18}_{-0.30}$	$6.49^{+0.14}_{-0.21}$	$6.57^{+0.17}_{-0.28}$
log (N/O)	...	...	...	$-1.09^{+0.16}_{-0.26}$	...	...	$-1.10^{+0.17}_{-0.28}$	$-0.67^{+0.14}_{-0.20}$	...

Property	S138 IR 22308b	S138	S138	S255	RCW 16-1	RCW 16-2	S257	S257	S288
Reference	peeters02	This work	caplan00	shaver83	shaver83	shaver83	caplan00	shaver83	rudolph97
R	11.00	11.00	11.00	11.00	11.00	11.00	11.01	11.01	11.02
n_e	768 ± 286	1040 ± 220	400 ± 40	400 ± 40	200 ± 20	250 ± 25	160 ± 16	100 ± 10	310 ± 130
T_e (10^3 K)	8.4 ± 0.8	10.0 ± 1.0	8.3 ± 0.8	8.8 ± 0.9	7.8 ± 0.8	7.6 ± 0.8	9.3 ± 0.9	9.1 ± 0.9	10.0 ± 1.0
log (N^+/H^+)	...	...	...	$7.44^{+0.13}_{-0.18}$	$7.18^{+0.10}_{-0.12}$	$7.43^{+0.12}_{-0.16}$	...	$7.29^{+0.11}_{-0.15}$	...
log (N^{++}/H^+)	$6.69^{+0.19}_{-0.33}$	$7.14^{+0.12}_{-0.16}$	...	...	...	...	...	...	...
log (O^+/H^+)	...	...	...	$8.58^{+0.13}_{-0.20}$	$8.44^{+0.15}_{-0.22}$	...	$8.10^{+0.12}_{-0.17}$	...	...

TABLE 6—*Continued*

Property	S138 IR 22308b	S138	S138	S255	RCW 16-1	RCW 16-2	S257	S257	S288
log (O^{++}/H^+)	$7.28^{+0.15}_{-0.23}$	$7.42^{+0.10}_{-0.12}$	$7.27^{+0.15}_{-0.22}$	$6.98^{+0.14}_{-0.21}$	$8.49^{+0.11}_{-0.15}$	$8.16^{+0.12}_{-0.16}$	...	...	$7.54^{+0.17}_{-0.29}$
log (S^+/H^+)	...	...	...	$6.01^{+0.09}_{-0.12}$	$6.10^{+0.09}_{-0.12}$	$6.21^{+0.10}_{-0.13}$	...	$6.20^{+0.09}_{-0.12}$	...
log (S^{++}/H^+)	$6.36^{+0.17}_{-0.28}$	$6.62^{+0.13}_{-0.18}$	...	...	$7.16^{+0.17}_{-0.29}$	$6.79^{+0.17}_{-0.29}$	...	...	$6.31^{+0.21}_{-0.42}$
log (S^{+++}/H^+)	...	...	...	...	...	...	...	...	...
log (N^+/O^+)	...	...	...	$-1.14^{+0.17}_{-0.30}$	$-1.25^{+0.17}_{-0.28}$	...	...	...	...
log (N^{++}/O^{++})	$-0.59^{+0.22}_{-0.48}$	$-0.29^{+0.14}_{-0.22}$	...	...	...	...	...	...	...
$T_{\rm eff}$ (10^3 K)	35.1 ± 0.6	34.8 ± 0.4	36.0 ± 2.0	33.6 ± 0.4	36.2 ± 0.5	36.2 ± 0.5	36.0 ± 2.0	36.0 ± 2.0	35.9 ± 0.7
icf (N^+)	...	...	...	0.87 ± 0.07	0.56 ± 0.06	0.54 ± 0.06	...	0.60 ± 0.20	...
icf (N^{++})	0.19 ± 0.07	0.17 ± 0.04	...	...	...	...	...	...	...
log (N/H)	$7.41^{+0.23}_{-0.54}$	$7.91^{+0.15}_{-0.23}$	...	$7.50^{+0.13}_{-0.18}$	$7.44^{+0.10}_{-0.14}$	$7.70^{+0.12}_{-0.17}$	...	$7.52^{+0.17}_{-0.28}$	...
icf (O^+)	...	...	...	0.91 ± 0.07	0.58 ± 0.06	...	0.61 ± 0.21	...	...
icf (O^{++})	0.13 ± 0.09	0.10 ± 0.05	0.30 ± 0.62	0.03 ± 0.01	0.33 ± 0.09	0.36 ± 0.06	...	...	0.26 ± 0.22
log (O/H)	$8.16^{+0.28}_{-1.11}$	$8.41^{+0.21}_{-0.43}$	$7.80^{+0.26}_{-0.75}$	$8.59^{+0.18}_{-0.33}$	$8.77^{+0.18}_{-0.30}$	$8.61^{+0.14}_{-0.20}$	$8.32^{+0.18}_{-0.32}$	...	$8.13^{+0.27}_{-0.88}$
icf (S^+)	...	...	...	0.13 ± 0.01	...	...	...	0.12 ± 0.04	...
icf (S^{++})	0.75 ± 0.02	0.76 ± 0.02	...	...	...	...	...	...	0.72 ± 0.02
log (S/H)	$6.49^{+0.17}_{-0.28}$	$6.74^{+0.13}_{-0.18}$	...	$6.89^{+0.10}_{-0.13}$	$7.19^{+0.19}_{-0.34}$	$6.89^{+0.19}_{-0.35}$	...	$7.12^{+0.16}_{-0.25}$	$6.46^{+0.21}_{-0.42}$
log (N/O)	$-0.76^{+0.22}_{-0.48}$	$-0.50^{+0.14}_{-0.22}$	...	$-1.12^{+0.17}_{-0.30}$	$-1.23^{+0.17}_{-0.28}$	...	...	...	...

Property	S206	BFS31	S148	S152	S152	S152	WB 73	BFS64	S156 IR 23030
Reference	caplan00	vilchez96ind	caplan00	afflerbach97	This work	caplan00	This work	fich91	peeters02
R	11.10	11.30	11.40	11.41	11.41	11.41	11.70	11.70	12.30
n_e	502 ± 50	200 ± 20	235 ± 23	400 ± 40	870 ± 145	455 ± 45	590 ± 220	100 ± 10	806 ± 205
T_e (10^3 K)	9.2 ± 0.9	5.0 ± 0.5	8.5 ± 0.9	8.4 ± 0.8	10.0 ± 1.0	8.4 ± 0.8	10.0 ± 1.0	8.4 ± 0.8	8.8 ± 0.9
log (N^+/H^+)	...	$8.18^{+0.12}_{-0.17}$	...	...	...	...	...	$7.32^{+0.13}_{-0.18}$	$7.40^{+0.12}_{-0.17}$
log (N^{++}/H^+)	...	...	...	...	$7.19^{+0.09}_{-0.11}$	...	$7.24^{+0.17}_{-0.29}$	...	$7.13^{+0.12}_{-0.18}$
log (O^+/H^+)	$7.88^{+0.12}_{-0.16}$	...	$8.27^{+0.12}_{-0.17}$	...	...	$8.26^{+0.12}_{-0.17}$	...	...	...
log (O^{++}/H^+)	$8.19^{+0.14}_{-0.20}$	...	$6.61^{+0.14}_{-0.22}$	$7.25^{+0.07}_{-0.09}$	$7.76^{+0.08}_{-0.10}$	$7.47^{+0.14}_{-0.22}$	$7.62^{+0.15}_{-0.22}$	...	$7.62^{+0.11}_{-0.15}$
log (S^+/H^+)	...	$7.23^{+0.12}_{-0.16}$	...	...	...	...	...	$6.25^{+0.10}_{-0.14}$	...
log (S^{++}/H^+)	...	$6.33^{+0.19}_{-0.33}$	...	$6.63^{+0.08}_{-0.10}$	$6.76^{+0.10}_{-0.14}$	...	$6.80^{+0.20}_{-0.38}$	...	$6.45^{+0.13}_{-0.19}$
log (S^{+++}/H^+)	...	...	...	...	...	...	...	...	$5.37^{+0.12}_{-0.16}$
log (N^+/O^+)	...	...	...	...	...	...	...	...	...
log (N^{++}/O^{++})	...	...	...	...	$-0.56^{+0.12}_{-0.16}$	...	$-0.39^{+0.21}_{-0.43}$	...	$-0.48^{+0.16}_{-0.26}$
$T_{\rm eff}$ (10^3 K)	36.0 ± 2.0	36.0 ± 2.0	36.0 ± 2.0	34.5 ± 0.3	35.3 ± 0.3	36.0 ± 2.0	34.9 ± 0.6	36.0 ± 2.0	35.7 ± 0.5
icf (N^+)	...	0.57 ± 0.21	...	...	...	...	...	0.60 ± 0.20	0.57 ± 0.05
icf (N^{++})	...	...	...	...	0.22 ± 0.05	...	0.17 ± 0.07	...	0.27 ± 0.09
log (N/H)	...	$8.43^{+0.19}_{-0.33}$	...	...	$7.86^{+0.13}_{-0.18}$	...	$8.01^{+0.24}_{-0.59}$	$7.55^{+0.18}_{-0.31}$	$7.59^{+0.16}_{-0.27}$
icf (O^+)	0.57 ± 0.22	...	0.60 ± 0.21	...	...	0.58 ± 0.22	...	...	...
icf (O^{++})	0.30 ± 0.63	...	0.28 ± 0.60	0.07 ± 0.02	0.16 ± 0.06	0.30 ± 0.62	0.11 ± 0.08	...	0.23 ± 0.13
log (O/H)	$8.36^{+0.17}_{-0.29}$	...	$8.28^{+0.18}_{-0.31}$	$8.42^{+0.15}_{-0.23}$	$8.56^{+0.18}_{-0.33}$	$8.33^{+0.18}_{-0.31}$	$8.60^{+0.29}_{-1.20}$	...	$8.26^{+0.27}_{-0.80}$
icf (S^+)	...	...	...	...	...	...	...	0.12 ± 0.04	...
icf (S^{++})	...	...	...	0.76 ± 0.01	0.74 ± 0.01	...	0.75 ± 0.02	...	...
log (S/H)	...	$7.28^{+0.21}_{-0.42}$	...	$6.75^{+0.08}_{-0.10}$	$6.89^{+0.10}_{-0.14}$	...	$6.93^{+0.20}_{-0.38}$	$7.17^{+0.16}_{-0.27}$	$6.49^{+0.17}_{-0.28}$
log (N/O)	...	...	...	...	$-0.70^{+0.12}_{-0.16}$	...	$-0.59^{+0.21}_{-0.43}$	...	$-0.56^{+0.16}_{-0.26}$

TABLE 6—*Continued*

Property	S156	S156	S219	S219	S219	RCW 6	IR 21190	S128 IR 21306	S128
Reference	simpson95	caplan00	caplan00	fich91	vilchez96ind	shaver83	peeters02	peeters02	rudolph97
R	12.30	12.30	12.50	12.50	12.50	12.60	12.65	12.70	12.70
n_e	1000 ± 100	907 ± 90	166 ± 16	90 ± 9	90 ± 9	100 ± 10	2882 ± 1429	214 ± 89	390 ± 50
T_e (10^3 K)	6.4 ± 0.6	8.5 ± 0.8	9.9 ± 1.0	8.8 ± 0.9	9.0 ± 0.9	7.3 ± 0.7	9.0 ± 0.9	8.9 ± 0.9	10.0 ± 1.0
log (N^+/H^+)	...	...	...	$7.45^{+0.12}_{-0.17}$	$7.37^{+0.08}_{-0.10}$	$7.37^{+0.13}_{-0.18}$	...	...	...
log (N^{++}/H^+)	$7.29^{+0.10}_{-0.14}$	...	...	...	...	...	...	...	$7.19^{+0.09}_{-0.11}$
log (O^+/H^+)	...	$8.34^{+0.12}_{-0.17}$	$8.19^{+0.12}_{-0.17}$	$8.84^{+0.14}_{-0.21}$	$8.29^{+0.13}_{-0.18}$	$8.54^{+0.15}_{-0.23}$	...	...	...
log (O^{++}/H^+)	$7.70^{+0.09}_{-0.12}$	$7.82^{+0.14}_{-0.22}$	...	...	$6.44^{+0.14}_{-0.21}$	$8.32^{+0.12}_{-0.17}$	$7.60^{+0.18}_{-0.32}$	$7.51^{+0.17}_{-0.28}$	$7.95^{+0.07}_{-0.08}$
log (S^+/H^+)	...	...	...	$6.32^{+0.10}_{-0.13}$	$6.29^{+0.09}_{-0.11}$	$6.10^{+0.10}_{-0.13}$	...	...	...
log (S^{++}/H^+)	$6.82^{+0.10}_{-0.13}$	...	...	...	$5.54^{+0.11}_{-0.14}$	...	$6.24^{+0.19}_{-0.36}$	...	$6.49^{+0.10}_{-0.13}$
log (S^{+++}/H^+)	...	...	...	...	...	...	$5.46^{+0.17}_{-0.28}$	...	...
log (N^+/O^+)	...	...	...	$-1.39^{+0.18}_{-0.31}$	$-0.92^{+0.15}_{-0.22}$	$-1.17^{+0.19}_{-0.34}$	...	...	...
log (N^{++}/O^{++})	$-0.41^{+0.13}_{-0.20}$	...	...	...	...	...	...	...	$-0.76^{+0.11}_{-0.15}$
$T_{\rm eff}$ (10^3 K)	35.0 ± 0.4	36.0 ± 2.0	36.0 ± 2.0	36.0 ± 2.0	35.3 ± 0.4	36.8 ± 2.0	36.0 ± 0.7	36.0 ± 2.0	36.6 ± 1.4
icf (N^+)	...	...	...	0.60 ± 0.20	0.67 ± 0.05	0.51 ± 0.21	...	...	...
icf (N^{++})	0.18 ± 0.04	...	...	...	...	...	...	...	0.40 ± 0.05
log (N/H)	$8.02^{+0.14}_{-0.20}$	...	...	$7.67^{+0.18}_{-0.30}$	$7.55^{+0.09}_{-0.11}$	$7.67^{+0.21}_{-0.42}$	...	...	$7.60^{+0.10}_{-0.13}$
icf (O^+)	...	0.56 ± 0.23	0.61 ± 0.21	0.62 ± 0.20	0.70 ± 0.05	0.53 ± 0.22	...	...	...
icf (O^{++})	0.12 ± 0.05	0.32 ± 0.66	...	...	0.12 ± 0.07	0.38 ± 0.10	0.35 ± 0.26	0.28 ± 0.59	0.42 ± 0.07
log (O/H)	$8.62^{+0.20}_{-0.36}$	$8.45^{+0.18}_{-0.31}$	$8.41^{+0.18}_{-0.31}$	$9.04^{+0.19}_{-0.33}$	$8.30^{+0.18}_{-0.31}$	$8.74^{+0.18}_{-0.32}$	$8.06^{+0.26}_{-0.78}$	$8.07^{+0.27}_{-0.83}$	$8.33^{+0.10}_{-0.12}$
icf (S^+)	...	...	...	0.12 ± 0.04	...	0.11 ± 0.02	...	...	...
icf (S^{++})	0.75 ± 0.02	...	...	...	...	...	...	...	0.68 ± 0.10
log (S/H)	$6.95^{+0.10}_{-0.13}$	...	...	$7.23^{+0.16}_{-0.26}$	$6.36^{+0.13}_{-0.19}$	$7.06^{+0.12}_{-0.16}$	$6.31^{+0.24}_{-0.57}$	...	$6.66^{+0.11}_{-0.15}$
log (N/O)	$-0.60^{+0.13}_{-0.20}$	...	...	$-1.37^{+0.18}_{-0.31}$	$-0.90^{+0.15}_{-0.22}$	$-1.15^{+0.19}_{-0.34}$	...	...	$-0.73^{+0.11}_{-0.15}$

Property	S128	S128	S128	S128	WB411	S301	S241	S271	S272
Reference	This work	caplan00	fich91	vilchez96dir	This work	fich91	fich91	fich91	fich91
R	12.70	12.70	12.70	12.70	12.90	12.90	13.20	13.20	13.20
n_e	380 ± 55	2438 ± 243	110 ± 11	110 ± 11	565 ± 115	100 ± 10	90 ± 9	370 ± 37	150 ± 15
T_e (10^3 K)	10.0 ± 1.0	9.0 ± 0.9	8.9 ± 0.9	11.6 ± 1.8	10.0 ± 1.0	7.7 ± 1.2	9.1 ± 0.9	9.1 ± 0.9	9.1 ± 0.9
log (N^+/H^+)	...	...	$7.13^{+0.10}_{-0.13}$	$6.74^{+0.10}_{-0.14}$	...	$7.41^{+0.16}_{-0.27}$	$7.40^{+0.10}_{-0.12}$	$7.46^{+0.12}_{-0.17}$	$7.39^{+0.12}_{-0.17}$
log (N^{++}/H^+)	$7.43^{+0.10}_{-0.12}$	...	...	...	$6.72^{+0.13}_{-0.19}$	...	...	...	...
log (O^+/H^+)	...	$8.52^{+0.12}_{-0.17}$	...	$7.72^{+0.13}_{-0.19}$	...	...	$8.23^{+0.14}_{-0.21}$	...	...
log (O^{++}/H^+)	$8.01^{+0.07}_{-0.09}$	$8.13^{+0.14}_{-0.21}$	$8.17^{+0.11}_{-0.15}$	$7.85^{+0.11}_{-0.15}$	$7.48^{+0.10}_{-0.12}$	$8.02^{+0.16}_{-0.24}$	...	...	...
log (S^+/H^+)	...	...	$5.77^{+0.10}_{-0.12}$	$5.50^{+0.10}_{-0.12}$	...	$6.19^{+0.13}_{-0.18}$	$6.34^{+0.09}_{-0.12}$	$5.76^{+0.11}_{-0.14}$	$6.09^{+0.10}_{-0.13}$
log (S^{++}/H^+)	$6.63^{+0.11}_{-0.15}$	...	...	$6.27^{+0.10}_{-0.13}$	$6.75^{+0.15}_{-0.23}$	...	...	...	...
log (S^{+++}/H^+)	...	...	...	...	...	...	...	...	...
log (N^+/O^+)	...	...	...	$-0.97^{+0.16}_{-0.26}$	...	...	$-0.83^{+0.16}_{-0.26}$	...	...
log (N^{++}/O^{++})	$-0.58^{+0.12}_{-0.16}$	...	...	...	$-0.75^{+0.16}_{-0.25}$	...	...	...	...
$T_{\rm eff}$ (10^3 K)	36.2 ± 0.3	36.0 ± 2.0	38.7 ± 1.8	38.5 ± 1.9	34.7 ± 0.5	35.6 ± 0.4	36.0 ± 2.0	36.0 ± 2.0	36.0 ± 2.0
icf (N^+)	...	...	0.33 ± 0.13	0.35 ± 0.14	...	0.63 ± 0.04	0.60 ± 0.20	0.55 ± 0.21	0.58 ± 0.20
icf (N^{++})	0.36 ± 0.03	...	...	...	0.15 ± 0.05	...	...	...	...
log (N/H)	$7.88^{+0.10}_{-0.13}$	...	$7.61^{+0.18}_{-0.32}$	$7.20^{+0.19}_{-0.36}$	$7.55^{+0.18}_{-0.32}$	$7.61^{+0.17}_{-0.27}$	$7.63^{+0.16}_{-0.26}$	$7.71^{+0.19}_{-0.36}$	$7.62^{+0.18}_{-0.32}$
icf (O^+)	...	0.53 ± 0.24	...	0.36 ± 0.15	...	...	0.62 ± 0.20	...	...
icf (O^{++})	0.36 ± 0.05	0.35 ± 0.70	0.50 ± 0.12	0.48 ± 0.12	0.09 ± 0.05	0.18 ± 0.10	...	...	...
log (O/H)	$8.45^{+0.09}_{-0.12}$	$8.67^{+0.18}_{-0.30}$	$8.48^{+0.14}_{-0.21}$	$8.09^{+0.17}_{-0.27}$	$8.54^{+0.28}_{-1.02}$	$8.76^{+0.28}_{-0.98}$	$8.44^{+0.18}_{-0.33}$	...	...
icf (S^+)	...	...	0.09 ± 0.01	...	...	0.13 ± 0.01	0.12 ± 0.04	0.09 ± 0.03	0.11 ± 0.04
icf (S^{++})	0.71 ± 0.02	...	...	...	0.76 ± 0.02	...	...	...	...

TABLE 6—*Continued*

Property	S128	S128	S128	S128	WB411	S301	S241	S271	S272
log (S/H)	$6.78^{+0.11}_{-0.15}$	...	$6.80^{+0.11}_{-0.15}$	$6.34^{+0.13}_{-0.19}$	$6.87^{+0.15}_{-0.23}$	$7.09^{+0.13}_{-0.19}$	$7.25^{+0.16}_{-0.25}$	$6.83^{+0.17}_{-0.29}$	$7.05^{+0.16}_{-0.26}$
log (N/O)	$-0.57^{+0.12}_{-0.16}$	...	...	$-0.96^{+0.16}_{-0.26}$	$-0.99^{+0.16}_{-0.25}$	...	$-0.81^{+0.16}_{-0.26}$	...	...

Property	S284	S217	S217	S298	G201.6+1.6	RCW 5-1	RCW 5-2	S211	S211
Reference	shaver83	caplan00	fich91	fich91	shaver83	shaver83	shaver83	caplan00	fich91
R	13.20	13.50	13.50	13.60	13.60	13.60	13.60	14.10	14.10
n_e	100 ± 10	48 ± 4	90 ± 9	100 ± 10	200 ± 20	200 ± 20	400 ± 40	135 ± 13	250 ± 25
T_e (10^3 K)	9.5 ± 0.9	9.2 ± 0.9	9.2 ± 0.9	9.3 ± 0.9	9.2 ± 0.9	10.3 ± 1.0	10.4 ± 1.0	10.2 ± 1.0	9.5 ± 0.9
log (N^+/H^+)	$7.05^{+0.10}_{-0.12}$	...	$7.35^{+0.10}_{-0.12}$	$7.04^{+0.12}_{-0.17}$	$7.21^{+0.10}_{-0.12}$	$6.45^{+0.09}_{-0.12}$	$6.85^{+0.12}_{-0.16}$	...	$7.38^{+0.09}_{-0.12}$
log (N^{++}/H^+)	...	...	...	...	...	...	...	...	...
log (O^+/H^+)	$8.27^{+0.14}_{-0.20}$	$8.09^{+0.12}_{-0.17}$	...	...	$8.53^{+0.14}_{-0.20}$	$7.52^{+0.13}_{-0.19}$	...	$7.91^{+0.12}_{-0.16}$	...
log (O^{++}/H^+)	$7.79^{+0.11}_{-0.14}$	$6.88^{+0.14}_{-0.21}$	...	$8.68^{+0.11}_{-0.14}$	$7.71^{+0.11}_{-0.15}$	$8.37^{+0.10}_{-0.13}$	$8.54^{+0.10}_{-0.13}$	$6.58^{+0.13}_{-0.19}$	...
log (S^+/H^+)	$5.88^{+0.09}_{-0.12}$	...	$6.16^{+0.10}_{-0.13}$	$6.18^{+0.10}_{-0.13}$	$6.08^{+0.09}_{-0.12}$	$5.62^{+0.09}_{-0.12}$	$5.89^{+0.09}_{-0.11}$	...	$6.01^{+0.09}_{-0.12}$
log (S^{++}/H^+)	...	...	...	...	...	$6.83^{+0.15}_{-0.23}$	...	...	...
log (S^{+++}/H^+)	...	...	...	...	...	...	...	...	...
log (N^+/O^+)	$-1.22^{+0.16}_{-0.25}$	...	...	...	$1.32^{+0.16}_{-0.26}$	$-1.07^{+0.15}_{-0.24}$	...	...	...
log (N^{++}/O^{++})	...	...	...	...	...	...	...	...	...
$T_{\rm eff}$ (10^3 K)	35.8 ± 0.3	36.0 ± 2.0	36.0 ± 2.0	39.9 ± 1.9	35.1 ± 0.3	37.8 ± 2.2	39.4 ± 1.7	36.0 ± 2.0	36.0 ± 2.0
icf (N^+)	0.61 ± 0.03	...	0.60 ± 0.20	0.26 ± 0.10	0.68 ± 0.04	0.38 ± 0.19	0.23 ± 0.10	...	0.57 ± 0.21
icf (N^{++})	...	...	...	...	...	...	...	...	...
log (N/H)	$7.26^{+0.10}_{-0.12}$	...	$7.58^{+0.16}_{-0.26}$	$7.63^{+0.19}_{-0.36}$	$7.38^{+0.10}_{-0.13}$	$6.87^{+0.23}_{-0.54}$	$7.49^{+0.21}_{-0.44}$	...	$7.63^{+0.18}_{-0.30}$
icf (O^+)	0.64 ± 0.03	0.64 ± 0.19	...	...	0.70 ± 0.04	0.40 ± 0.20	...	0.61 ± 0.21	...
icf (O^{++})	0.21 ± 0.08	0.24 ± 0.53	...	0.57 ± 0.14	0.11 ± 0.04	0.46 ± 0.13	0.59 ± 0.13	0.27 ± 0.57	...
log (O/H)	$8.40^{+0.16}_{-0.27}$	$8.12^{+0.17}_{-0.30}$	...	$8.93^{+0.14}_{-0.21}$	$8.59^{+0.17}_{-0.27}$	$8.43^{+0.16}_{-0.25}$	$8.77^{+0.13}_{-0.18}$	$7.93^{+0.17}_{-0.28}$	...
icf (S^+)	0.12 ± 0.01	...	0.12 ± 0.04	0.09 ± 0.01	0.12 ± 0.01	...	0.06 ± 0.01	...	0.10 ± 0.03
icf (S^{++})	...	...	...	...	...	...	...	...	...
log (S/H)	$6.78^{+0.10}_{-0.12}$	...	$7.07^{+0.16}_{-0.26}$	$7.25^{+0.11}_{-0.16}$	$7.00^{+0.10}_{-0.13}$	$6.86^{+0.17}_{-0.28}$	$7.10^{+0.11}_{-0.14}$	...	$7.04^{+0.16}_{-0.26}$
log (N/O)	$-1.21^{+0.16}_{-0.25}$	...	...	...	$-1.30^{+0.16}_{-0.26}$	$-1.05^{+0.15}_{-0.24}$	...	...	...

Property	S212	S212	S270	WB870	S285	S127A IR 21270	S127A	S127 B	S127
Reference	caplan00	fich91	fich91	rudolph97	fich91	peeters02	rudolph97	This work	caplan00
R	14.20	14.20	14.20	14.60	14.70	15.00	15.00	15.00	15.00
n_e	128 ± 12	100 ± 10	390 ± 39	1200 ± 380	100 ± 10	186 ± 63	320 ± 70	50 ± 25	545 ± 54
T_e (10^3 K)	9.7 ± 1.0	9.5 ± 0.9	9.5 ± 0.9	10.0 ± 1.0	9.7 ± 1.0	9.8 ± 1.0	10.0 ± 1.0	10.0 ± 1.0	9.4 ± 0.9
log (N^+/H^+)	...	$7.22^{+0.10}_{-0.12}$	$7.11^{+0.12}_{-0.17}$	...	$7.28^{+0.12}_{-0.17}$	...	...	...	...
log (N^{++}/H^+)	...	...	...	...	...	$6.78^{+0.16}_{-0.27}$	$7.18^{+0.13}_{-0.19}$	...	...
log (O^+/H^+)	$8.05^{+0.12}_{-0.16}$	$8.39^{+0.14}_{-0.20}$	...	...	...	...	...	...	$8.07^{+0.12}_{-0.16}$
log (O^{++}/H^+)	$7.73^{+0.14}_{-0.20}$	$7.52^{+0.11}_{-0.14}$	...	$7.61^{+0.13}_{-0.20}$	...	$7.54^{+0.15}_{-0.23}$	$8.04^{+0.10}_{-0.13}$	$7.25^{+0.21}_{-0.44}$	$7.62^{+0.14}_{-0.20}$
log (S^+/H^+)	...	$5.94^{+0.09}_{-0.12}$	$6.15^{+0.10}_{-0.13}$	...	$6.29^{+0.09}_{-0.12}$	...	...	...	...
log (S^{++}/H^+)	...	...	...	$6.25^{+0.17}_{-0.28}$	...	$5.65^{+0.18}_{-0.30}$	$6.18^{+0.15}_{-0.24}$	$6.64^{+0.25}_{-0.64}$	...
log (S^{+++}/H^+)	...	...	...	...	...	...	...	...	...
log (N^+/O^+)	...	$-1.16^{+0.16}_{-0.25}$	...	...	...	...	...	...	...
log (N^{++}/O^{++})	...	...	...	...	...	$-0.76^{+0.21}_{-0.41}$	$-0.86^{+0.16}_{-0.25}$	...	...
$T_{\rm eff}$ (10^3 K)	36.0 ± 2.0	35.2 ± 0.3	36.0 ± 2.0	36.0 ± 0.5	36.0 ± 2.0	41.5 ± 3.0	40.9 ± 2.3	34.7 ± 1.0	36.0 ± 2.0
icf (N^+)	...	0.68 ± 0.03	0.55 ± 0.21	...	0.60 ± 0.20	...	...	...	...

TABLE 6—*Continued*

Property	S212	S212	S270	WB870	S285	S127A IR 21270	S127A	S127 B	S127
icf (N^{++})	...	...	...	...	...	0.60 ± 0.10	0.57 ± 0.12	...	...
log (N/H)	...	$7.39^{+0.10}_{-0.12}$	$7.37^{+0.19}_{-0.36}$	...	$7.51^{+0.18}_{-0.30}$	$7.00^{+0.17}_{-0.29}$	$7.42^{+0.15}_{-0.23}$	...	...
icf (O^+)	0.61 ± 0.21	0.71 ± 0.03	...	...	...	...	...	...	0.57 ± 0.23
icf (O^{++})	0.27 ± 0.57	0.11 ± 0.04	...	0.34 ± 0.16	...	0.73 ± 0.17	0.69 ± 0.19	0.06 ± 0.08	0.31 ± 0.63
log (O/H)	$8.22^{+0.17}_{-0.29}$	$8.44^{+0.17}_{-0.27}$	...	$8.07^{+0.24}_{-0.57}$	...	$7.68^{+0.17}_{-0.29}$	$8.20^{+0.15}_{-0.23}$	$8.46^{+0.30}_{-1.65}$	$8.20^{+0.17}_{-0.29}$
icf (S^+)	...	0.14 ± 0.01	0.08 ± 0.03	...	0.12 ± 0.04	...	...	...	...
icf (S^{++})	...	...	...	0.71 ± 0.03	...	0.44 ± 0.10	0.44 ± 0.10	0.72 ± 0.01	...
log (S/H)	...	$6.80^{+0.10}_{-0.12}$	$7.22^{+0.17}_{-0.27}$	$6.40^{+0.17}_{-0.28}$	$7.21^{+0.16}_{-0.25}$	$6.01^{+0.19}_{-0.35}$	$6.53^{+0.17}_{-0.29}$	$6.79^{+0.25}_{-0.64}$	...
log (N/O)	...	$-1.15^{+0.16}_{-0.25}$	...	...	...	$-0.68^{+0.21}_{-0.41}$	$-0.78^{+0.16}_{-0.25}$	...	...

Property	S127	S127	S83	BFS54	S207	S208	S209	S209	S209
Reference	fich91	vilchez96dir	caplan00	fich91	caplan00	caplan00	caplan00	fich91	vilchez96ind
R	15.00	15.00	15.20	16.30	16.80	16.80	17.00	17.00	17.00
n_e	37 ± 3	370 ± 37	100 ± 10	100 ± 10	155 ± 15	74 ± 7	645 ± 64	550 ± 55	550 ± 55
T_e (10^3 K)	9.9 ± 1.0	10.7 ± 0.9	9.9 ± 1.0	10.4 ± 1.0	10.5 ± 1.1	10.5 ± 1.1	10.8 ± 1.1	8.8 ± 1.8	9.0 ± 0.9
log (N^+/H^+)	$7.17^{+0.10}_{-0.12}$	$6.94^{+0.08}_{-0.10}$	...	$7.28^{+0.12}_{-0.16}$	...	...	...	$7.11^{+0.18}_{-0.31}$	$6.93^{+0.09}_{-0.12}$
log (N^{++}/H^+)	...	...	...	...	...	...	...	...	...
log (O^+/H^+)	...	$8.00^{+0.10}_{-0.13}$	$7.76^{+0.12}_{-0.16}$	...	$7.95^{+0.11}_{-0.15}$	$7.90^{+0.11}_{-0.16}$	$8.01^{+0.11}_{-0.15}$	...	$8.02^{+0.12}_{-0.16}$
log (O^{++}/H^+)	...	$7.62^{+0.08}_{-0.10}$	$8.32^{+0.13}_{-0.20}$	...	$6.26^{+0.13}_{-0.19}$	$6.35^{+0.13}_{-0.19}$	$7.58^{+0.13}_{-0.19}$	...	$8.23^{+0.10}_{-0.13}$
log (S^+/H^+)	$6.10^{+0.09}_{-0.12}$	$5.60^{+0.07}_{-0.09}$	...	...	...	...	...	...	$5.71^{+0.09}_{-0.11}$
log (S^{++}/H^+)	...	$6.35^{+0.08}_{-0.10}$	...	...	...	...	...	...	$5.99^{+0.10}_{-0.12}$
log (S^{+++}/H^+)	...	...	...	...	...	...	...	...	...
log (N^+/O^+)	...	$-1.06^{+0.12}_{-0.17}$	...	...	...	...	...	...	$-1.08^{+0.14}_{-0.21}$
log (N^{++}/O^{++})	...	...	...	...	...	...	...	...	...
T_{eff} (10^3 K)	36.0 ± 2.0	36.0 ± 0.3	36.0 ± 2.0	36.0 ± 2.0	36.0 ± 2.0	36.0 ± 2.0	36.0 ± 2.0	36.0 ± 2.0	48.8 ± 4.4
icf (N^+)	0.63 ± 0.18	0.56 ± 0.03	...	0.60 ± 0.20	...	...	...	0.54 ± 0.22	0.07 ± 0.02
icf (N^{++})	...	...	...	...	...	...	...	...	...
log (N/H)	$7.37^{+0.15}_{-0.23}$	$7.19^{+0.08}_{-0.10}$	...	$7.50^{+0.17}_{-0.29}$	...	...	...	$7.38^{+0.23}_{-0.54}$	$8.12^{+0.18}_{-0.31}$
icf (O^+)	...	0.59 ± 0.03	0.62 ± 0.20	...	0.61 ± 0.21	0.63 ± 0.20	0.57 ± 0.23	...	0.06 ± 0.02
icf (O^{++})	...	0.28 ± 0.09	0.26 ± 0.56	...	0.27 ± 0.58	0.25 ± 0.55	0.31 ± 0.64	...	0.88 ± 0.04
log (O/H)	...	$8.15^{+0.12}_{-0.17}$	$8.42^{+0.17}_{-0.28}$	...	$7.96^{+0.17}_{-0.27}$	$7.91^{+0.17}_{-0.27}$	$8.15^{+0.16}_{-0.26}$	...	$8.44^{+0.15}_{-0.22}$
icf (S^+)	0.16 ± 0.05	...	...	...	...	...	...	...	...
icf (S^{++})	...	...	...	...	...	...	...	...	...
log (S/H)	$6.91^{+0.15}_{-0.24}$	$6.42^{+0.11}_{-0.14}$	...	...	...	...	...	...	$6.17^{+0.12}_{-0.18}$
log (N/O)	...	$-1.04^{+0.12}_{-0.17}$	...	...	...	...	...	...	$-1.09^{+0.14}_{-0.21}$

Property	S283	S283	S266	S266A	S266B
Reference	fich91	vilchez96ind	fich91	vilchez96dir	vilchez96dir
R	17.01	17.01	17.90	17.90	17.90
n_e	170 ± 17	170 ± 17	400 ± 40	400 ± 40	400 ± 40
T_e (10^3 K)	10.8 ± 1.1	10.0 ± 1.0	11.1 ± 1.1	9.9 ± 2.2	10.2 ± 1.9
log (N^+/H^+)	$7.18^{+0.12}_{-0.16}$	$7.07^{+0.08}_{-0.10}$	$6.46^{+0.11}_{-0.16}$	$6.80^{+0.14}_{-0.20}$	$7.31^{+0.11}_{-0.15}$
log (N^{++}/H^+)	...	...	...	...	...
log (O^+/H^+)	...	$8.22^{+0.13}_{-0.19}$	...	$7.55^{+0.19}_{-0.35}$	$7.92^{+0.16}_{-0.25}$
log (O^{++}/H^+)	...	$7.12^{+0.12}_{-0.17}$	$6.20^{+0.13}_{-0.18}$	$5.61^{+0.21}_{-0.42}$	$5.50^{+0.17}_{-0.30}$

TABLE 6—*Continued*

Property	S283	S283	S266	S266A	S266B
log (S^+/H^+)	$6.07^{+0.10}_{-0.12}$	$6.25^{+0.08}_{-0.10}$	$5.01^{+0.09}_{-0.11}$	$5.76^{+0.13}_{-0.20}$	$6.32^{+0.11}_{-0.15}$
log (S^{++}/H^+)	...	$6.07^{+0.10}_{-0.12}$	...	$4.83^{+0.12}_{-0.17}$	$5.44^{+0.10}_{-0.13}$
log (S^{+++}/H^+)	...	...	...	...	...
log (N^+/O^+)	...	$-1.15^{+0.15}_{-0.23}$	...	$-0.74^{+0.22}_{-0.47}$	$-0.61^{+0.19}_{-0.33}$
log (N^{++}/O^{++})	...	...	...	...	...
$T_{\rm eff}$ (10^3 K)	36.0 ± 2.0	35.6 ± 0.4	34.0 ± 0.3	34.9 ± 0.6	33.4 ± 2.0
icf (N^+)	0.58 ± 0.20	0.62 ± 0.04	0.80 ± 0.05	0.68 ± 0.08	0.91 ± 0.34
icf (N^{++})	...	...	...	...	...
log (N/H)	$7.41^{+0.18}_{-0.31}$	$7.27^{+0.09}_{-0.11}$	$6.56^{+0.12}_{-0.16}$	$6.97^{+0.14}_{-0.21}$	$7.35^{+0.13}_{-0.19}$
icf (O^+)	...	0.65 ± 0.04	...	0.71 ± 0.08	0.95 ± 0.34
icf (O^{++})	...	0.17 ± 0.09	0.04 ± 0.02	0.10 ± 0.07	0.02 ± 0.05
log (O/H)	...	$8.25^{+0.17}_{-0.28}$	$7.59^{+0.20}_{-0.39}$	$7.55^{+0.26}_{-0.77}$	$7.92^{+0.22}_{-0.47}$
icf (S^+)	0.11 ± 0.03	...	0.12 ± 0.01	...	...
icf (S^{++})	...	...	...	...	...
log (S/H)	$7.05^{+0.16}_{-0.26}$	$6.47^{+0.12}_{-0.17}$	$5.92^{+0.09}_{-0.12}$	$5.81^{+0.17}_{-0.29}$	$6.37^{+0.14}_{-0.22}$
log (N/O)	...	$-1.13^{+0.15}_{-0.23}$	...	$-0.72^{+0.22}_{-0.47}$	$-0.59^{+0.19}_{-0.33}$

Note.—Table 6 is also available in machine-readable form in the electronic edition of the *Astrophysical Journal Supplement*.

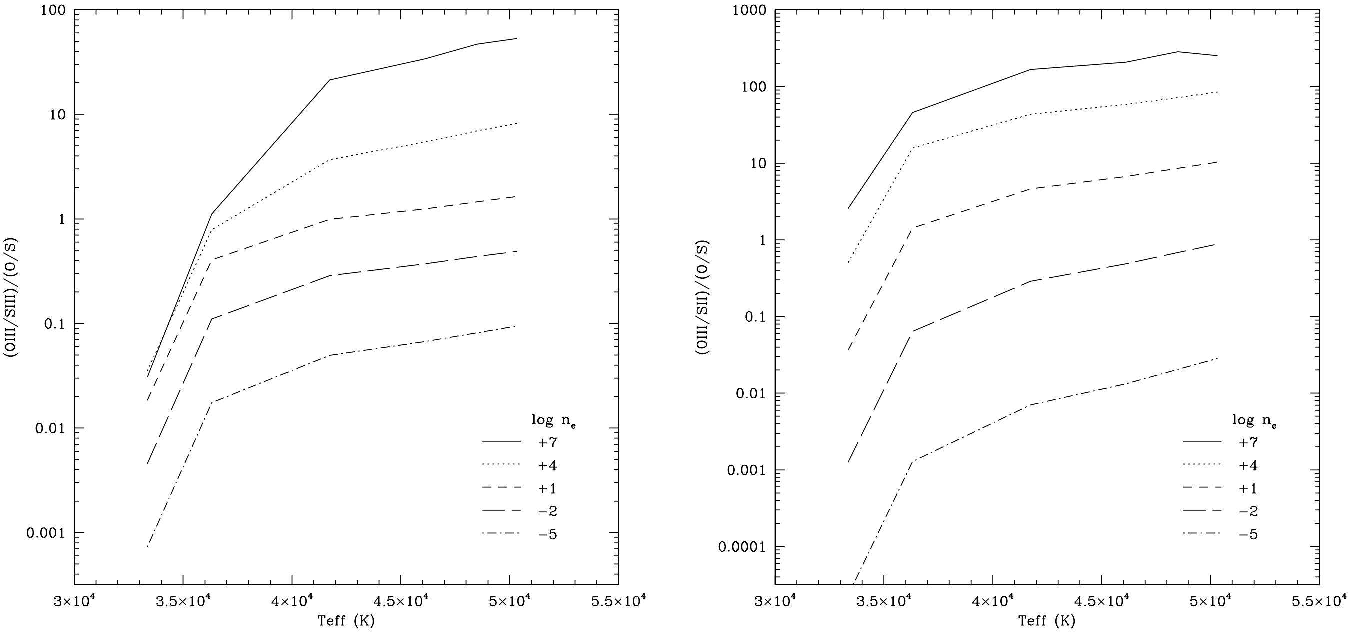

FIG. 2.—(*a*) Plot of the ratio (O III/S III)/(O/S) vs. stellar effective temperature for the models of Stasińska & Schaerer (1997). This ratio is used to determine effective temperatures for the FIR studies. (*b*) Plot of the ratio (O III/S II)/(O/S) vs. stellar effective temperature for the models of Stasińska & Schaerer (1997). This ratio is used to determine effective temperatures for the optical studies.

our final abundances are on average 4.4 ± 2.5 percent lower than the Deharveng et al. values.

6. DISTANCES

Accurate galactocentric distances of the sources in the fit to an abundance gradient (or any Galactic gradient) are equally as important as the abundances themselves. Many studies have used kinematic distances for the sources we are studying, which are both model dependent and inherently inaccurate due to random and streaming motions of gas in the Galaxy. For example, Shaver et al. (1983) derived kinematic distances for all of the sources they studied using a Schmidt rotation curve and $R_0 = 10$ kpc. Many more modern studies that have compared their gradient results to those of Shaver have incorrectly scaled Shaver's galactocentric distances to an $R_0 = 8.5$ kpc without accounting for the additional change to a flat rotation curve in the outer parts of the Galaxy (Fich et al. 1989).

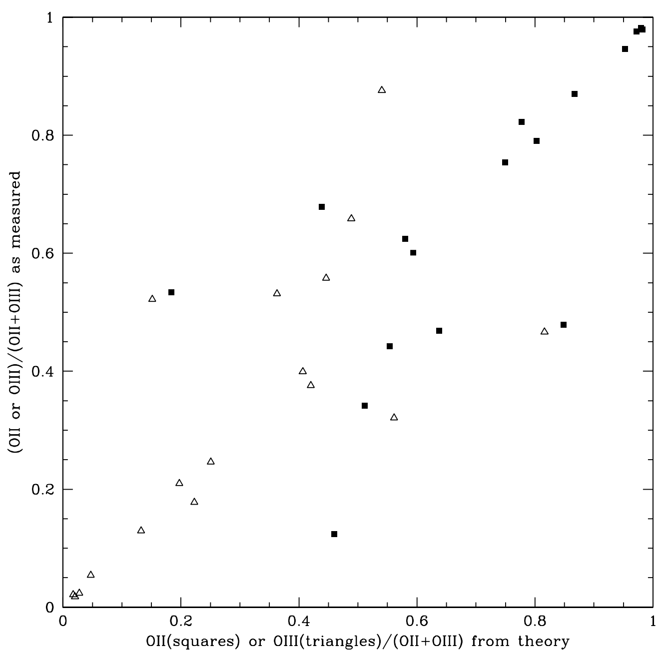

FIG. 3.—Plot of O II/(O II+O III) (*filled squares*) and O III/(O II+O III) (*open triangles*) as measured by Shaver et al. (1983) vs. the same quantity calculated from the models of Stasińska & Schaerer (1997), using effective temperatures determined from the data in Fig. 2*b*.

In order to minimize the effects of inaccuracies in distances on our analysis of abundance gradients in the Galaxy, we have searched the literature for the most accurate distances possible for all the sources observed in the six studies we analyzed. Table 4 shows the results of this work. The first column lists the name of the source as used by the first of the six groups to observe that source. The second and third columns list the galactocentric distance (R) and distance from the Sun (d) of the source, including our best estimates of the uncertainties in these quantities. The fourth and fifth columns list the method used to determine the distance (SP: spectrophotometric; K: kinematic; GC: Galactic center; M: maser proper motions) and the reference from which the distance or data used to determine the distance were taken. The sixth column lists any additional names for the source we could identify, and the seventh and last column lists those of the six groups who have observed each source. Throughout this analysis, we assumed a flat rotation curve, and used the IAU accepted values of distance to the Galactic center ($R_0 = 8.5$ kpc) and circular velocity of the local standard of rest ($\Theta_0 = 220$ km s^{-1}).

We began by searching for spectrophotometric distances to these objects (some studies already had listed such distances, and we took those, where available). Of the 117 sources listed in the table, we were able to find spectrophotometric distances to 55 of them. For those that had no uncertainty given, we assigned an uncertainty of 20%. Of the remaining sources, two have distances determined by the method of maser proper motions (Orion and W51); and one source, G7.47+0.06, is associated with the "3 kpc arm," which puts it at a distance of 6.3 kpc with $R_0 = 10$ kpc (Wink et al. 1982), or 5.4 kpc with $R_0 = 8.5$ kpc. For these 40 sources with relatively well-determined distances from the literature, we then determined their galactocentric distances (R) and

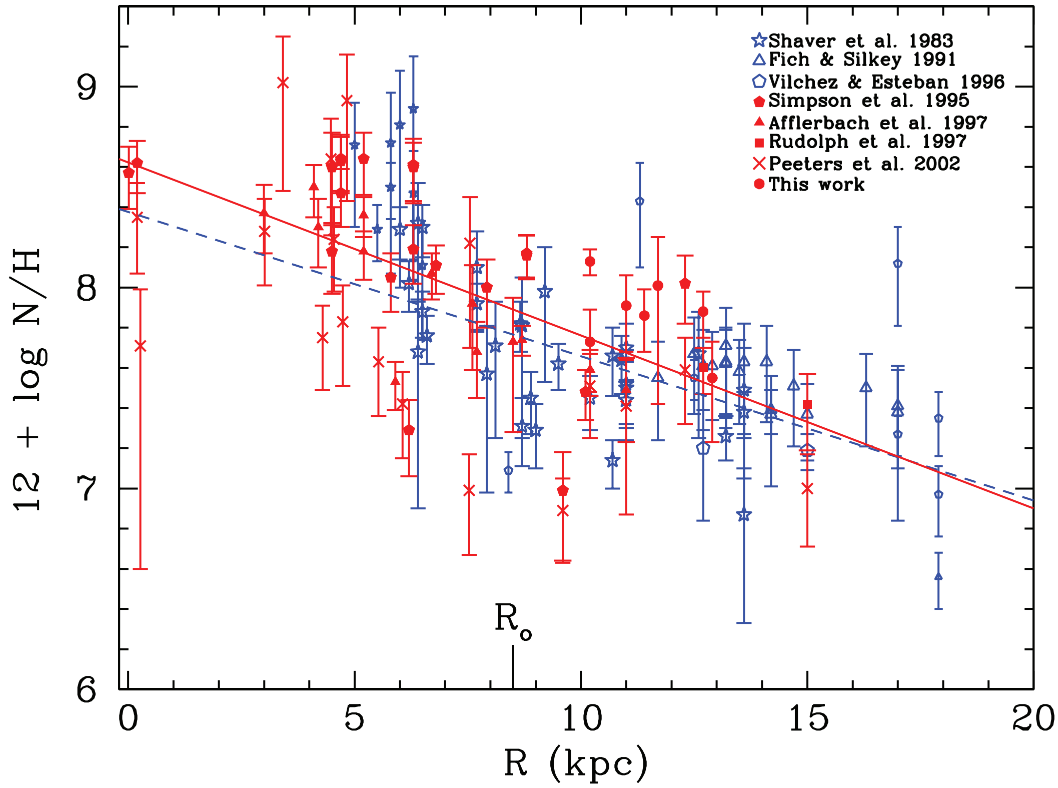

FIG. 4.—Newly determined nitrogen abundances (N/H) plotted vs. galactocentric radius (*R*) for the six studies reanalyzed and the new data presented here. Optical studies are indicated with open blue symbols; FIR studies are indicated filled red symbols. The best fit to the optical data (excluding certain sources indicated with smaller symbols; see text for details) is shown as a dashed blue line. The best fit to the FIR data is shown as a solid red line. Distances are taken from Table 4.

uncertainties in *R*, the latter by standard methods of error propagation. Another two sources are in the Galactic center, which assigns them an *R* of zero and a distance of 8.5 kpc.

For all but one of the remaining 64 sources, we used radial velocities from the literature to determine kinematic and galactocentric distances. Where two references in the table occur, the second reference was used to resolve the near/far distance ambiguity. Following Fich & Silkey (1991), we derived uncertainties in the kinematic distances by assuming a 7 km s^{-1} uncertainty in the radial velocities, corresponding to the observed velocity dispersion of local molecular clouds (Stark 1984). The last source, λ Cen, has a forbidden velocity, and we assigned it a galactocentric distance corresponding to the tangent point appropriate for its Galactic longitude.

7. ABUNDANCE GRADIENTS

From the derived abundances in Table 6 we can study the distribution of Galactic abundances with galactocentric radius (*R*). Figures 4, 5, 6, and 7 show plots of the newly determined N/H, O/H, S/H, and N/O plotted versus galactocentric radius for the six studies reanalyzed plus the new data presented here. To make it easier to distinguish between the two data sets, the optical data are plotted as open symbols, while the FIR data are plotted as solid symbols. Linear fits to the optical and FIR results are plotted as dashed and solid lines, respectively (see § 7.1 for details of the fitting procedure). For all four abundances, but particularly for N/O, there is evidence of an offset between the optical and FIR results.

7.1. *Abundance Gradient Fitting*

Given the amount of scatter evident in Figures 4–7 we considered a number of different fitting techniques and fitting functions. However, we concluded that a linear fit is still the simplest way to characterize the data, and we leave the fitting of more complex functions to eventual comparisons to detailed theoretical models (see, e.g., Hou et al. 2000).

To determine linear abundance gradients, we used the straight line fitting routine, FIT, from Press et al. (1986) and fitted to a linear function of ($R - 8.5$ kpc). This routine allows one to fit data in which different points have different, known uncertainties and uses those individual uncertainties to produce estimates of the uncertainties in each of the fitted parameters (the intercept and the slope) as well as an overall goodness-of-fit of the data to the model line (to simplify calculations of gradients, all asymmetric uncertainties were averaged, leading to final uncertainties that are symmetric in the linear abundances for fitting purposes). In all cases we found that the goodness-of-fit parameter suggested that the input uncertainties for each data point were too small; in other words, the data at a given galactocentric radius, *R*, are more scattered than the observational uncertainties, including both the distance uncertainties and the measurement uncertainties, alone would suggest. This suggests that there is a real spread in abundances.

To measure this additional spread, we introduce a parameter we call the "intrinsic scatter," which is added in quadrature to the uncertainty for each data point. The use of the intrinsic scatter parameter had no noticeable effect on the fit parameters, but may have some significance as a measure of the intrinsic variation of abundances at a given radius, *R*. Its use also leads to more meaningful uncertainties in the fitted parameters. For each element we chose the smallest possible value of the intrinsic scatter required to obtain a meaningful fit, according to the goodness-of-fit parameter. This additional scatter was typically between 0.10 and 0.20 dex. Afflerbach et al. (1997), in fitting their data, followed a similar procedure to find what they also call the "intrinsic scatter"

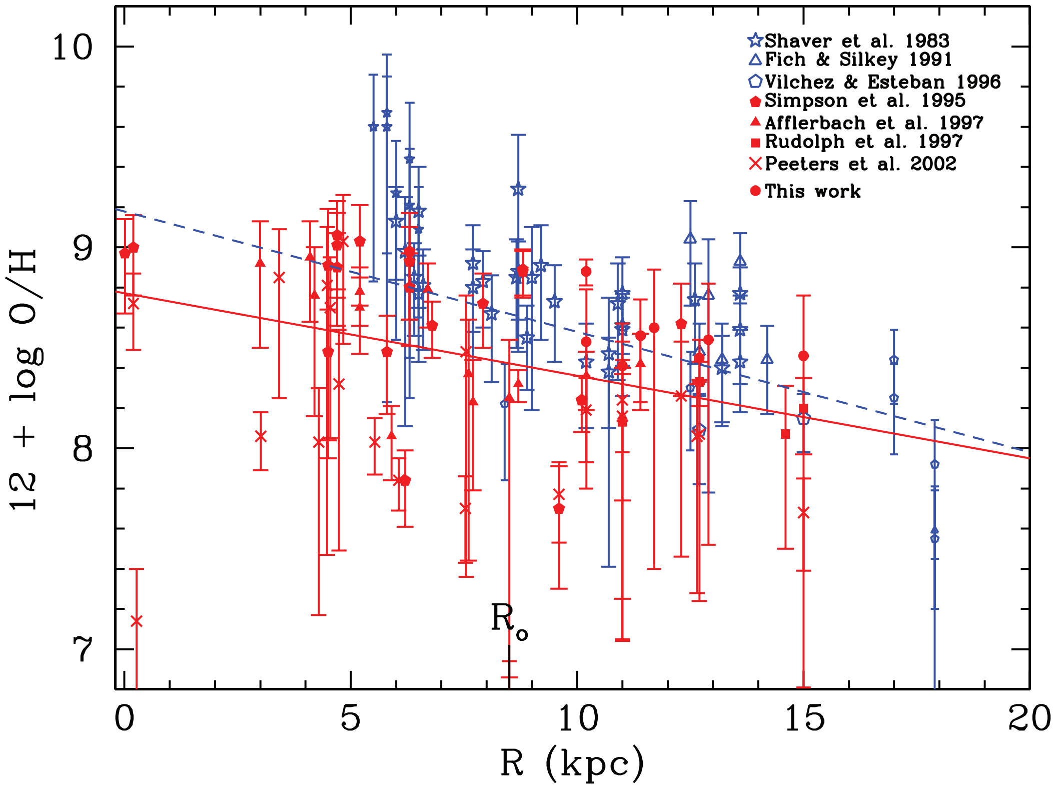

FIG. 5.—Newly determined oxygen abundances (O/H) plotted vs. galactocentric radius (*R*) for the six studies reanalyzed and the new data presented here. Optical studies are indicated with open blue symbols; FIR studies are indicated filled red symbols. The best fit to the optical data (excluding certain sources indicated with smaller symbols; see text for details) is shown as a dashed blue line. The best fit to the FIR data is shown as a solid red line. Distances are taken from Table 4.

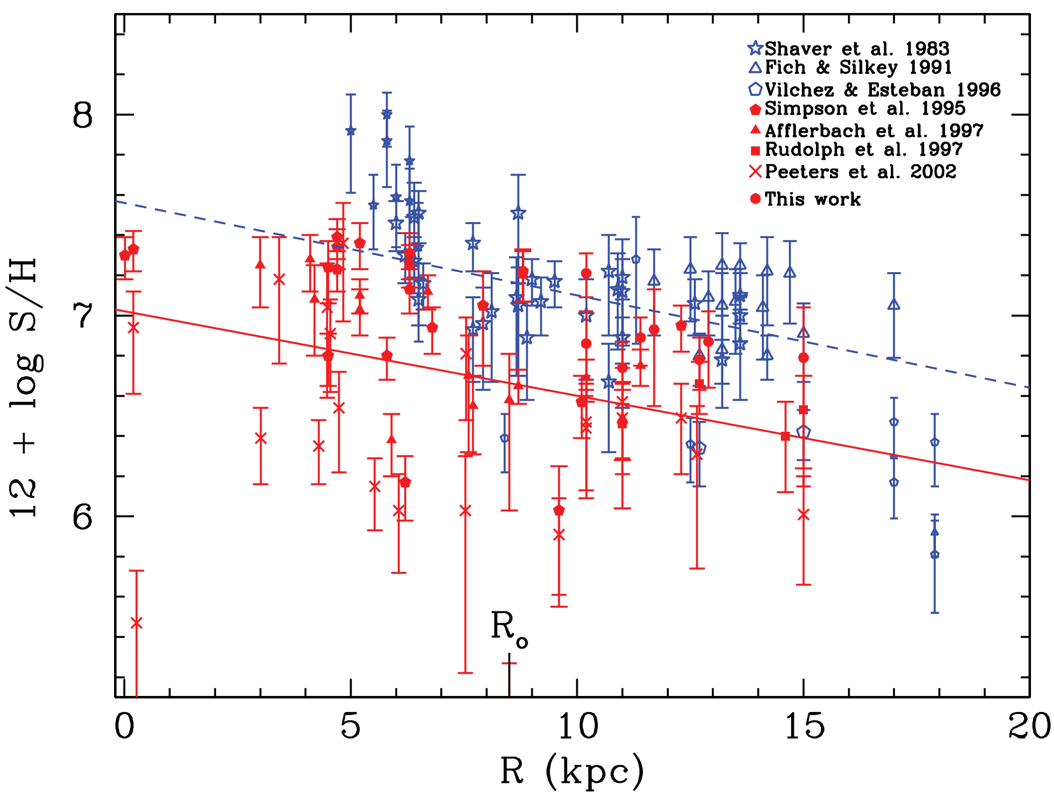

FIG. 6.—Newly determined sulfur abundances (S/H) plotted vs. galactocentric radius (*R*) for the six studies reanalyzed and the new data presented here. Optical studies are indicated with open blue symbols; FIR studies are indicated filled red symbols. The best fit to the optical data (excluding certain sources indicated with smaller symbols; see text for details) is shown as a dashed blue line. The best fit to the FIR data is shown as a solid red line. Distances are taken from Table 4.

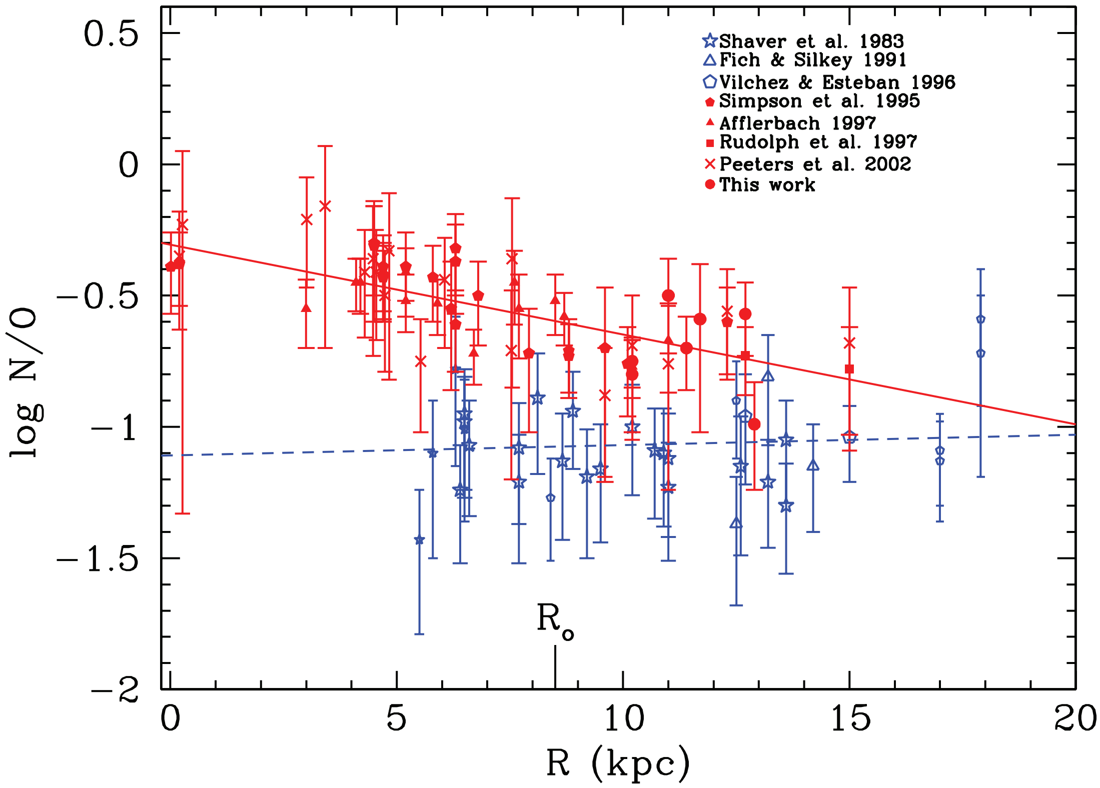

FIG. 7.—Newly determined nitrogen-to-oxygen abundance ratios (N/O) plotted vs. galactocentric radius (R) for the six studies reanalyzed and the new data presented here. Optical studies are indicated with open blue symbols; FIR studies are indicated closed red symbols. The best fit to the optical data is shown as a dashed blue line. The best fit to the FIR data is shown as a solid red line. Distances are taken from Table 4.

in the data and find values from 0.10 to 0.16, in good agreement with our values. These nonzero values of the scatter may indicate that the gas is not as well mixed as in commonly thought.

To determine if the results from the optical and FIR data sets could be combined into a single fit, we fitted straight line gradients to each result separately as well as to the combined data set. The fit to the combined data set gave slopes considerably different from either individual data set and was not as good as the separate fits because the two data sets had significant offsets between them. Thus, we chose to use the separate fits for the optical and FIR data sets as our final results.

In addition, the fits to the complete optical data set gave extremely steep slopes for O/H and S/H, largely due to some extremely high points from the Shaver et al. study around $R =$ 5–6 kpc. Upon closer inspection, we discovered that all of these points corresponded to regions whose abundances Shaver et al. did not consider "well-determined." Furthermore, all these regions were very cool ($T_e < 6000$ K), making the estimates of their ionic abundances *very* sensitive to uncertainties in electron temperature. Deharveng et al. (2000) in their reanalysis of the Shaver et al. data concluded that the Shaver et al. estimates of the electron temperatures for these regions are too cool.

Thus, we chose to exclude these data points from the fits to the optical data. We also excluded the data for S266 (which is known to have anomalously low abundances; Fich & Silkey 1991; Deharveng et al. 2000), and for the Vílchez & Esteban regions with model-dependent determinations of electron temperature. These data points excluded from the optical fit are plotted as smaller symbols in the plots.

Table 7 shows the final fits to each data set as well as the ratio of the slopes and the offsets in both the intercept and in the abundance (X/H) at the solar circle ($R_0 = 8.5$ kpc).

7.2. N/H

The final derived nitrogen abundances are shown in Figure 4. As given in Table 7, the FIR gradient of -0.085 dex kpc^{-1} is slightly steeper than the optical gradient of -0.071 dex kpc^{-1} and the fitted line for the FIR is higher almost everywhere, especially

TABLE 7

FINAL ABUNDANCE GRADIENTS FITS

Data Used	Slope	Abundance at 8.5 kpc	Number of Points
	12+log (N/H)		
Optical	-0.071 ± 0.010	7.76 ± 0.04	50
FIR	-0.085 ± 0.010	7.90 ± 0.04	60
Ratio/offset	0.84 ± 0.15	0.14 ± 0.06	
	12+log (O/H)		
Optical	-0.060 ± 0.010	8.67 ± 0.04	70
FIR	-0.041 ± 0.014	8.42 ± 0.05	68
Ratio/offset	1.46 ± 0.55	0.25 ± 0.06	
	12+log (S/H)		
Optical	-0.046 ± 0.009	7.17 ± 0.04	48
FIR	-0.042 ± 0.013	6.66 ± 0.05	68
Ratio/offset	1.10 ± 0.40	0.51 ± 0.06	
	log (N/O)		
Optical	0.004 ± 0.016	-1.08 ± 0.06	25
FIR	-0.034 ± 0.006	-0.60 ± 0.02	60

at small galactocentric distances. Other observers have also found a relatively wide variation in nitrogen abundance gradients (see Table 3). The original result of Shaver et al., using only the sources with "well-determined" abundances, and recomputed with the new distances from Table 4, is -0.066 dex kpc^{-1}; Afflerbach et al. find -0.072 dex kpc^{-1}; while Simpson et al., together with Rudolph et al. find -0.111 dex kpc^{-1}. In studies of B stars, Gummersbach et al. (1998) found a gradient of N/H of -0.08 ± 0.02 dex kpc^{-1}, and Rolleston et al. found a gradient of N/H of -0.09 ± 0.01 dex kpc^{-1}. Thus, there is no consistent result for the gradient of N/H, either between FIR studies or between FIR and optical studies, but it should be noted that the spread in the results is not very much larger than the uncertainties in the fitted slopes.

Besides the difference in slopes between the optical and FIR data sets, the most visible feature in this plot is the lack of many data points below the optical fit inside of $R \approx 5.5$ kpc. There are no useful optical observations inside of this galactocentric distance, and *most* of the FIR observations are above the best fit to the optical data. Hence, the FIR data are not consistent with the optical fit in the innermost parts of the Galaxy.

The inclusion of the innermost optical data points (i.e., the Shaver et al. sources that were left out of the optical fit) would lead to a steeper nitrogen gradient or a break in the gradient through a step around 7 kpc or a strong flattening of the nitrogen abundance gradient in the outer Galaxy. Both of these possibilities have been discussed previously (Fich & Silkey 1991; Simpson et al. 1995). Without these data points, the evidence for a flattening of the nitrogen gradient at large R is not as compelling. The mean nitrogen abundance at $R_0 = 8.5$ kpc shows that the FIR observations produce abundances that are slightly higher than those from the optical measurements, though this result is not statistically very significant.

7.3. O/H

Figure 5 shows the final derived abundances for oxygen. The figure shows that the optical gradient is steeper than that determined from the FIR observations. However, as given in Table 7 the difference is not statistically significant (the ratio of the slopes are less than 1 σ from 1.00). Within the uncertainties these results are not different from those found for other kinds of objects. Henry & Worthey (1999), who simply collected all the H II region and PNe abundance data in the literature and fitted it simultaneously, found a gradient of -0.06 ± 0.01 dex kpc^{-1}. Our result is also consistent with gradients found from observations of abundances in B stars by Smartt & Rolleston (1997; -0.07 ± 0.01) and Gummersbach et al. (1998; -0.07 ± 0.02).

There is a vertical shift of 0.25 dex between the fits to the optical and FIR oxygen gradients at $R = 8.5$ kpc and this is statistically significant at the 4 σ level. There is less evidence for a flattening or step function in the oxygen gradient, even before excluding the optical data near 6 kpc.

7.4. S/H

Although one expects the sulfur abundances to track well with the oxygen abundances, Figure 6 shows that the optical measurements of sulfur do not follow this rule. The FIR result is constrained by the analysis method to give the same gradient for oxygen and sulfur. The optical observations give a slightly shallower slope of -0.046 dex kpc^{-1}. This is strongly influenced by approximately a dozen data points from the work of Fich & Silkey, all of which are higher than the FIR results in the same range in galactocentric distances. The offset between FIR and optical data sets at $R = 8.5$ kpc is very significant in this analysis.

7.5. N/O

The most glaring display of the difference between the optical and FIR abundances is shown in Figure 7, where the ratio of the nitrogen to oxygen abundances (N/O) are shown. Except at the outer edge of the Galaxy the two sets of observations appear to span completely different ranges in this abundance ratio. This is to be expected from the N/H and O/H results. The FIR determined N/H results give higher values and a slightly steeper slope than the optically determined results. On the other hand the FIR determined O/H results are lower and have a less steep slope than the optically determined results. Dividing N/H by O/H values naturally leads to the more dramatic differences seen in Figure 7.

The FIR observations lead to abundance ratios that are approximately 0.5 dex higher than those found from the optical data. The FIR observations are best fitted by a slightly negative abundance ratio gradient of -0.036 ± 0.006 kpc^{-1}, while the distribution of the optical data appears flat. This fit to the FIR data agrees quite well with the N/O gradient of -0.04 ± 0.02 dex kpc^{-1} found in a study of B star abundances (Rolleston et al. 2000).

8. CONCLUSIONS

This work was motivated by the hope that a single analysis of all of the available data, both optical and infrared, would lead to a resolution of the differences found in various abundance studies of H II regions in the Milky Way. This has not been successful. We now know that these differences are *not* due to the use of different distance scales in the Galaxy, the use of different physical constants for the various quantum processes modeled, or the use of different ionization correction schemes. The optical and infrared studies of the H II region abundances still give systematically different results, most evident in the ratio of N/O.

To a first approximation the use of a different distance scale in the Milky Way (i.e., changing R_0 from 10 to 8.5 kpc) does not result in any change in the gradient. When comparing gradients from studies using different values of R_0 the gradient should not be automatically rescaled by the ratio of the R_0 values (see § 4).

Although the physical constants used in this analysis are now consistent across the analysis there is still more work to be done on the detailed physics of the analysis. In particular, there may be important excitation processes that have not yet been accounted for in this analysis and these processes may differ for the dominant lines in the optical and the FIR. For example, as suggested by Rubin et al. (1988), it is possible that recombination excitation could be important in the optical lines.

The biggest weaknesses in the FIR studies are the relative insensitivity of FIR telescopes (this will improve with SOFIA); the need to determine the hydrogen column density from other data (typically radio continuum images) in order to determine X/H, and the difficulty in doing this accurately (see Rudolph et al. 1997 for a discussion of this point) and the fact that the corrections from N^{++}/O^{++} to N/O can be large (though the small error bars on the FIR points in Figure 7 suggest this effect may not be as large as has been suggested).

The biggest weaknesses in the optical studies are the extreme sensitivity to extinction (making it difficult or impossible to observe some parts of the Galaxy) and to the assumed electron temperature. *This latter point cannot be emphasized enough.* Even the determination of N/O from N^{+}/O^{+} (which are nominally equal in the models of Stasińska & Schaerer 1997) is heavily dependent on the assumed electron temperature (as evidenced by the large error bars on the optical data points in Fig. 7). The recent study of Deharveng et al. (2000), in which they reanalyzed a number of the same optical H II region studies we did, but with a different method for determining the electron temperature, led to a significantly shallower slope of O/H than had been seen previously, highlighting this problem.

The abundances in a handful of H II regions have been studied in great detail (e.g., by Esteban et al. 1990, 1998; Peimbert & Torres-Peimbert 1990). These studies looked at numerous lines of sight in one or two individual H II regions and obtained sensitive measurements of the line intensities of numerous line at optical wavelengths. These allowed the authors of these studies to make much more precise determinations of the conditions within each nebula and to examine each for variations in quantities such as extinction and electron temperature. All of the resulting abundances from those studies are consistent with the abundances found in this current study.

While it is now well established that there is an overall abundance gradient in the Milky Way, the size of that gradient is still uncertain, and it is clear that it may be different for different elements. Thus, it is probably misleading to refer to a single ''abundance gradient'' for the Milky Way. There also may not be a single gradient for all *R*, though the evidence for this result is not yet compelling.

It is tempting, in the face of such discrepancies between the optical and FIR data sets, to conclude that our place in the disk of our Galaxy is the major cause of these differences. One might even be tempted to question the usefulness of Galactic studies of abundance in favor of extragalactic studies, which do not suffer from such severe extinction problems. We believe, however, that our study is a cautionary tale for anyone who wishes to study abundance variations in galaxies. Our inability to reconcile the optical and FIR data sets, particularly the N/O data, suggest that there is still fundamental physics we do not understand well enough, physics that will affect any determination of nebular abundances, Galactic or extragalactic.

We wish to thank the KAO staff for excellent support while these observations were being made and Jim Baltz, Steve Lord, and Sean Colgan for their assistance with the observations. A. L. R. wishes to acknowledge the support of NASA grant NAG 2-960, and the NSF Young Faculty Career Development CAREER Program via NSF grant 96-24924.

REFERENCES

Afflerbach, A., Churchwell, E., Acord, J. M., Hofner, P., Kurtz, S., & Depree, C. G. 1996, ApJS, 106, 423
Afflerbach, A., Churchwell, E., & Werner, M. W. 1997, ApJ, 478, 190
Antonopoulou, E., & Pottasch, S. R. 1987, A&A, 173, 108
Balser, D. S., Bania, T. M., Brockway, C. J., Rood, R. T., & Wilson, T. L. 1994, ApJ, 430, 667
Bézard, B., Gautier, D., & Marten, A. 1986, A&A, 161, 387
Bharat, R. 1994, in Infrared Astronomy with Arrays: The Next Generation, ed. I. S. McLean (Dordrecht: Kluwer), 376
Blitz, L., Fich, M., & Stark, A. A. 1982, ApJS, 49, 183
Blum, R. D., & Pradhan, A. K. 1992, ApJS, 80, 425
Born, M., & Wolf, E. 1964, in Principles of Optics (Oxford: Pergamon), 416
Brand, J., & Blitz, L. 1993, A&A, 275, 67
Brocklehurst, M. 1971, MNRAS, 153, 471
Bronfman, L., Nyman, L., & May, J. 1996, A&A, 115, 81
Caplan, J., Deharveng, L., Peña, M., Costero, R., & Blondel, C. 2000, MNRAS, 311, 317
Cardelli, J. A., Clayton, G. C., & Mathis, J. S. 1989, ApJ, 345, 245
Caswell, J. L., & Haynes, R. F. 1987, A&A, 171, 261
Chan, G., & Fich, M. 1995, AJ, 106, 2611
Chini, R., Elsaesser, H., & Neckel, T. 1980, A&A, 91, 186
Churchwell, E., Walmsley, C. M., & Cesaroni, R. 1990, A&AS, 83, 119
Corbel, S., Wallyn, P., Dame, T. M., Durouchoux, P., Mahoney, W. A., Vilhu, O., & Gindlay, J. E. 1997, ApJ, 478, 624
Deharveng, L., Peña, M., Caplan, J., & Costero, R. 2000, MNRAS, 311, 329
Dinerstein, H. L. 1990, in The Interstellar Medium in Galaxies, ed. H. A. Thronson, Jr., & J. M. Shull (Dordrecht: Kluwer), 257
Drissen, L., Moffat, A. F. J., Walborn, N. R., & Shara, M. M. 1995, AJ, 110, 2235
Erickson, E. F., Haas, M. R., Colgan, S. W. J., Simpson, J. P., & Rubin, R. H. 1995, in ASP Conf. Ser. 73, Airborne Astronomy Symposium on the Galactic Ecosystem: From Gas to Stars to Dust, ed. M. R. Haas, J. A. Davidson, & E. F. Erickson (San Francisco: ASP), 523
Erickson, E. F., Matthews, S., Augason, G. C., Houck, J. R., Harwit, M. O., & Rank, D. M. 1984, Proc. SPIE, 509, 129
Esteban, C., Peimbert, M., Torres-Peimbert, S., & Escalante, V. 1998, MNRAS, 295, 401
Esteban, C., Vilchez, J. M., Manchado, A., & Edmunds, M. G. 1990, A&A, 227, 515
Feinstein, A. 1994, Rev. Mex. AA, 29, 141
Fich, M. 1986, AJ, 92, 787
———. 1993, ApJS, 86, 475
Fich, M., Blitz, L., & Stark, A. A. 1989, ApJ, 342, 272
Fich, M., & Silkey, M. 1991, ApJ, 366, 107
Galavís, M. E., Mendoza, C., & Zeippen, C. J. 1995, A&AS, 111, 347
Garay, G., Lizano, S., & Gomez, Y. 1994, ApJ, 429, 268
Georgelin, Y. M., & Georgelin, Y. P. 1976, A&A, 49, 57
Girardi, L., Bica, E., Pastoriza, M. G., & Winge, C. 1997, ApJ, 486, 847
Giveon, U., Sternberg, A., Lutz, D., Feuchtgruber, H., & Pauldrach, A. W. A. 2002, ApJ, 566, 880
Goldader, J. D., & Wynn-Williams, C. G. 1994, ApJ, 433, 164
Gummersbach, C. A., Kaufer, A., Schäfer, D. R., Szeifert, T., & Wolf, B. 1998, A&A, 338, 881
Haas, M. R., Erickson, E. F., McKibbin, D. D., Goorvitch, D., & Caroff, L. J. 1982, Icarus, 51, 476
Hackwell, J. A., Gehrz, R. D., Smith, J. R., & Briotta, D. A. 1978, ApJ, 221, 797
Haikala, L. K. 1995, A&A, 294, 89
Hanel, R. A., Conrath, B. J., Kunde, V. G., Pearl, J. C., & Pirraglia, J. A. 1983, Icarus, 53, 262
Henry, R. B. C., & Worthey, G. 1999, PASP, 111, 919
Heydari-Malayeri, M. 1988, A&A, 202, 240
Hillenbrand, L. A. 1997, AJ, 113, 1733
Hillenbrand, L. A., Massey, P., Strom, S. E., & Merrill, K. M. 1993, AJ, 106, 1906
Hofner, P., Kurtz, S., Churchwell, E., Walmsley, C. M., & Cesaroni, R. 1994, ApJ, 429, L85
Hou, J. L., Prantzos, N., & Boissier, S. 2000, A&A, 362, 921
Hunter, D. A. 1992, ApJS, 79, 469
Jenkner, H., Lasker, B. M., Sturch, C. R., McLean, B. J., Shara, M. M., & Russell, J. L. 1990, AJ, 99, 2082
Kuchar, T. A., & Bania, T. M. 1994, ApJ, 436, 117
Kurucz, R. L. 1979, ApJS, 40, 1
Lasker, B. M., Sturch, C. R., McLean, B. J., Russell, J. L., Jenkner, H., & Shara, M. M. 1990, AJ, 99, 2019
Lennon, D. J., & Burke, V. M. 1994, A&AS, 103, 273
Lester, D. F., Dinerstein, H. L., Werner, M. W., Watson, D. M., Genzel, R., & Storey, J. W. V. 1987, ApJ, 320, 573
Liszt, H. S., & Spiker, R. W. 1995, ApJS, 98, 259
Lockman, F. J. 1989, ApJS, 71, 469
Lord, S. D. 1992, NASA Tech. Memo. 103957
Martin, P. G., & Whittet, D. C. B. 1990, ApJ, 357, 113
Martín-Hernández, N. L., et al. 2002, A&A, 381, 606
Mathis, J. S. 1985, ApJ, 291, 247
Matthews, S., & Erickson, E. F. 1977, NASA Tech. Memo. X-73, 204
Mendoza, C. 1983, in IAU Symp. 103, Planetary Nebulae (Dordrecht: Reidel), 143
Mooney, T., Sievers, A., Mezger, P. G., Solomon, P. M., Kreysa, E., Haslam, C. G. T., & Lemke, R. 1995, A&A, 299, 869
Muzzio, J. C., & Celotti de Frecha, M. B. 1979, MNRAS, 189, 159
Osterbrock, D. E. 2000, Astrophysics of Gaseous Nebulae and Active Galactic Nuclei (Mill Valley: University Science Books)
Pagel, B. E. J. 1997, Nucleosynthesis and Chemical Evolution of Galaxies (Cambridge: Cambridge Univ. Press)
Peeters, E., et al. 2002, A&A, 381, 571
Peimbert, M. 1967, ApJ, 150, 825
Peimbert, M., & Torres-Peimbert, S. 1990, Rev. Mex. AA, 24, 155
Pradhan, A. K., & Peng, J. 1995, in STScI Symp. 8, The Analysis of Emission Lines, ed. R. E. Williams & M. Livio (Cambridge: Cambridge Univ. Press), 8
Press, W. H., Flannery, B. P., Teukolsky, S. A., & Vetterling, W. T. 1986, Numerical Recipes, The Art of Scientific Computing (Cambridge: Cambridge Univ. Press)

Reifenstein, E. C., Wilson, T. L., Burke, B. F., Mezger, P. G., & Altenhoff, W. J. 1970, A&A, 4, 357
Rieke, G. H., & Lebofsky, M. J. 1985, ApJ, 288, 618
Rolleston, W. R. J., Smartt, S. J., Dufton, P. L., & Ryans, R. S. I. 2000, A&A, 363, 537
Rubin, R. H. 1985, ApJS, 57, 349
Rubin, R. H., Simpson, J. P., Erickson, E. F., & Haas, M. R. 1988, ApJ, 327, 377
Rubin, R. H., Simpson, J. P., Haas, M. R., & Erickson, E. F. 1991, ApJ, 374, 564
Rudolph, A. L., de Geus, E. J., Brand, J., & Wouterloot, J. G. A. 1996, ApJ, 458, 653
Rudolph, A. L., Simpson, J. P., Haas, M. R., Erickson, E. F., & Fich, M. 1997, ApJ, 489, 94
Saraph, H. E., & Storey, P. J. 1999, A&AS, 134, 369
Schaerer, D., & de Koter, A. 1997, A&A, 322, 598
Seaton, M. J. 1979, MNRAS, 187, 73
Shaver, P. A., McGee, R. X., Newton, L. M., Danks, A. C., & Pottasch, S. R. 1983, MNRAS, 204, 53
Simpson, J. P., Colgan, S. W. J., Rubin, R. H., Erickson, E. F., & Haas, M. R. 1995, ApJ, 444, 721
Simpson, J. P., & Rubin, R. H. 1990, ApJ, 354, 165
Smartt, S. J., & Rolleston, W. R. J. 1997, ApJ, 481, L47
Stark, A. A. 1984, ApJ, 281, 624
Stasińska, G. 1980, A&A, 84, 320
———. 1982, A&AS, 48, 299
Stasińska, G., & Schaerer, D. 1997, A&A, 322, 615
Tapia, M., Roth, M., Marraco, H., & Ruiz, M. T. 1988, MNRAS, 232, 661
van den Ancker, M. E., The, P. S., Feinstein, A., Vazquez, R. A., de Winter, D., & Perez, M. R. 1997, A&AS, 123, 63
Vílchez, J. M., & Esteban, C. 1996, MNRAS, 280, 720
Walmsley, C. M., Churchwell, E., & Terzian, Y. 1981, A&A, 96, 278
Whitford, A. E. 1958, AJ, 63, 201
Wink, J. E., Altenhoff, W. J., & Mezger, P. G. 1982, A&A, 108, 227
Wood, D. O. S., & Churchwell, E. 1989, ApJS, 69, 831
Wouterloot, J. G. A., & Brand, J. 1989, A&AS, 80, 149